

UNCLASSIFIED

AD NUMBER
AD839442
NEW LIMITATION CHANGE
TO Approved for public release, distribution unlimited
FROM Distribution authorized to U.S. Gov't. agencies and their contractors; Critical Technology; 26 JUN 1968. Other requests shall be referred to Naval Ordnance Lab., White Oak, MD.
AUTHORITY
NOL ltr, 15 Nov 1971

THIS PAGE IS UNCLASSIFIED

NOL  
TR-68-124  
C. 1

NOLTR 68-124

AD-839442

ON THE FREQUENCY FILTERING OF  
TRANSIENT NOISE SIGNALS

RETURN TO  
TECHNICAL LIBRARY BRANCH  
NAVAL ORDNANCE SYSTEMS COMMAND  
Dept. of Navy  
Washington 25, D. C., 20380

Do not forward this copy to other activities  
without authorization of NAVORDSYSCOM (ORD-9132)

26 JUNE 1968

NOL

UNITED STATES NAVAL ORDNANCE LABORATORY, WHITE OAK, MARYLAND

NOLTR 68-124

This document is subject to special export controls  
and each transmittal to foreign governments or  
foreign nationals may be made only with prior  
approval of NOL.

2

## ON THE FREQUENCY FILTERING OF TRANSIENT NOISE SIGNALS

Prepared by:

Edward C. Whitman

ABSTRACT: A class of transient random signals is modeled as the product of a deterministic, square integrable envelope function and a Gaussian random process having a well-defined power spectrum. The passage of an ensemble of such random signals through a linear filter is studied with particular emphasis on the mean and variance of the total output energy. It is found that an important role is played in these considerations by the covariance function between values of the energy density spectrum of a sample function evaluated at different frequency arguments. Accordingly, the form of this function is derived and portrayed as a surface lying above a two-dimensional frequency plane. Examples of these spectral covariance surfaces are presented and discussed for both rectangular and decaying exponential pulses of both broad and narrow band Gaussian noise, and their general characteristics are identified. Finally, the problem of idealized narrow band filtering is specifically approached and approximate expressions derived for the mean, variance, and normalized standard deviation of the output energy of a narrow band filter excited by rectangular pulses of narrow band Gaussian noise. The approximate relationships of the filter bandwidth, pulse duration, and underlying noise spectrum are explored for their effects on spectral resolution and statistical stability, leading to an uncertainty principle. The implications of these findings for spectral analysis and monopulse signal processing are discussed in the light of this uncertainty principle and the limitations it imposes on the simultaneous precision of frequency resolution and spectral amplitude.

PUBLISHED 26 JUNE 1968

U. S. NAVAL ORDNANCE LABORATORY  
White Oak, Maryland

NOLTR 68-124

26 June 1968

ON THE FREQUENCY FILTERING OF TRANSIENT NOISE SIGNALS

In a previous paper (NOLTR 67-25), a class of random signals was modeled as the product of a transient, deterministic envelope waveform and a continuing random process, and the autocorrelation and spectrum of this class studied in some detail. In the present report, this study is extended to treat the covariance properties of the random transient spectra and the statistical characteristics of the outputs of filters excited by such waveforms. The work on this project was funded under Task MAT-03L-000/F008-98-01, Problem Assignment 009. The report will be of interest to those concerned with statistical communication and detection theory, monopulse signal processing, measurement planning for spectral analysis, and noise immunity studies.

The author wishes to acknowledge with thanks the aid of Mr. Ralph Ferguson and Mrs. Mary Beth Beszterczei of the Computer Applications Division for their advice in preparing the computer programming that lies behind many of the findings; and also the helpful criticism of Dr. Earl A. Schuchard of the Magnetics and Electrical Division in preparing the final manuscript.

E. F. SCHREITER  
Captain, USN  
Commander

*E. H. Beach*  
E. H. BEACH  
By direction

CONTENTS

	Page
Chapter I, INTRODUCTION .....	1
Chapter II, FREQUENCY FILTERING OF RANDOM TRANSIENT WAVEFORMS .....	6
Chapter III, SPECTRAL COVARIANCE SURFACES FOR RANDOM TRANSIENT ENSEMBLES .....	11
Chapter IV, IDEAL BAND PASS FILTERING OF RANDOM TRANSIENT WAVEFORMS .....	53
Chapter V, CONCLUSIONS AND SUGGESTIONS FOR FUTURE RESEARCH ,.....	76
APPENDIX A, THE SPECTRAL NORMALIZATION PROBLEM .....	A-1
APPENDIX B, THE "WIDTH" OF THE CONVOLUTION OF TWO FUNCTIONS .....	B-1
APPENDIX C, AN ALTERNATIVE APPROACH TO THE NARROW BAND FILTERING PROBLEM WITH A SOLUTION FOR AN IMPORTANT SPECIAL CASE ....	C-1

ILLUSTRATIONS

Figure	Title	Page
1	A Model for the Generation of Random Transients .....	2
2	Linear Filtering of Random Transient Waveforms .....	8
3a	The $\omega - \omega'$ Plane Showing the Symmetry Axes .....	16
3b	Three Dimensional Representation of the Spectral Covariance Symmetry Planes .....	16
4	Rectangular Envelope Functions and Associated $p(t, x)$ .....	17
5	Exponential Envelope Function and Associated $p(t, x)$ .....	17
6a	Rectangular Low-Pass Broad Band Spectrum .....	21
6b	Rectangular Narrow Band Spectrum .....	21
7	Spectral Expected Value for a Rectangular Burst of Low-Pass Broad Band Noise with $q = 10.0$ .....	26
8	Normalized Spectral Standard Deviation for a Rectangular Burst of Low-Pass Broad Band Noise with $q = 10.0$ .....	26
9	Normalized Spectral Covariance Surface for a Rectangular Pulse of Low-Pass Broad Band Noise with $q = 10.0$ .....	28
10	Important Lines in the $r - s$ Plane .....	29
11	Normalized Spectral Variance for a Rectangular Pulse of Low-Pass Broad Band Noise with $q = 10.0$ .....	29
12	Sections Through the Spectral Covariance Surface for a Rectangular Pulse of Low-Pass Broad Band Noise with $q = 10.0$ .....	31
13	Normalized Spectral Expected Value for a Rectangular Burst of Low-Pass Broad Band Noise with $q = 1.0$ .....	32
14	Normalized Spectral Standard Deviation for a Rectangular Burst of Low-Pass Broad Band Noise with $q = 1.0$ .....	32
15	Normalized Spectral Covariance Surface for a Rectangular Pulse of Low-Pass Broad Band Noise with $q = 1.0$ .....	33

ILLUSTRATIONS

Figure	Title	Page
16	Normalized Spectral Variance for a Rectangular Pulse of Low-Pass Broad Band Noise with $q = 1.0$ .....	34
17	Sections through the Spectral Covariance Surface for a Rectangular Pulse of Low-Pass Broad Band Noise with $q = 1.0$ .....	35
18	The Region of Appreciable Covariance for a Rectangular Pulse of Low-Pass Broad Band Noise as Delineated in the $r - s$ Plane .....	37
19	Normalized Spectral Expected Value for a Rectangular Burst of Narrow Band Noise with $q = 50.0$ and $z = 0.1$ .....	41
20	Normalized Spectral Variance for a Rectangular Burst of Narrow Band Noise with $q = 50.0$ and $z = 0.1$ .....	41
21	Normalized Spectral Covariance Surface for a Rectangular Pulse of Narrow Band Noise with $q = 50.0$ and $z = 0.1$ .....	42
22	Sections Through the Spectral Covariance Surface for a Rectangular Pulse of Narrow Band Noise with $q = 50.0$ and $z = 0.1$ .....	43
23	Normalized Spectral Expected Value for a Rectangular Burst of Narrow Band Noise with $q = 10.0$ and $z = 0.01$ .....	45
24	Normalized Spectral Variance for a Rectangular Burst of Narrow Band Noise with $q = 10.0$ and $z = 0.01$ .....	45
25	Normalized Spectral Covariance Surface for a Rectangular Pulse of Narrow Band Noise with $q = 10.0$ and $z = 0.01$ .....	46
26	Sections through the Spectral Covariance Surface for a Rectangular Pulse of Narrow Band Noise with $q = 10.0$ and $z = 0.01$ .....	47
27	The Region of Appreciable Spectral Covariance for a Rectangular Pulse of Narrow Band Noise Delineated in the $r - s$ Plane .....	48
28	Comparison of the Spectral Expected Values for Rectangular and Decaying Exponential Pulses of Narrow Band Noise with $q = 10.0$ and $z = 0.1$ .....	49
29	Comparison of Sections Through the Spectral Covariance Surface for Rectangular and Decaying Exponential Pulses of Narrow Band Noise for $q = 10.0$ and $z = 0.1$ . Here, the Center Frequency has been Chosen Equal to the Center Frequency of the Underlying Noise Process .....	50
30	A Comparison of the Energy Density Spectra for a Rectangular Pulse of Length $T$ and a Decaying Exponential Pulse of Time Constant $T$ .....	51
31	Ideal Narrow-Band Filter Function .....	54
32	$\text{Var}[F(H)]$ Portrayed as the Volume of a Prism Lying Under the Spectral Covariance Surface .....	54
33	An Interpretation of the Calculation of $E_A[F(H)]$ as the Area of Overlap of Two Rectangular Functions .....	58
34	Approximations for the Expected Value of the Output Energy of a Narrow Band Filter when Excited by a Rectangular Pulse of Narrow Band Noise .....	60

ILLUSTRATIONS

Figure	Title	Page
35	An Approximation for the Form of the Normalized Spectral Covariance Surface for a Rectangular Pulse of Narrow Band Noise .....	61
36	A Geometric Interpretation of the Approximate Output Energy Variance as Proportional to that Area of the "Covariance Hexagon" Overlapped by the "Filter Square" .....	63
37	Approximations for the Variance of the Output Energy of a Narrow Band Filter when Excited by a Rectangular Pulse of Narrow Band Noise .....	66
38	Approximations for the Normalized Standard Deviation of the Energy Output of a Narrow Band Filter when Excited by a Rectangular Pulse of Narrow Band Noise .....	69
39	The Normalized Standard Deviation of the Energy Out of a Narrow Band Filter as a Function of Normalized Filter Bandwidth when the Filter is Centered on the Center Frequency of the Underlying Input Noise Process .....	70
40	A Graphical Interpretation of the Determination of $R^2(B', \Delta)$ as the Ratio of Two Areas Overlapped by the Filter Square .....	73
B-1	The Convolution of Two Rectangular Pulses .....	B-5
B-2	Convolution of Double-sided Decaying Exponential Pulses for Two Sets of Parameter Values. All Amplitudes have been Normalized to Unity at the Origin .....	B-6

REFERENCES

- (a) Whitman, E.C., NOLTR 67-25 "On the Statistical Properties of Transient Noise Signals," U.S. Naval Ordnance Laboratory, White Oak, Maryland, 8 Mar 1967
- (b) Lee, Y.W., Statistical Theory of Communication, New York, 1960
- (c) Davenport, W.B., Jr. and Root, W.L., An Introduction to the Theory of Random Signals and Noise, New York, 1958
- (d) Parzen, E., Modern Probability Theory and Its Applications, New York, 1960
- (e) Parzen, E., Stochastic Processes, San Francisco, 1962
- (f) Bureau of Ships, Navy Dept, Washington, D. C., NAVSHIPS Rpt 0967-129-3010, "Introduction to Sonar Technology," Dec 1965
- (g) Harman, W.W., Principles of the Statistical Theory of Communication, New York, 1963
- (h) Bendat, J.S. and Piersol, A.G., Measurement and Analysis of Random Data, New York, 1966
- (i) Blackman, R.B. and Tukey, J.W., The Measurement of Power Spectra, New York, 1958
- (j) Born, Max, The Natural Philosophy of Cause and Chance, Oxford, 1949
- (k) Mason, S.J. and Zimmermann, H.J., Electronic Circuits, Signals, and Systems, New York, 1960
- (l) Schwartz, Mischa, Information Transmission, Modulation, and Noise, New York, 1959
- (m) Papoulis, A., Probability, Random Variables, and Stochastic Processes, New York, 1965

## Chapter I

## INTRODUCTION

In the predecessor of this report, reference (a), a study was made of the statistical characteristics of a class of transient, random waveforms appearing similar to sonar reverberation and EER returns, by assuming a relatively simple mathematical model for these phenomena and following the statistical implications of the model to their logical conclusion. The intent of that study was to prepare the groundwork for a theory that would provide some guidelines for predicting the result of operating on such waveforms for purposes of signal processing and/or measurement. Also raised were certain philosophical questions about the extent to which accurate predictions of random transient phenomena could be made and about the measurement interpretation of the harmonic spectrum of such signals. This report deals with a considerable amplification of the latter point.

The model treated in reference (a) is shown in Figure 1. It consists of generating an ensemble of random transient waveforms by the simple expedient of multiplying a continuing, stationary, zero-mean random process by a deterministic, square-integrable transient which is taken to be zero for  $t < 0$ . By considering an infinite ensemble of stationary random processes and a single transient "envelope waveform," one generates an infinite ensemble of non-stationary random transients each differing from the other in detail, but all characterized by the same time-varying variance, as the following shows.

If we denote a typical output ensemble member by  $s(t)$ , the continuing stationary input process by  $n(t)$ , and the multiplying transient waveform by  $e(t)$ , then evidently

$$s(t) = e(t) n(t) \quad (1)$$

If  $\sigma_n^2$  is the variance of  $n(t)$ , and  $\sigma_s^2$  that of  $s(t)$ , then since  $e(t)$  is assumed deterministic and hence does not enter into the averaging process for the variance,

$$\sigma_s^2(t) = e^2(t) \sigma_n^2 \quad (2)$$

which, as noted above, is a function of time.

For each member  $s(t)$  of the ensemble of random transients, one can compute the time autocorrelation function defined by

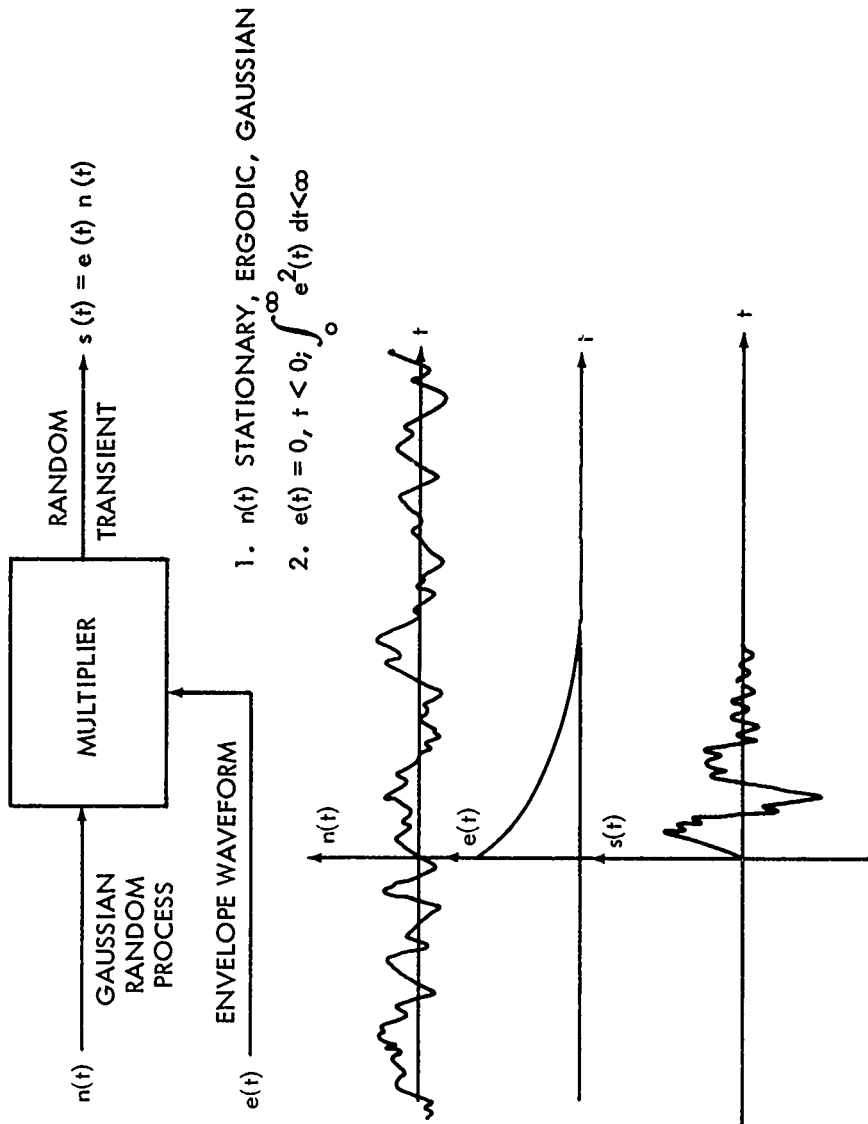


FIG.1 A MODEL FOR THE GENERATION OF RANDOM TRANSIENTS.

$$\phi_{SS}(\tau) \equiv \int_0^{\infty} s(t) s(t+\tau) dt \quad (3)$$

and the Fourier integral

$$S(\omega) \equiv \frac{1}{2\pi} \int_0^{\infty} s(t) e^{-j\omega t} dt \quad (4)$$

The energy density spectrum of the ensemble member is then given by

$$\phi_{SS}(\omega) = 2\pi S(\omega) \overline{S(\omega)} = 2\pi |S(\omega)|^2 \quad (5)$$

where the superscript bar denotes complex conjugation. From the Wiener-Khintchine relation, we know also that

$$\phi_{SS}(\omega) = \frac{1}{2\pi} \int_{-\infty}^{\infty} \phi_{SS}(\tau) e^{-j\omega\tau} d\tau \quad (6)$$

which is to say that the time autocorrelation function of equation (3) and the energy density spectrum of equation (5) constitute a Fourier transform pair.\* If the time autocorrelation function and energy density spectrum are computed for each of a large number of sample waveforms, they will turn out to be different from sample to sample since they result from operations on randomly different waveforms. Thus, for every value of their arguments, these quantities are random variables which may be considered statistics of the ensemble. It is not possible to speak of a single deterministic, predictable autocorrelation function or spectrum valid for the entire ensemble, since each ensemble member will yield a different function which can not be predicted with exactitude before the event.

Since the time autocorrelation function and energy density spectrum of a random transient are random variables, parameterized in a sense by their respective arguments, it becomes interesting to study the expected values of these variables and also their variances. In practical terms, the expected values represent the average

---

\*NOTE: The convention of reference (a) will be followed here in that autocorrelation functions and spectra for "energy" (i.e., transient) signals will be denoted  $\phi$  and  $\psi$  respectively (using upper and lower case phi); whereas autocorrelation functions and spectra for "power" (i.e., continuing) signals will be respectively denoted  $\Psi$  and  $\psi$  (upper and lower case psi).

at a point obtained over a large number of samples, and the variances indicate the extent to which the spectrum and autocorrelation of a single sample can be expected to depart from the average at a point. In reference (a), these means and variances were derived both in general and in particular simple cases where the spectral character of the continuing process and the form of the envelope transient were specified. The principal results were the following:

If  $s(t) = e(t)n(t)$  and  $\phi_{SS}(\tau)$  and  $\phi_{SS}(\omega)$  are given by equations (3) - (6), then

$$E[\phi_{SS}(\tau)] = \psi_{nn}(\tau)\phi_{ee}(\tau) \quad (7)$$

and

$$E[\phi_{SS}(\omega)] = \frac{1}{2\pi} \int_{-\infty}^{\infty} \psi_{nn}(x) \phi_{ee}(x) e^{-j\omega x} dx \quad (8)$$

where  $E[\cdot]$  denotes an ensemble average,  $\psi_{nn}(\tau)$  is the autocorrelation function of the continuing stationary process and  $\phi_{ee}(\tau)$  is the autocorrelation of the envelope waveform. The second of these relations can be expressed as

$$\begin{aligned} E[\phi_{SS}(\omega)] &= \int_{-\infty}^{\infty} \psi_{nn}(\omega') \phi_{ee}(\omega - \omega') d\omega' \\ &= \psi_{nn}(\omega) \otimes \phi_{ee}(\omega) \end{aligned} \quad (9)$$

where  $\psi_{nn}(\omega)$  is the power spectral density of the noise process,  $\phi_{ee}(\omega)$  is the energy density spectrum of the transient envelope, and  $\otimes$  represents the operation of convolution. The expected value of  $\phi_{SS}(\tau)$  is thus seen to be the product of the autocorrelation functions of the two signals whose product forms the random transient, and not surprisingly the expected value of the energy density spectrum turns out to be given by the convolution of the power density spectrum of the continuing stationary process and the energy density spectrum of the envelope waveform.

If  $n(t)$  is further restricted to be a Gaussian random process, the following expressions for the variances can be derived:

$$\text{Var}[\phi_{SS}(\tau)] = 2 \int_0^{\infty} \phi_{pp}(u, \tau) [\psi_{nn}^2(u) + \psi_{nn}(u+\tau)\psi_{nn}(u-\tau)] du \quad (10)$$

where  $\phi_{pp}(u, \tau)$  is the autocorrelation function of

$$p(t, \tau) \equiv e(t) e(t-\tau) \quad (11)$$

that is

$$\phi_{pp}(u, \tau) = \int_0^{\infty} p(t, \tau) p(t+u, \tau) dt \quad (12)$$

$$\text{Var}[\phi_{ss}(\omega)] = \{E[\phi_{ss}(\omega)]\}^2 \quad (13)$$

$$+ \left| \frac{1}{2\pi} \int_0^{\infty} \int_0^{\infty} e(t)e(u)\psi_{nn}(t-u)e^{-j\omega(t+u)} dt du \right|^2$$

The study reported here is an extension of the approach described in reference (a) and concentrates on the energy density spectrum of random transient signals. In particular, it will be aimed at predicting the result of frequency filtering such waveforms and at the somewhat broader question of describing the distribution of energy over the spectral band of the signals. If one considers a narrow band filter, for example, and passes an ensemble member through it, the output energy observed is an indication of the "strength" of the signal in the particular frequency band passed by the filter. Upon repeating the experiment with other ensemble members, however, it will be found that in general this output energy will vary from sample to sample and is thus a random variable parameterized not only by the characteristics of the random transient ensemble, but also by the bandwidth and center frequency of the filter. It is of interest to know the expected value and variance of this output energy as an aid to measurement planning or performance prediction, and this is the task undertaken in the following pages. It will be seen that the resulting analysis bears a strong resemblance to that underlying traditional power spectrum measurement, which indeed can be viewed as a special case of the more general problem treated here. One of the goals of the present study is the development of a proper interpretation of the energy density spectrum of a transient signal and its relationship to physical measurements of the signal energy.

## Chapter II

## FREQUENCY FILTERING OF RANDOM TRANSIENT WAVEFORMS

To study the effects of frequency filtering on random transient signals, one need only make a fairly straightforward application of linear system theory. If the filter of interest is modeled as a linear system with impulse response  $h(t)$ , it is well known (reference (b), Chapter 13) that if  $s(t)$  is the input to the filter, then the output  $f(t)$  is given by

$$f(t) = \int_0^{\infty} s(x) h(t-x) dx \quad (14)$$

which is the convolution of the input signal and the impulse response of the filter. In terms of energy density spectra this becomes

$$\Phi_{ff}(\omega) = |H(\omega)|^2 \Phi_{ss}(\omega) \quad (15)$$

where  $\Phi_{ss}(\omega)$  and  $\Phi_{ff}(\omega)$  are the input and output spectra, respectively, and  $H(\omega)$  is the system function of the filter, given by the Fourier transform of  $h(t)$ :

$$H(\omega) = \int_{-\infty}^{\infty} h(t) e^{-j\omega t} dt \quad (16)$$

Since  $\Phi_{ss}(\omega)$  is a random variable, it should come as no surprise that for every value of  $\omega$ ,  $\Phi_{ff}(\omega)$  is a random variable also. From equation (15), however, it is immediately obvious that

$$\begin{aligned} E[\Phi_{ff}(\omega)] &= |H(\omega)|^2 E[\Phi_{ss}(\omega)] \\ &= |H(\omega)|^2 [\Psi_{nn}(\omega) \otimes \Phi_{ee}(\omega)] \end{aligned} \quad (17)$$

where  $E[\phi_{SS}(\omega)]$  is given by equations (8) or (9). Similarly,

$$\text{Var} [\phi_{ff}(\omega)] = |H(\omega)|^4 \text{Var}[\phi_{SS}(\omega)] \quad (18)$$

with  $\text{Var} [\phi_{SS}(\omega)]$  given by equation (13). Since the second term of equation (13) is always positive, it is apparent that

$$\text{Var} [\phi_{SS}(\omega)] > \{E[\phi_{SS}(\omega)]\}^2 \quad (19)$$

and in turn that

$$\text{Var} [\phi_{ff}(\omega)] > \{E[\phi_{ff}(\omega)]\}^2 \quad (20)$$

This is to say that the standard deviation of  $\phi_{ff}(\omega)$  will always be larger than the mean of  $\phi_{ff}(\omega)$ , regardless of  $H(\omega)$ , which implies that the distribution of  $\phi_{ff}(\omega)$  is rather broad for every  $\omega$ . In practical terms, this means that in calculating  $\phi_{ff}(\omega)$  for a number of sample functions and comparing the results for some given  $\omega$ , a large variability will be found. If one is seeking a statistic of the random transient ensemble that remains fairly constant from sample to sample, the value of  $\phi_{ff}(\omega)$  at a point clearly falls far short of the ideal. The situation here is rather similar to that faced in attempting a spectral analysis on the basis of the so-called "periodogram" (reference (c), pages 107-108) which can be shown to have little statistical reliability as an estimate of the deterministic spectrum of a stationary continuing stochastic process, unless a number are computed and ensemble averaged.

To gain a possibly more reliable statistic for the ensemble of random transients processed through the filter  $H(\omega)$ , we will consider integrating the output spectrum  $\phi_{ff}(\omega)$  over all  $\omega$  to obtain an expression for the total energy in  $f(t)$ . An important special case will be that in which  $|H(\omega)|$  is very narrow compared to the spectral width of  $s(t)$ , in which event the filter, with a tunable center frequency, provides in some sense an empirical measurement of  $\phi_{SS}(\omega)$ . It will be important to examine the statistical reliability of such measurements, i.e., the extent to which a single measurement accurately reflects the ensemble as a whole. This evidently has an important bearing on the validity of attempting to measure or predict the spectrum of a sample random transient to arbitrary precision.

A diagrammatic representation of the problem of interest is shown in Figure 2. Let  $F(H)$  represent the total energy of  $s(t)$  remaining after it is passed through the filter  $H(\omega)$ . In terms of  $f(t)$ , the output signal,

$$F(H) = \int_{-\infty}^{\infty} f^2(t) dt \quad (21)$$

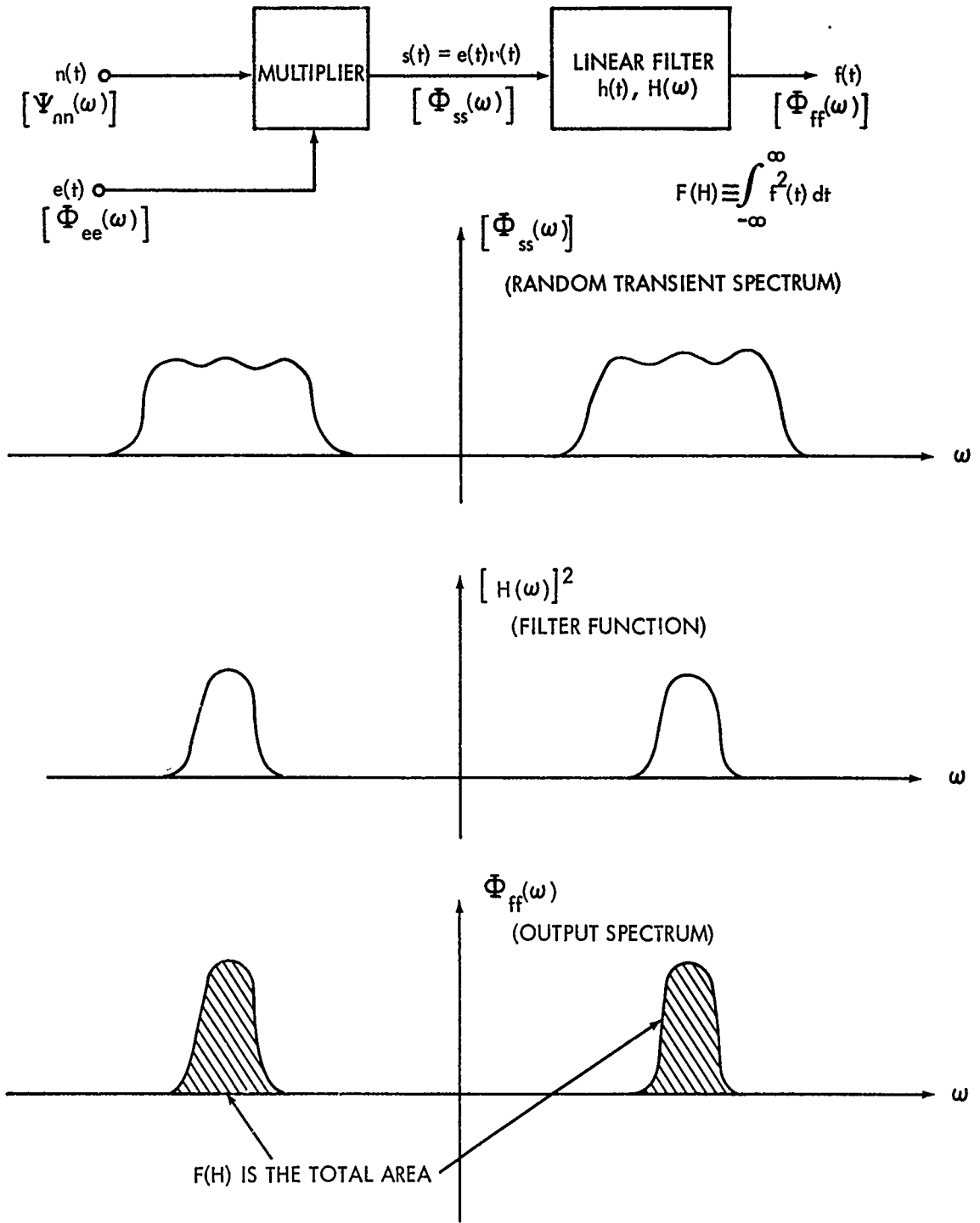


FIG. 2 LINEAR FILTERING OF RANDOM TRANSIENT WAVEFORMS.

and in terms of the various spectra,

$$F(H) = \int_{-\infty}^{\infty} \phi_{ff}(\omega) d\omega = \int_{-\infty}^{\infty} |H(\omega)|^2 \phi_{SS}(\omega) d\omega \quad (22)$$

$F(H)$  is a random variable whose mean is given by

$$\begin{aligned} E[F(H)] &= \int_{-\infty}^{\infty} |H(\omega)|^2 E[\phi_{SS}(\omega)] d\omega \\ &= \int_{-\infty}^{\infty} |H(\omega)|^2 [\psi_{nn}(\omega) \otimes \phi_{ee}(\omega)] d\omega \quad \text{by equation (9)} \end{aligned} \quad (23)$$

To find the variance of  $F(H)$ , we will use the relationship

$$\text{Var}[F(H)] = E[F^2(H)] - \{E[F(H)]\}^2 \quad (24)$$

$$\begin{aligned} F^2(H) &= \int_{-\infty}^{\infty} |H(\omega)|^2 \phi_{SS}(\omega) d\omega \int_{-\infty}^{\infty} |H(\omega')|^2 \phi_{SS}(\omega') d\omega' \\ &= \int_{-\infty}^{\infty} \int_{-\infty}^{\infty} |H(\omega)|^2 |H(\omega')|^2 \phi_{SS}(\omega) \phi_{SS}(\omega') d\omega d\omega' \end{aligned} \quad (25)$$

Taking the expected value yields

$$E[F^2(H)] = \int_{-\infty}^{\infty} \int_{-\infty}^{\infty} |H(\omega)|^2 |H(\omega')|^2 E[\phi_{SS}(\omega) \phi_{SS}(\omega')] d\omega d\omega' \quad (26)$$

Now using equations (23) and (24),

$$\begin{aligned} \text{Var}[F(H)] &= \int_{-\infty}^{\infty} \int_{-\infty}^{\infty} |H(\omega)|^2 |H(\omega')|^2 E[\phi_{SS}(\omega) \phi_{SS}(\omega')] d\omega d\omega' \\ &\quad - \int_{-\infty}^{\infty} |H(\omega)|^2 E[\phi_{SS}(\omega)] d\omega \int_{-\infty}^{\infty} |H(\omega')|^2 E[\phi_{SS}(\omega')] d\omega' \end{aligned} \quad (27)$$

A little manipulation then gives

$$\begin{aligned} \text{Var}[F(H)] = & \int_{-\infty}^{\infty} \int_{-\infty}^{\infty} |H(\omega)|^2 |H(\omega')|^2 \{E[\phi_{ss}(\omega)\phi_{ss}(\omega')] \\ & - E[\phi_{ss}(\omega)] E[\phi_{ss}(\omega')]\} d\omega d\omega' \end{aligned} \quad (28)$$

The quantity in the brackets can immediately be identified as the covariance of  $\phi_{ss}(\omega)$  and  $\phi_{ss}(\omega')$  since it can be easily shown that

$$\text{Cov}(x, y) = E(xy) - E(x)E(y) \quad (29)$$

(see reference (d), Ch. 8, Sec. 2). We may thus finally write that

$$\text{Var}[F(H)] = \int_{-\infty}^{\infty} \int_{-\infty}^{\infty} |H(\omega)|^2 |H(\omega')|^2 \text{Cov}[\phi_{ss}(\omega), \phi_{ss}(\omega')] d\omega d\omega'. \quad (30)$$

At this point, it is well to pause for an interpretation of the results attained thus far. In the situation considered here, sample members of an ensemble of random transients, generated according to the description in Chapter I, are passed through a linear system represented by  $H(\omega)$ . As noted above, each sample input waveform will have a different computed spectrum  $\phi_{ss}(\omega)$ , and hence each output waveform will have a correspondingly different spectrum  $\phi_{ff}(\omega)$ . The quantity of interest here is the total energy of the filter output, denoted  $F(H)$  and given by the integral of  $\phi_{ff}(\omega)$  over all  $\omega$ .  $F(H)$  is a random variable whose mean is given by equation (23). This is the result to be expected in averaging the total output energy over a large number of sample transients. Graphically,  $E[F(H)]$  can be visualized as the area under the curve formed by plotting  $E[\phi_{ss}(\omega)]$  over all frequencies and then weighing by the function  $|H(\omega)|^2$ . The square root of the variance of  $F(H)$ , namely the standard deviation  $\sigma_{F(H)}$ , is an indication of the spread of the probability distribution of the total output energy about its mean.  $\sigma_{F(H)}^2$  is given by equation (30) above and can be interpreted as the volume under a surface defined over the  $\omega - \omega'$  frequency plane. The height of this surface above the plane is given by the product of  $\text{Cov}[\phi_{ss}(\omega), \phi_{ss}(\omega')]$  and  $|H(\omega)|^2 |H(\omega')|^2$ . Alternatively, one can visualize a "spectral covariance surface" whose height above the  $\omega - \omega'$  plane is given by the function  $\text{Cov}[\phi_{ss}(\omega), \phi_{ss}(\omega')]$ . The variance integral can be considered to yield the volume under such a surface after each volume element has been weighted by  $|H(\omega)|^2 |H(\omega')|^2$ . The spectral covariance surface thus plays a central role in the study of the frequency filtering of an ensemble, particularly when  $|H(\omega)|$  is relatively constant, and its properties will be examined in the next chapter.

Chapter III

SPECTRAL COVARIANCE SURFACES FOR RANDOM TRANSIENT ENSEMBLES

In this chapter, we shall study the properties of the covariance of (or between) values of  $\phi_{SS}(\omega)$  for two arguments  $\omega$  and  $\omega'$ . From elementary statistics,

$$\text{Cov}[\phi_{SS}(\omega), \phi_{SS}(\omega')] = E[\phi_{SS}(\omega) \phi_{SS}(\omega')] - E[\phi_{SS}(\omega)] E[\phi_{SS}(\omega')] \quad (31)$$

If the Fourier Transform of  $s(t)$  is given by

$$S(\omega) = \frac{1}{2\pi} \int_0^{\infty} s(t) e^{-j\omega t} dt, \quad (32)$$

then

$$\phi_{SS}(\omega) = 2\pi S(\omega) \overline{S(\omega)} = 2\pi |S(\omega)|^2 \quad (33)$$

Recalling that  $s(t) = e(t)n(t)$ ,

$$\begin{aligned} \phi_{SS}(\omega) &= \frac{1}{2\pi} \int_0^{\infty} e(t)n(t) e^{-j\omega t} dt \int_0^{\infty} e(x)n(x) e^{j\omega x} dx \\ &= \frac{1}{2\pi} \int_0^{\infty} \int_0^{\infty} e(t)e(x)n(t)n(x) e^{-j\omega(t-x)} dt dx \end{aligned} \quad (34)$$

Changing one of the variables of integration to  $a = t-x$  yields

$$\phi_{SS}(\omega) = \frac{1}{2\pi} \int_{-\infty}^{\infty} \int_0^{\infty} e(t)e(t-a)n(t)n(t-a) e^{-j\omega a} dt da \quad (35)$$

In taking the expected value, we use the fact that  $n(t)$  is stationary such that

$$E[n(t)n(t-a)] = \psi_{nn}(a) \quad (36)$$

and that 
$$\int_0^{\infty} e(t)e(t-a)dt \equiv \phi_{ee}(a) \quad (37)$$

Thus, 
$$E[\phi_{SS}(\omega)] = \frac{1}{2\pi} \int_{-\infty}^{\infty} \int_0^{\infty} e(t)e(t-a)\psi_{nn}(a)e^{-j\omega a} dt da \quad (38)$$

$$= \frac{1}{2\pi} \int_{-\infty}^{\infty} \phi_{ee}(a)\psi_{nn}(a)e^{-j\omega a} da$$

which was previously given ex cathedra as equation (8).

Similarly, the product  $\phi_{SS}(\omega) \phi_{SS}(\omega')$  may be written as

$$\phi_{SS}(\omega) \phi_{SS}(\omega') = \frac{1}{4\pi^2} \int_0^{\infty} \int_0^{\infty} \int_0^{\infty} \int_0^{\infty} e(t)e(x)e(u)e(v)n(t)n(x)n(u)n(v)e^{-j\omega(t-x)}e^{-j\omega'(u-v)} dt dx du dv \quad (39)$$

If  $n(t)$  is a Gaussian random process, it may be shown (reference (e), page 93) that

$$E[n(t)n(x)n(u)n(v)] = \psi_{nn}(t-x)\psi_{nn}(u-v) + \psi_{nn}(t-u)\psi_{nn}(x-v) + \psi_{nn}(t-v)\psi_{nn}(x-u) \quad (40)$$

and therefore,

$$E[\phi_{SS}(\omega)\phi_{SS}(\omega')] = \frac{1}{4\pi^2} \int_0^{\infty} \int_0^{\infty} \int_0^{\infty} \int_0^{\infty} e(t)e(x)e(u)e(v)\psi_{nn}(t-x)\psi_{nn}(u-v)e^{-j\omega(t-x)}e^{-j\omega'(u-v)} dt dx du dv + \frac{1}{4\pi^2} \int_0^{\infty} \int_0^{\infty} \int_0^{\infty} \int_0^{\infty} e(t)e(x)e(u)e(v)\psi_{nn}(t-u)\psi_{nn}(x-v)e^{-j\omega(t-x)}e^{-j\omega'(u-v)} dt dx du dv + \frac{1}{4\pi^2} \int_0^{\infty} \int_0^{\infty} \int_0^{\infty} \int_0^{\infty} e(t)e(x)e(u)e(v)\psi_{nn}(t-v)\psi_{nn}(x-u)e^{-j\omega(t-x)}e^{-j\omega'(u-v)} dt dx du dv \quad (41)$$

which will be abbreviated as

$$E[\phi_{ss}(\omega) \phi_{ss}(\omega')] = I_1 + I_2 + I_3 \quad (42)$$

where  $I_1$ ,  $I_2$ , and  $I_3$  represent the three integrals of equation (41).

$I_1$  can immediately be written as

$$I_1 = \frac{1}{4\pi^2} \int_0^\infty \int_0^\infty e(t)e(x)\psi_{nn}(t-x)e^{-j\omega(t-x)} dt dx \int_0^\infty \int_0^\infty e(u)e(v)\psi_{nn}(u-v)e^{-j\omega'(u-v)} du dv \quad (43)$$

Considering the expected value of both sides of equation (34) shows that

$$I_1 = E[\phi_{ss}(\omega)] E[\phi_{ss}(\omega')] \quad (44)$$

Continuing

$$I_2 = \frac{1}{4\pi^2} \int_0^\infty \int_0^\infty e(t)e(u)\psi_{nn}(t-u)e^{-j(\omega t + \omega' u)} dt du \int_0^\infty \int_0^\infty e(x)e(v)\psi_{nn}(x-v)e^{j(\omega x + \omega' v)} dx dv \quad (45)$$

Noting that the two double integrals are complex conjugates of each other, one writes

$$I_2 = \left| \frac{1}{2\pi} \int_0^\infty \int_0^\infty e(t)e(u)\psi_{nn}(t-u)e^{-j(\omega t + \omega' u)} dt du \right|^2 \quad (46)$$

Now using the change of variables  $a = t-u$ ,

$$\begin{aligned} I_2 &= \left| \frac{1}{2\pi} \int_{-\infty}^\infty \int_0^\infty e(t)e(t-a)\psi_{nn}(a)e^{-j\omega t} e^{-j\omega'(t-a)} da dt \right|^2 \\ &= \left| \frac{1}{2\pi} \int_{-\infty}^\infty \psi_{nn}(a)e^{j\omega'a} \left\{ \int_0^\infty e(t)e(t-a)e^{-j(\omega+\omega')t} dt \right\} da \right|^2 \end{aligned} \quad (47)$$

A further simplification can be wrought by using the function defined in equation (11):

$$p(t, x) \equiv e(t)e(t-x)$$

This has a Fourier transform

$$P(\omega, x) = \frac{1}{2\pi} \int_0^{\infty} p(t, x) e^{-j\omega t} dt \quad (48)$$

$I_2$  may now be expressed as

$$I_2 = \left| \frac{1}{2\pi} \int_{-\infty}^{\infty} \psi_{nn}(x) P(\omega + \omega') e^{j\omega' x} dx \right|^2 \quad (49)$$

Similarly it may be shown that

$$I_3 = \left| \frac{1}{2\pi} \int_{-\infty}^{\infty} \psi_{nn}(x) P(\omega - \omega', x) e^{-j\omega' x} dx \right|^2 \quad (50)$$

Note that  $I_3$  is merely equal to  $I_2$  with  $\omega'$  replaced by  $(-\omega')$ . Finally, by equations (31) and (44),

$$\begin{aligned} \text{Cov}[\phi_{SS}(\omega), \phi_{SS}(\omega')] &= E[\phi_{SS}(\omega) \phi_{SS}(\omega')] - E[\phi_{SS}(\omega)] E[\phi_{SS}(\omega')] \\ &= I_1 + I_2 + I_3 - I_1 \\ &= I_2 + I_3 \end{aligned} \quad (51)$$

$$\text{Cov}[\phi_{SS}(\omega), \phi_{SS}(\omega')] =$$

$$\begin{aligned} &\left| \frac{1}{2\pi} \int_{-\infty}^{\infty} \psi_{nn}(x) P(\omega + \omega', x) e^{j\omega' x} dx \right|^2 \\ &+ \left| \frac{1}{2\pi} \int_{-\infty}^{\infty} \psi_{nn}(x) P(\omega - \omega', x) e^{-j\omega' x} dx \right|^2 \end{aligned} \quad (52)$$

where  $P(\omega, x)$  is given by equation (48).

Some fundamental properties of the spectral covariance function can be appreciated at once by considering the form of equation (52). First we note that due to the very definition of covariance, the function will not be changed in value if  $\omega$  and  $\omega'$  are interchanged. From equation (52), it is apparent that replacing  $\omega'$  by  $-\omega'$  will similarly have no effect on the value of the function. From these two facts, it becomes obvious that  $\omega$  and  $-\omega$  are also interchangeable, and thus that  $\text{Cov}[\phi_{SS}(\omega), \phi_{SS}(\omega')]$  is an even function of  $\omega$  and  $\omega'$  separately and also a symmetrical function of  $\omega$  and  $\omega'$ . Geometrically, this means that the covariance function, defined as a surface over the  $\omega - \omega'$  plane, must be symmetrical about the vertical planes defined by the equations  $\omega = \omega'$  and  $\omega = -\omega'$ , and preserve the same shape (except, of course, for a rotation) above all four quadrants of the  $\omega - \omega'$  plane.  $\text{Cov}[\phi_{SS}(\omega), \phi_{SS}(\omega')]$  can thus be said to

possess a cruciform symmetry about vertical planes inclined  $45^\circ$  with respect to those defined by the equations  $\omega' = 0$  and  $\omega = 0$ . This is shown in Figure 3. Evidently, it is necessary to study the function only in a single quadrant to visualize it everywhere. Another interesting property of  $\text{Cov} [\phi_{SS}(\omega), \phi_{SS}(\omega')]$  that emerges directly from equation (52) is that it is always positive. This was by no means obvious at the outset, since two random variables may in general exhibit negative covariance even if it can be shown that they are separately always positive (as  $\phi_{SS}(\omega)$  and  $\phi_{SS}(\omega')$  are here). Values of a sample spectrum for two different arguments are therefore always positively correlated. It is not really clear at this point what deeper significance this may hold.

To continue this investigation of the form of the spectral covariance surface, it is necessary to turn to specific expressions for the envelope function. Accordingly, the two forms treated in reference (a) will be considered: a rectangular pulse of duration  $T$  seconds, and a decaying exponential pulse having a time constant of  $T$  seconds.

For the first of these, shown in Figure 4,

$$\begin{aligned} e(t) &= 1, & 0 \leq t \leq T \\ &= 0, & \text{elsewhere} \end{aligned} \tag{53}$$

From equation (11), for  $0 \leq x \leq T$ ,

$$\begin{aligned} p(t, x) &= 1, & x \leq t \leq T \\ &= 0, & \text{elsewhere} \end{aligned} \tag{54}$$

and for  $-T \leq x \leq 0$

$$\begin{aligned} p(t, x) &= 1, & 0 \leq t \leq T + x \\ &= 0, & \text{elsewhere} \end{aligned} \tag{55}$$

Evidently for  $|x| > T$ ,  $p(t, x) = 0$  everywhere. The function  $p(t, x)$  is plotted in Figure 4 as a function of  $t$  with  $x$  treated as a parameter. Now taking the Fourier transform with respect to  $t$  as in equation (48) yields

$$P_R(\omega, x) = \frac{T - |x|}{2\pi} \frac{\sin \omega \left( \frac{T - |x|}{2} \right)}{\omega \left( \frac{T - |x|}{2} \right)} e^{-j\omega \left( \frac{T+x}{2} \right)} \tag{56}$$

for  $-T \leq x \leq T$  and  $-\infty < \omega < \infty$ .

where the subscript R on  $P_R(\omega, x)$  denotes the rectangular pulse case.

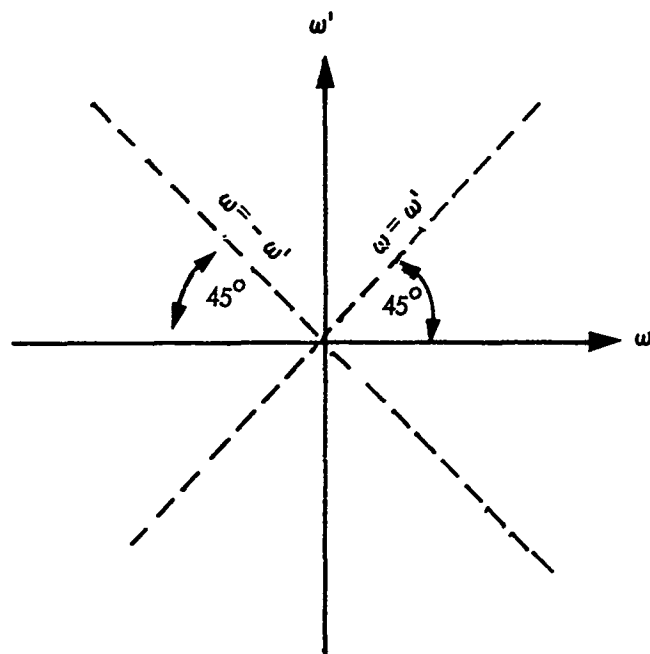


FIG.3a THE  $\omega$ - $\omega'$  PLANE SHOWING THE SYMMETRY AXES.

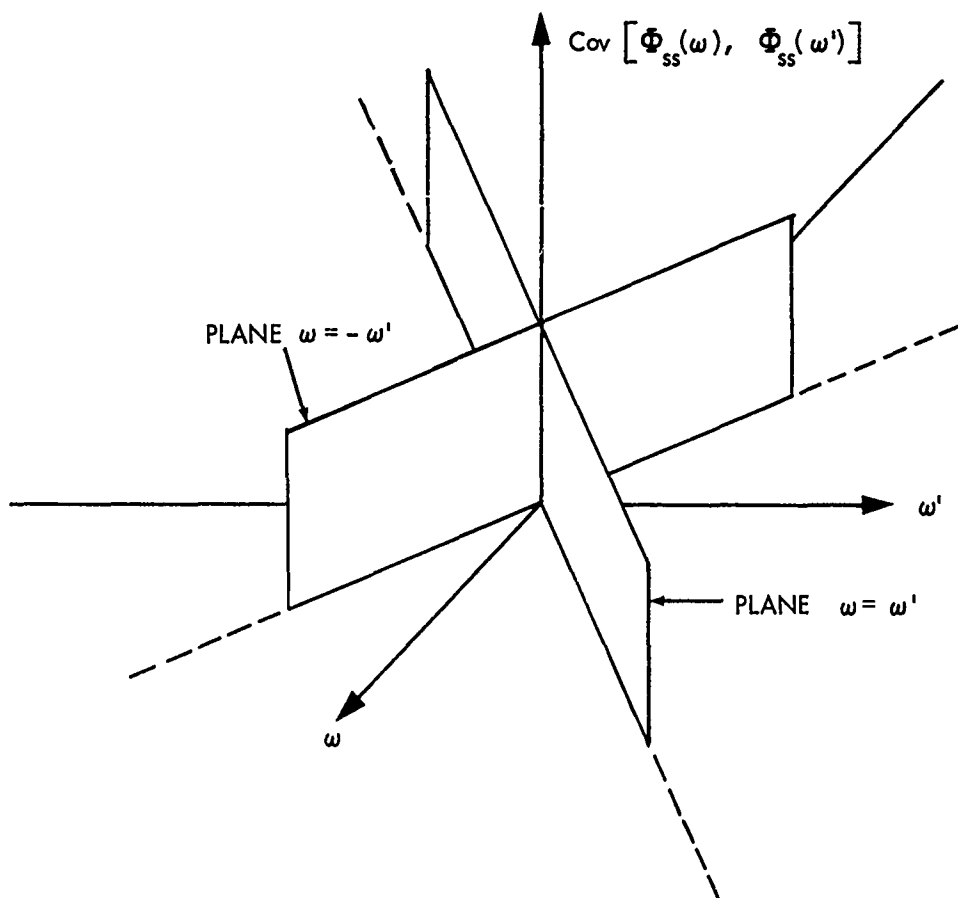


FIG.3b 3-DIMENSIONAL REPRESENTATION OF THE SPECTRAL COVARIANCE SYMMETRY PLANES.

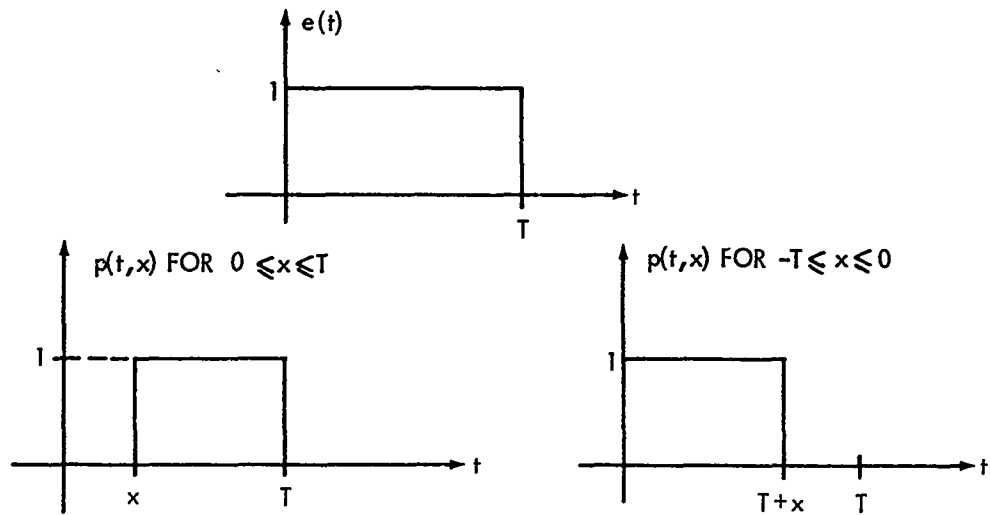


FIG.4 RECTANGULAR ENVELOPE FUNCTION AND ASSOCIATED  $p(t,x)$ .

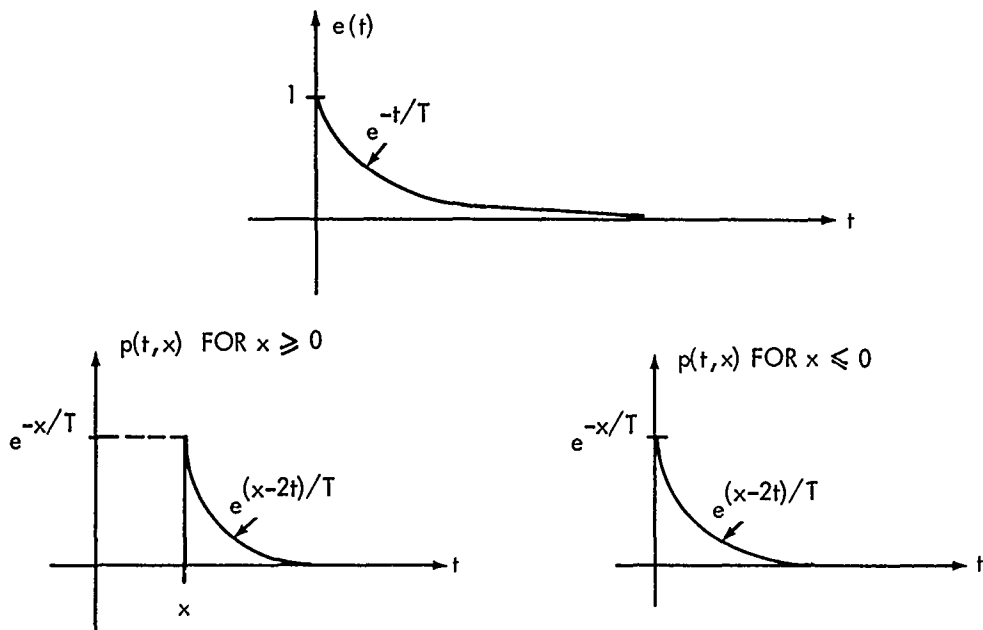


FIG.5 EXPONENTIAL ENVELOPE FUNCTION AND ASSOCIATED  $p(t,x)$ .

When  $|x| > T$ ,  $P_R(\omega, x) = 0$  for all  $\omega$ .

For the exponential envelope case, shown in Figure 5,

$$\begin{aligned} e(t) &= e^{-t/T}, \quad t \geq 0 \\ &= 0, \quad t < 0 \end{aligned} \tag{57}$$

Accordingly, for  $x \geq 0$ ,

$$\begin{aligned} p(t, x) &= e^{x/T} e^{-2t/T}, \quad t \geq x \\ &= 0, \quad t < x \end{aligned} \tag{58}$$

and for  $x < 0$ ,

$$\begin{aligned} p(t, x) &= e^{x/T} e^{-2t/T}, \quad t \geq 0 \\ &= 0, \quad t < 0 \end{aligned} \tag{59}$$

From equation (48), with  $P_E(\omega, x)$  denoting the Fourier transform appropriate to the decaying exponential case,

$$P_E(\omega, x) = \frac{1}{2\pi} \frac{e^{-x/T}}{\frac{2}{T} + j\omega} e^{-j\omega x}, \quad -\infty < \omega < \infty \tag{60}$$

for  $x \geq 0$

$$P_E(\omega, x) = \frac{1}{2\pi} \frac{e^{x/T}}{\frac{2}{T} + j\omega}, \quad -\infty < \omega < \infty \tag{61}$$

for  $x < 0$

Having derived expressions for  $P(\omega, x)$  in the two envelope cases of interest, it is now possible to continue the development by substituting these into equations (49) and (50) for  $I_2(\omega, \omega')$  and  $I_3(\omega, \omega')$ . Again using the subscript R to denote the rectangular envelope case,

$$\begin{aligned} I_{2R}(\omega, \omega') &= \left| \int_{-T}^T \psi_{nn}(x) \frac{T-|x|}{2\pi} \frac{\sin(\omega+\omega')\left(\frac{T-|x|}{2}\right)}{(\omega+\omega')\left(\frac{T-|x|}{2}\right)} e^{-j(\omega+\omega')\left(\frac{T+x}{2}\right)} e^{j\omega'x} dx \right|^2 \\ &= \left| e^{-j(\omega+\omega')\frac{T}{2}} \int_{-T}^T \psi_{nn}(x) \frac{T-|x|}{2\pi} \frac{\sin(\omega+\omega')\left(\frac{T-|x|}{2}\right)}{(\omega+\omega')\left(\frac{T-|x|}{2}\right)} e^{-j(\omega-\omega')\frac{x}{2}} dx \right|^2 \end{aligned} \tag{62}$$

Noting that the integrand, except for the exponential, is an even function of  $x$ , and using the Euler relations, one writes

$$I_{2R}(\omega, \omega') = \frac{1}{\pi^2} \left| e^{-j(\omega+\omega')\frac{T}{2}} \int_0^T \psi_{nn}(x) (T-x) \frac{\sin(\omega+\omega') \left(\frac{T-x}{2}\right)}{(\omega+\omega') \left(\frac{T-x}{2}\right)} \cos(\omega-\omega')\frac{x}{2} dx \right|^2 \quad (63)$$

The magnitude of  $e^{-j(\omega+\omega')\frac{T}{2}}$  is unity, and the integral is real, so

$$I_{2R}(\omega, \omega') = \frac{1}{\pi^2} \left[ \int_0^T \psi_{nn}(x) (T-x) \frac{\sin(\omega+\omega') \left(\frac{T-x}{2}\right)}{(\omega+\omega') \left(\frac{T-x}{2}\right)} \cos(\omega-\omega')\frac{x}{2} dx \right]^2 \quad (64)$$

Recalling that  $I_3(\omega, \omega') = I_2(\omega, -\omega')$ , we have

$$I_{3R}(\omega, \omega') = \frac{1}{\pi^2} \left[ \int_0^T \psi_{nn}(x) (T-x) \frac{\sin(\omega-\omega') \left(\frac{T-x}{2}\right)}{(\omega-\omega') \left(\frac{T-x}{2}\right)} \cos(\omega+\omega')\frac{x}{2} dx \right]^2 \quad (65)$$

The sum of equations (64) and (65) gives the covariance function for the rectangular envelope case when  $\psi_{nn}(x)$  is the autocorrelation function associated with the input noise process.

For the exponential envelope case, the same procedures yield the following results:

$$I_{2E}(\omega, \omega') = \frac{1}{4\pi^2} \frac{1}{\left(\frac{2}{T}\right)^2 + (\omega+\omega')^2} \left| \int_0^\infty \psi_{nn}(x) e^{-x/T} [e^{-j\omega'x} + e^{-j\omega x}] dx \right|^2 \quad (66a)$$

$$I_{3E}(\omega, \omega') = \frac{1}{4\pi^2} \frac{1}{\left(\frac{2}{T}\right)^2 + (\omega-\omega')^2} \left| \int_0^\infty \psi_{nn}(x) e^{-x/T} [e^{j\omega'x} + e^{-j\omega x}] dx \right|^2 \quad (66b)$$

or defining

$$I_a \equiv \int_0^\infty \psi_{nn}(x) e^{-x/T} [\cos \omega'x + \cos \omega x] dx \quad (67a)$$

$$I_b \equiv \int_0^{\infty} \psi_{nn}(x) e^{-x/T} [\sin \omega'x + \sin \omega x] dx \quad (67b)$$

$$I_c \equiv \int_0^{\infty} \psi_{nn}(x) e^{-x/T} [\sin \omega'x - \sin \omega x] dx \quad (67c)$$

$$\begin{aligned} \text{Cov}_E[\phi_{SS}(\omega), \phi_{SS}(\omega')] &= \frac{1}{4\pi^2} \frac{1}{\left(\frac{2}{T}\right)^2 + (\omega + \omega')^2} [I_a^2 + I_b^2] \\ &+ \frac{1}{4\pi^2} \frac{1}{\left(\frac{2}{T}\right)^2 + (\omega - \omega')^2} [I_a^2 + I_c^2] \end{aligned} \quad (68)$$

Further progress toward a description of the spectral covariance surfaces unfortunately requires the use of specific expressions for the input noise autocorrelation functions. This, to be sure, destroys the generality of the results (which to some extent has been sacrificed already by using specific envelope functions), but by carefully choosing the noise spectra of interest, one can arrive at fairly general conclusions about the form of the covariance surface for an arbitrary noise type. In reference (a), two examples of idealized noise spectra were treated, and the same will be used here. These are the rectangular broad band spectrum, based on zero frequency, and a rectangular narrow band spectrum centered at some  $\omega_0$ . The two spectra are portrayed in Figure 6.

The first can be described mathematically as

$$\begin{aligned} \psi_{nn}(\omega) &= N_0, \quad -\omega_2 \leq \omega \leq \omega_2 \\ &= 0, \quad \text{elsewhere} \end{aligned} \quad (69)$$

The corresponding autocorrelation function is

$$\psi_{nn}(\tau) = 2N_0\omega_2 \frac{\sin \omega_2 \tau}{\omega_2 \tau}, \quad -\infty < \tau < \infty \quad (70)$$

The second spectrum is given by

$$\begin{aligned} \psi_{nn}(\omega) &= N_0, \quad \omega_1 \leq |\omega| \leq \omega_2 \\ &= 0, \quad \text{elsewhere} \end{aligned} \quad (71)$$

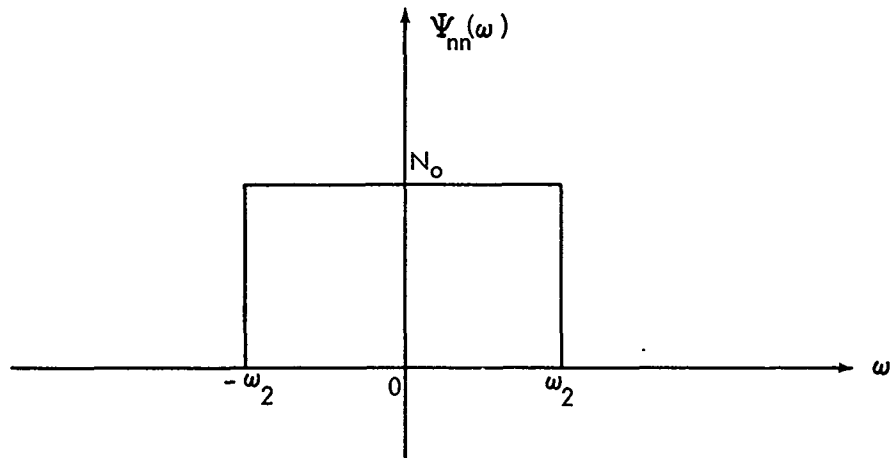


FIG.6a. RECTANGULAR LOW-PASS BROAD BAND SPECTRUM.

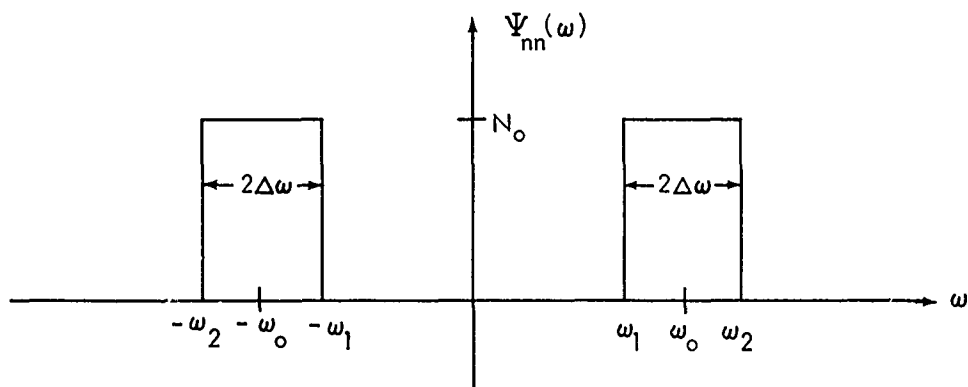


FIG.6b. RECTANGULAR NARROW BAND SPECTRUM.

$$\psi_{nn}(\tau) = 4\Delta\omega N_0 \frac{\sin(\Delta\omega)\tau}{(\Delta\omega)\tau} \cos \omega_0\tau, \quad -\infty < \tau < \infty \quad (72)$$

where

$$\Delta\omega \equiv \frac{\omega_2 - \omega_1}{2}, \quad \text{the half bandwidth} \quad (73a)$$

$$\omega_0 \equiv \frac{\omega_1 + \omega_2}{2}, \quad \text{the center frequency} \quad (73b)$$

These expressions have been used in equations (64), (65), (67), and (68) to derive integral representations for the spectral covariance surfaces of both rectangular and decaying exponential bursts of both broad and narrow band noise. These expressions have in turn been evaluated on the IBM-7090 computer at NOL to gain an understanding of the form of the surface. Indeed, much of the manipulation leading up to the final expressions for  $\text{Cov}[\phi_{SS}(\omega), \phi_{SS}(\omega')]$  was specifically intended to reduce the problem to one of evaluating Gaussian quadratures - a task amenable to a computer algorithm. We will now consider several of the cases in detail.

A. Rectangular Pulse of Low-Pass Broad Band Noise

For the rectangular function described in equation (53) it is easily shown that

$$\begin{aligned} \phi_{ee}(\tau) &= T - |\tau|, \quad -T \leq \tau \leq T \\ &= 0, \quad \text{elsewhere} \end{aligned} \quad (74)$$

Thus, from equation (38),

$$\begin{aligned} E[\phi_{SS}(\omega)] &= \frac{1}{2\pi} \int_{-\infty}^{\infty} \phi_{ee}(x) \psi_{nn}(x) e^{-j\omega x} dx \\ &= \frac{1}{\pi} \int_0^T (T-x) \psi_{nn}(x) \cos \omega x dx \end{aligned} \quad (75)$$

and from equations (64) and (65),

$$\text{Cov}[\phi_{SS}(\omega), \phi_{SS}(\omega')] =$$

$$\begin{aligned} &\frac{1}{\pi^2} \left[ \int_0^T \psi_{nn}(x)(T-x) \frac{\sin(\omega+\omega') \left(\frac{T-x}{2}\right)}{(\omega+\omega') \left(\frac{T-x}{2}\right)} \cos(\omega - \omega') \frac{x}{2} dx \right]^2 \\ &+ \frac{1}{\pi^2} \left[ \int_0^T \psi_{nn}(x)(T-x) \frac{\sin(\omega-\omega') \left(\frac{T-x}{2}\right)}{(\omega-\omega') \left(\frac{T-x}{2}\right)} \cos(\omega-\omega') \frac{x}{2} dx \right]^2 \end{aligned} \quad (76)$$

It is also convenient to recall that

$$\text{Var}[\phi_{SS}(\omega)] = \text{Cov}[\phi_{SS}(\omega), \phi_{SS}(\omega)] \quad (77)$$

or from equation (76) with  $\omega = \omega'$ ,

$$\begin{aligned} \text{Var}[\phi_{SS}(\omega)] &= \frac{1}{\pi^2} \left[ \int_0^T \psi_{nn}(x)(T-x) \frac{\sin \omega(T-x)}{\omega(T-x)} dx \right]^2 \\ &+ \frac{1}{\pi^2} \left[ \int_0^T \psi_{nn}(x)(T-x) \cos \omega x dx \right]^2 \\ &= I_{2R}(\omega, \omega) + \{E[\phi_{SS}(\omega)]\}^2 \end{aligned} \quad (78)$$

where in the last expression we have used equations (64) and (75).

To obtain the final expressions, we substitute  $\psi_{nn}(x)$  from equation (70) above into equations (75), (76), and (78),

$$E[\phi_{SS}(\omega)] = \frac{2N_o \omega_2 T}{\pi} \int_0^T \left(1 - \frac{x}{T}\right) \frac{\sin \omega_2 x}{\omega_2 x} \cos \omega x dx \quad (79)$$

$$\text{Cov}[\phi_{SS}(\omega), \phi_{SS}(\omega')] = \frac{4N_o^2 \omega_2^2 T^2}{\pi^2} X$$

$$\left\{ \begin{aligned} &\left[ \int_0^T \left(1 - \frac{x}{T}\right) \frac{\sin \omega_2 x}{\omega_2 x} \frac{\sin(\omega - \omega')\left(\frac{T-x}{2}\right)}{(\omega - \omega')\left(\frac{T-x}{2}\right)} \cos(\omega + \omega')\left(\frac{x}{2}\right) dx \right]^2 \\ &+ \left[ \int_0^T \left(1 - \frac{x}{T}\right) \frac{\sin \omega_2 x}{\omega_2 x} \frac{\sin(\omega + \omega')\left(\frac{T-x}{2}\right)}{(\omega + \omega')\left(\frac{T-x}{2}\right)} \cos(\omega - \omega')\left(\frac{x}{2}\right) dx \right]^2 \end{aligned} \right\} \quad (80)$$

$$\text{Var}[\phi_{SS}(\omega)] = \{E[\phi_{SS}(\omega)]\}^2 + \frac{4N_o^2 \omega_2^2 T^2}{\pi^2} \left[ \int_0^T (1-\frac{x}{T}) \frac{\sin \omega_2 x}{\omega_2 x} \frac{\sin \omega(T-x)}{\omega(T-x)} dx \right]^2 \quad (81)$$

For greater generality of presentation, these expressions will be normalized and parameterized by defining the following quantities, as in reference (a):

$$q \equiv \frac{\omega_2 T}{2\pi}, \text{ the number of periods of the highest noise frequency contained in a pulse length.} \quad (82a)$$

$$r \equiv \frac{\omega}{\omega_2}, \omega \text{ expressed as a fraction of } \omega_2. \quad (82b)$$

$$s \equiv \frac{\omega'}{\omega_2}, \omega' \text{ expressed as a fraction of } \omega_2. \quad (82c)$$

The generalized expressions then become

$$E_N[\phi_{SS}(r)] = 2q \int_0^1 (1-x) \frac{\sin 2\pi qx}{2\pi qx} \cos 2\pi qxr \, dx \quad (83)$$

$$\text{Cov}_N[\phi_{SS}(r), \phi_{SS}(s)] =$$

$$4q^2 \left\{ \left[ \int_0^1 (1-x) \frac{\sin 2\pi qx}{2\pi qx} \frac{\sin \pi q(1-x)(r+s)}{\pi q(1-x)(r+s)} \cos \pi qx(r-s) \, dx \right]^2 + \left[ \int_0^1 (1-x) \frac{\sin 2\pi qx}{2\pi qx} \frac{\sin \pi q(1-x)(r-s)}{\pi q(1-x)(r-s)} \cos \pi qx(r+s) \, dx \right]^2 \right\} \quad (84)$$

$$\text{Var}_N[\phi_{SS}(r)] = \{E_N[\phi_{SS}(r)]\}^2 + 4q^2 \left[ \int_0^1 (1-x) \frac{\sin 2\pi qx}{2\pi qx} \frac{\sin 2\pi qr(1-x)}{2\pi qr(1-x)} \, dx \right]^2 \quad (85)$$

The normalization included in the above three equations is described in Appendix A and has been chosen such that

$$\int_{-\infty}^{\infty} E_N[\phi_{SS}(r)] dr = 1 \quad (86)$$

The relationship between the normalized and unnormalized versions is given by the following:

$$E[\phi_{SS}(\omega)] = 2N_0 T E_N[\phi_{SS}(r = \frac{\omega}{\omega_2})] \quad (87a)$$

$$\text{Cov}[\phi_{SS}(\omega), \phi_{SS}(\omega')] = 4N_0^2 T^2 \text{Cov}_N[\phi_{SS}(r = \frac{\omega}{\omega_2}), \phi_{SS}(s = \frac{\omega'}{\omega_2})] \quad (87b)$$

with a corresponding expression for the spectral variance.

A Fortran IV computer program was written to calculate and plot the normalized results derived above. Because of the symmetry properties of  $\text{Cov}_N[\phi_{SS}(r), \phi_{SS}(s)]$ , it is necessary to study the behavior of the function only over the upper right-hand quadrant of the r-s plane. Similarly, since  $E_N[\phi_{SS}(r)]$  is an even function of r, it is presented only for r positive. The reader will recall that this data applies to the case where an input noise process with a rectangular low pass spectrum, as in Figure 6a, is gated by a rectangular pulse of duration T, as in Figure 4. The most important parameter of the situation is q, defined to equal the number of periods of the highest noise frequency contained in the pulse duration T - the higher q becomes, the longer becomes the "piece" of the input process gated by the pulse. The results are plotted against frequency variables expressed as a percentage of the highest noise frequency  $\omega_2$ . Hopefully, this approach will divorce the data from particular parameter values.

Figure 7 shows a plot of  $E_N[\phi_{SS}(r)]$  for this case with  $q = 10.0$ . Because q is appreciably larger than unity, reciprocal spreading arguments show that the energy density spectrum of e(t) is considerably narrower than the power spectrum of n(t). Thus, the convolution implied in the calculation of  $E_N[\phi_{SS}(r)]$  yields a spectrum of approximately the same shape and width as that of n(t). (The width of  $E[\phi_{SS}(\omega)]$  is therefore approximately  $\omega_2$ , and that of  $E_N[\phi_{SS}(r)]$  about  $\omega_2 / \omega_2 = 1$  in units of the variable r.) The normalized expected spectrum is seen to be roughly rectangular with amplitude approximately 1/2 and half-width unity. This checks the normalization which was intended to set the area under the curve equal to unity. The "tail" of the spectrum, extending beyond  $r = 1.0$ , is the most obvious effect of the gating process on the input spectrum.

Figure 8 shows a plot of the standard deviation of  $\phi_{SS}(r)$  as a fraction of the mean of  $\phi_{SS}(r)$ , i.e.,

$$\sigma_N(r) = \frac{\sqrt{\text{Var}_N[\phi_{SS}(r)]}}{E_N[\phi_{SS}(r)]} \quad (88)$$

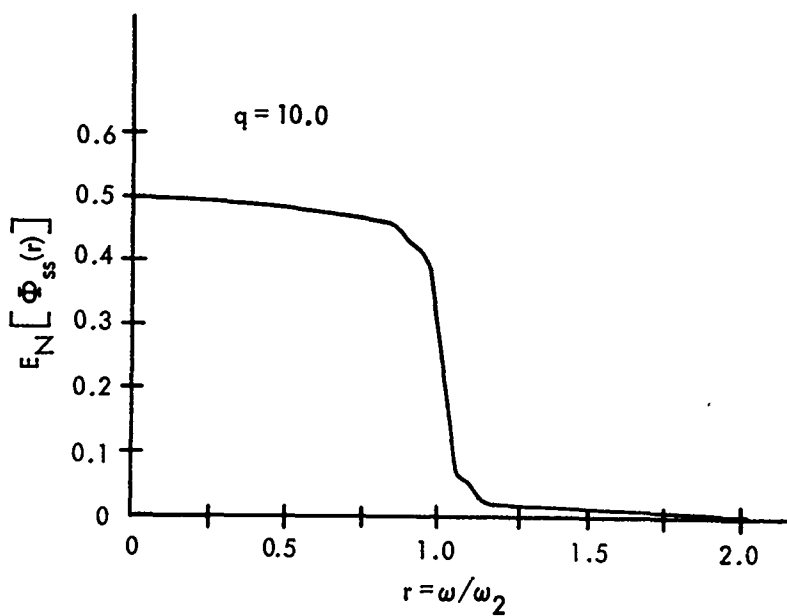


FIG.7 SPECTRAL EXPECTED VALUE FOR A RECTANGULAR BURST OF LOW-PASS BROAD BAND NOISE WITH  $q = 10.0$ .

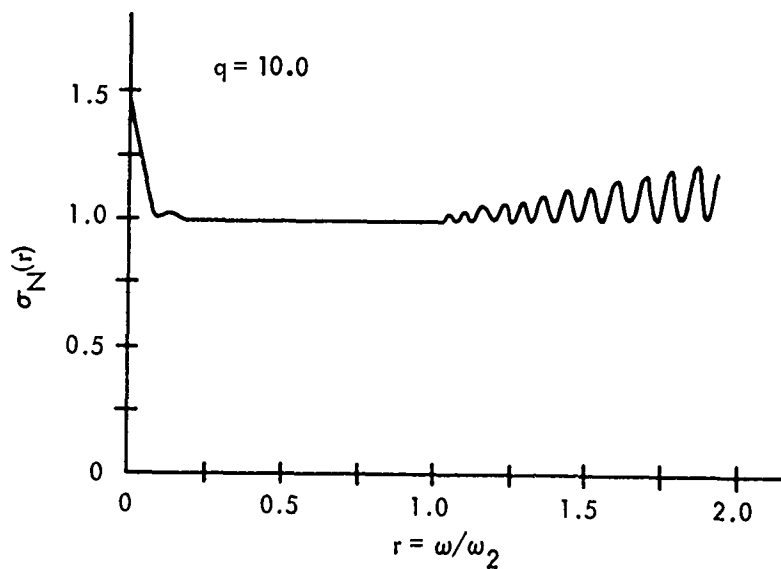


FIG.8 NORMALIZED SPECTRAL STANDARD DEVIATION FOR A RECTANGULAR BURST OF LOW-PASS BROAD BAND NOISE WITH  $q = 10.0$ .

As noted above, this ratio must always be greater than unity, and near the origin achieves its maximum value of  $\sqrt{2}$ . This is because it can be shown from equation (75) and the first form in equation (78) with  $\omega = 0$  that

$$\text{Var}_N[\phi_{ss}(0)] = 2\{E_N[\phi_{ss}(0)]\}^2 \quad (89)$$

The fact that for large values of  $r$ ,  $\sigma_N(r) \approx 1$  implies that

$$\text{Var}_N[\phi_{ss}(r)] \approx \{E_N[\phi_{ss}(r)]\}^2 \text{ for } r \gg 0 \quad (90)$$

or alternatively, that  $I_{2R}(\omega, \omega)$  of equation (78) makes negligible contribution to the variance for  $\omega \gg 0$ .

A three-dimensional rendering of the normalized spectral covariance surface for the upper right-hand quadrant of the  $r$ - $s$  plane is shown in Figure 9. It is seen that the surface has the form of a sharp, narrow ridge symmetrical about the plane  $r = s$ , running from the origin to the point  $r = s = 1$  and then tapering off. From equation (77), we know that the height of the surface above the line  $r = s$  is a measure of  $\text{Var}_N[\phi_{ss}(r)]$ . Accordingly, the height of the surface at the origin is roughly twice that found elsewhere along the line  $r = s$ , in agreement with equations (89) and (90).

As an aid to relating the height and length of the covariance ridge to the parameters of the random transient, let us examine the  $r$ - $s$  plane itself as shown in Figure 10. As noted several times before, the covariance surface is symmetrical about the plane defined by the relationship  $r = s$ . Consider any line in the  $r$ - $s$  plane parallel to that representing  $r = s$ . The equation of such a line is

$$s = a + r$$

OR

$$s - r = a \quad (91)$$

where  $a$  is the intercept on the  $s$  axis. Evidently, along such paths,  $s$  and  $r$  have a constant difference equal to  $a$ . In the present case, such lines represent the loci of points for which the arguments of the covariance function have a given (normalized) difference equal to  $a$ . Similarly, lines lying perpendicular to the symmetry axis have equations of the form

$$s + r = b \quad (92)$$

and on such loci, the sum of  $r$  and  $s$  is a constant. In particular, since  $(s + r)/2$  is the arithmetic average of the two normalized frequency arguments, such a line represents the loci of points for which the center frequency of the two is constant and equal to  $b/2$ . Furthermore, it can be shown that a translation of magnitude  $d$  parallel to the direction of the line  $r = s$  produces a change in the center frequency equal to  $d/\sqrt{2}$  while leaving the center frequency unchanged.

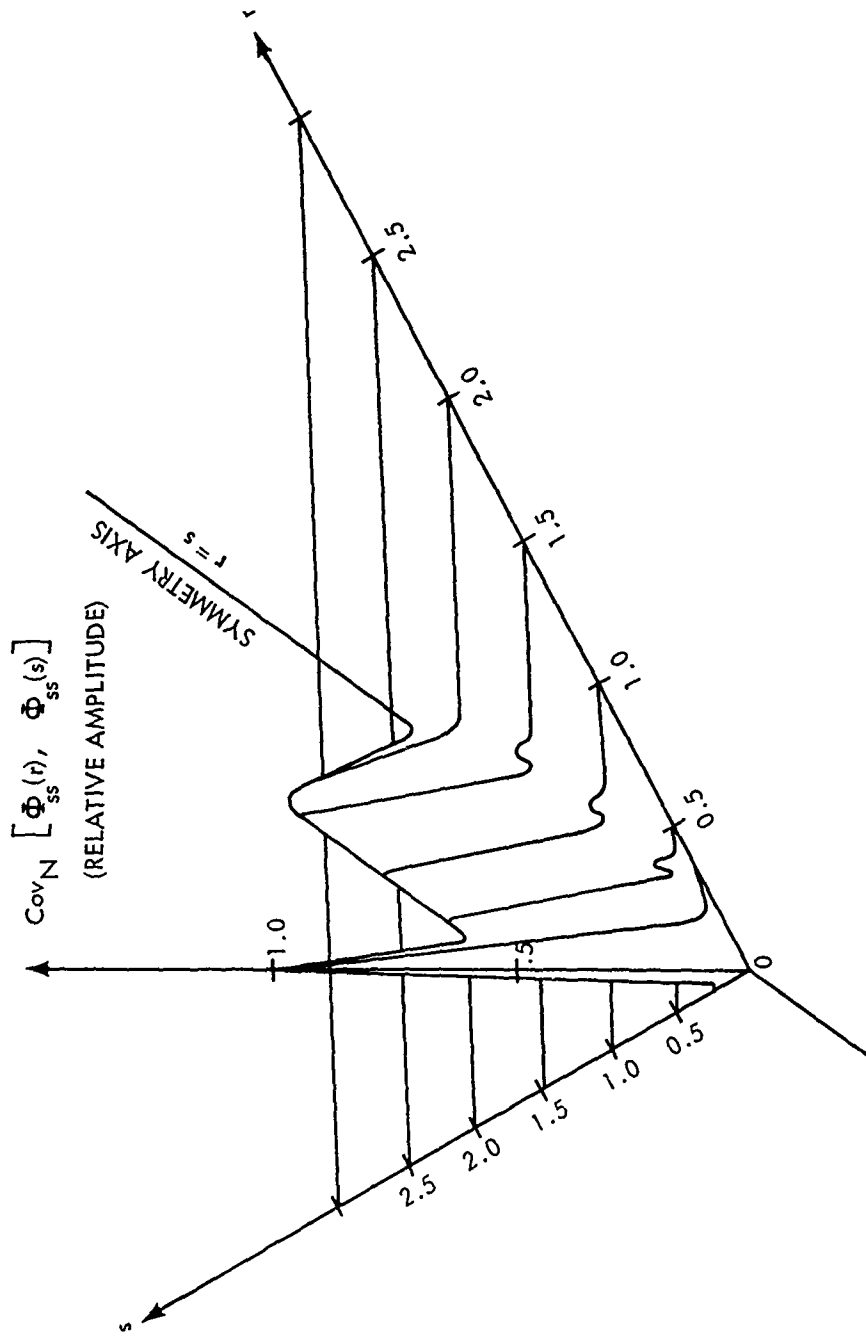


FIG.9 NORMALIZED SPECTRAL COVARIANCE SURFACE FOR A RECTANGULAR PULSE OF LOW-PASS BROAD BAND NOISE WITH  $q \approx 10.0$ .

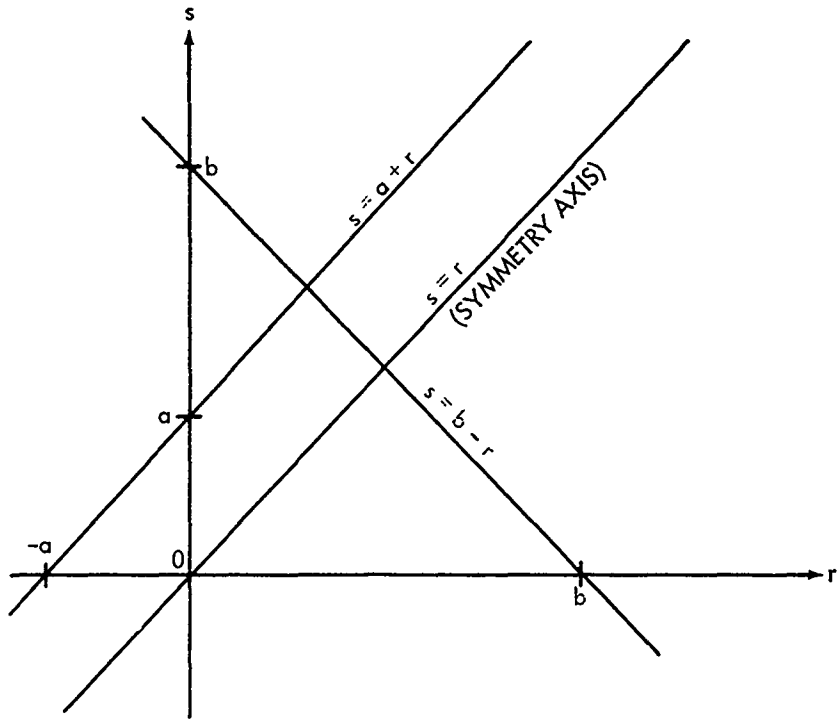


FIG. 10 IMPORTANT LINES IN THE  $r - s$  PLANE.

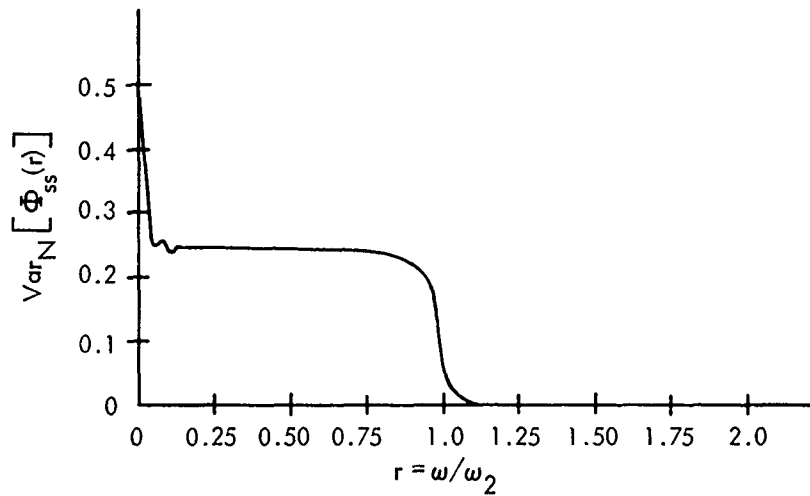


FIG. 11 NORMALIZED SPECTRAL VARIANCE FOR A RECTANGULAR PULSE OF LOW-PASS BROAD BAND NOISE WITH  $q = 10.0$ .

Returning now to the case portrayed in Figure 9, Figure 11 shows essentially a section through the covariance surface along the plane of symmetry  $r = s$ . This can be interpreted as a graph of  $\text{Var}_N[\phi_{ss}(r)]$  plotted along an axis scaled by a factor of  $\sqrt{2}$ . Along the line  $r = s$ , the covariance arguments have zero difference, and the covariance reduces immediately to the variance. From another point of view, one obtains a section through the plane of symmetry by graphing the variance as a function of  $r$ , and then "stretching" the graph along the  $r$  axis by a factor of  $\sqrt{2}$ . In Figure 12 are shown two plots of  $\text{Cov}_N[\phi_{ss}(r), \phi_{ss}(s)]$  where a constant center frequency has been chosen as a parameter and the covariance plotted as a function of the difference between the two arguments. In other words, we portray  $\text{Cov}_N(r, s)$  where

$$r = c + d/2 \quad (93a)$$

and

$$s = c - d/2 \quad (93b)$$

This is an even function of  $d$ , so only half of each plot has been presented. From the discussion immediately above, it becomes obvious that such graphs represent cross-sections of the covariance surface perpendicular to the plane of symmetry and intersecting the latter above the point  $r = s = c$ . The normalized frequency difference  $d$  represents a translation perpendicular to the plane of symmetry of length  $d/\sqrt{2}$ . The family of graphs thus represents a series of cross-sections of the surface, taken perpendicular to the axis of the "ridge".

In Figures 13 through 17, a similar series of graphs are shown for the case of a rectangular pulse of low-pass broad band noise with  $q = 1.0$ . It is seen that the covariance surface now appears as a relatively smoothly sloping "pile" which decreases gradually in all directions with distance from the origin. Recalling the definition of the parameter  $q$ , the difference between the two random transient examples treated thus far is that in the former case, where  $q = 10.0$ , a relatively large number of cycles of the highest frequency present in  $n(t)$  are found in pulse length  $T$ , whereas for  $q = 1.0$ , only a single cycle is possible. The  $q = 10.0$  case essentially presents a longer "piece" of the noise process  $n(t)$ .

Some general characteristics of the spectra of rectangular noise pulses can be immediately discerned by studying Figures 7 through 17. It turns out that an interesting parameter of the random transient spectrum is its effective width, essentially defined as that positive frequency spread for which  $E[\phi_{ss}(\omega)]$  is significantly different from zero. It will be recalled that this expected value can be expressed as the convolution of the energy density spectrum of the envelope function and the power density spectrum of the underlying noise process. Roughly speaking, the width of the convolution of two even functions is equal to the sum of the widths of the functions themselves. The justification of this approximation is discussed in Appendix B. If one spectrum is significantly wider than the other, the width of the convolution of the two will essentially be that of the former. In the present case, the positive frequency width of the (double-sided) noise process spectrum is simply  $\omega_2$  (or 1 in terms of the normalized frequency variables). The energy density spectrum of a rectangular pulse of length  $T$  and unit amplitude is given by

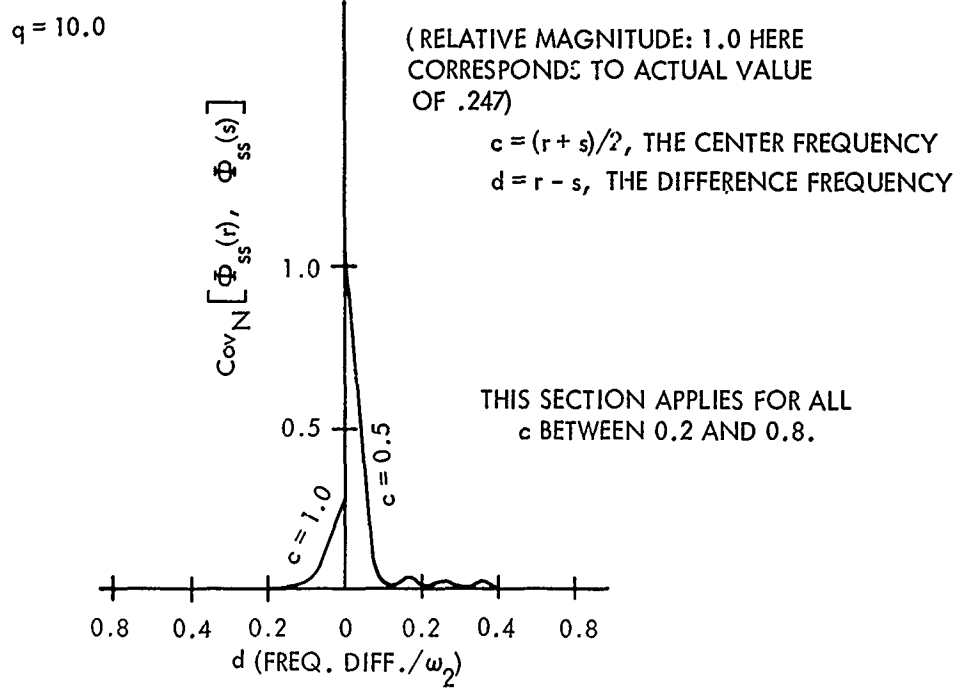


FIG. 12 SECTIONS THROUGH THE SPECTRAL COVARIANCE SURFACE FOR A RECTANGULAR PULSE OF LOW-PASS BROAD BAND NOISE WITH  $q = 10.0$ .

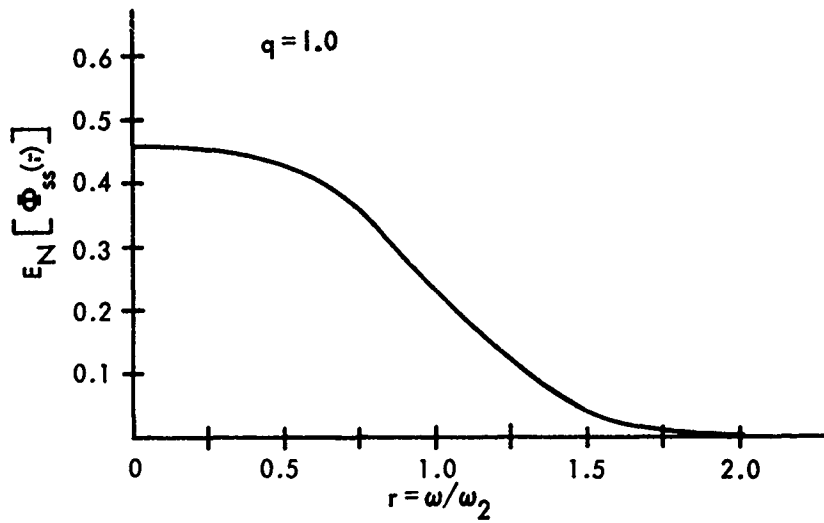


FIG. 13 NORMALIZED SPECTRAL EXPECTED VALUE FOR A RECTANGULAR BURST OF LOW-PASS BROAD BAND NOISE WITH  $q = 1.0$ .

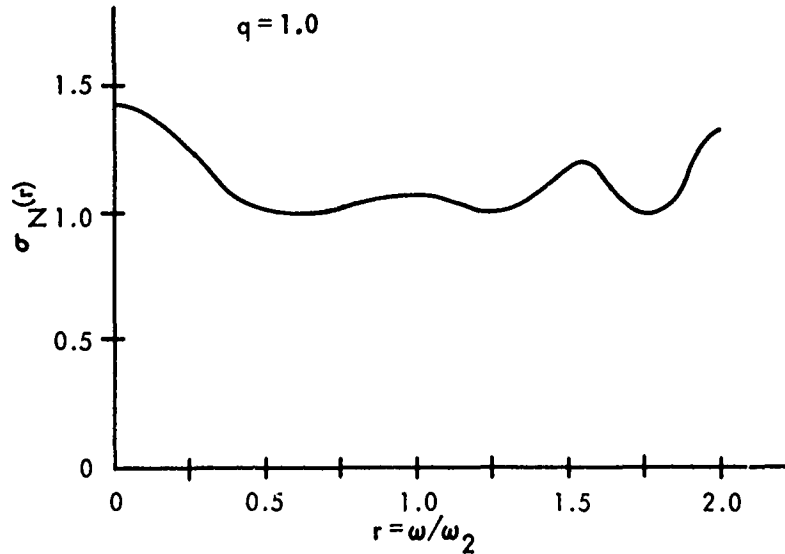


FIG. 14 NORMALIZED SPECTRAL STANDARD DEVIATION FOR A RECTANGULAR BURST OF LOW-PASS BROAD BAND NOISE WITH  $q = 1.0$ .

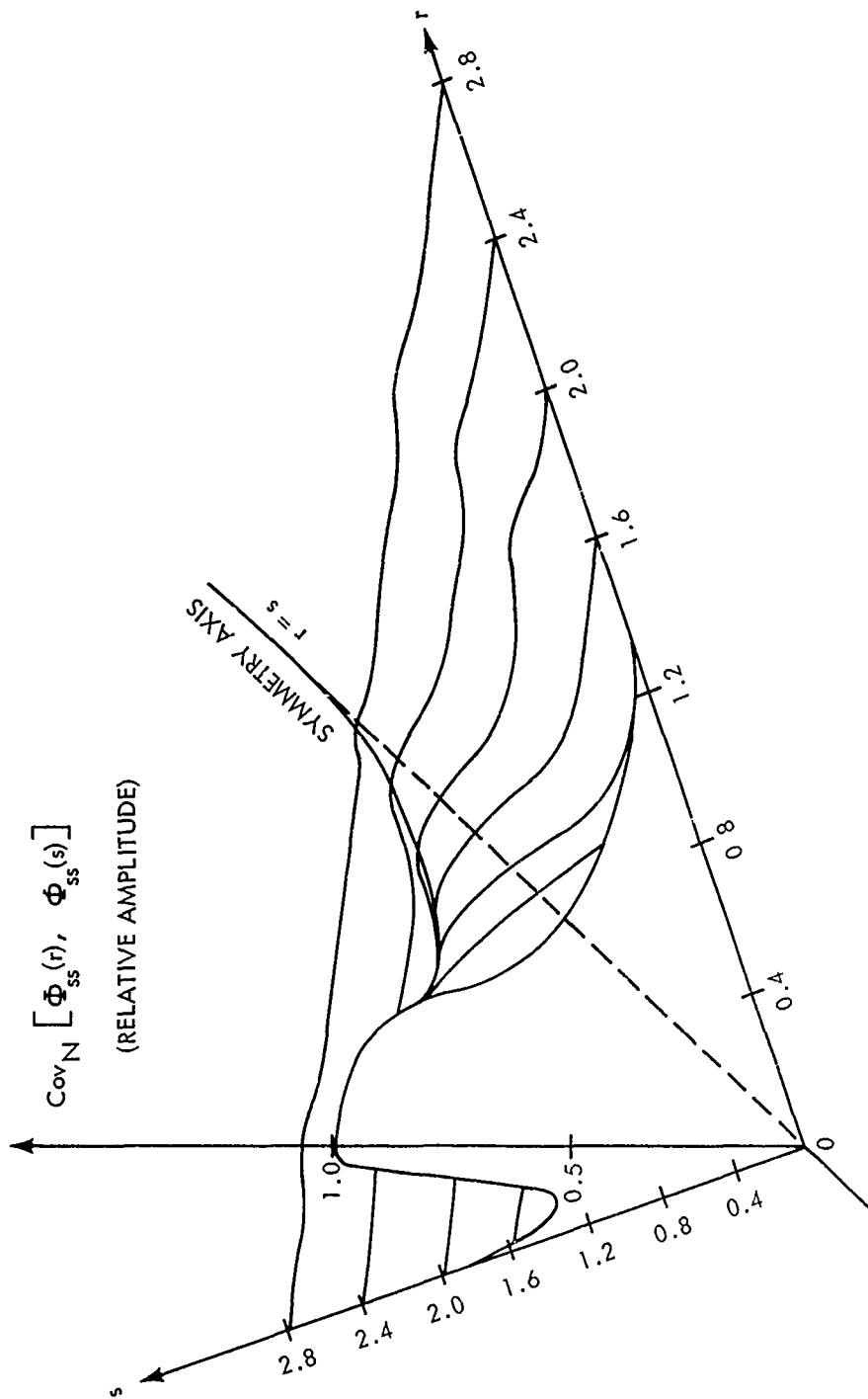


FIG. 15 NORMALIZED SPECTRAL COVARIANCE SURFACE FOR A RECTANGULAR PULSE OF LOW-PASS BROAD BAND NOISE WITH  $q = 1.0$ .

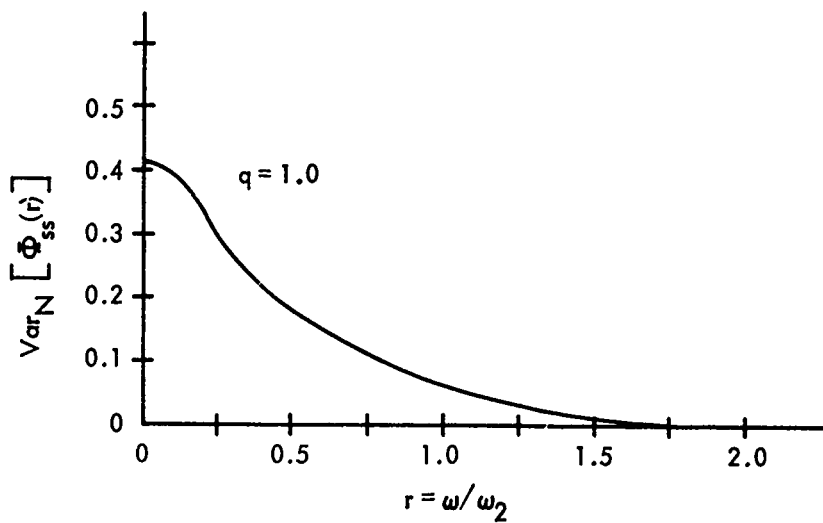


FIG. 16 NORMALIZED SPECTRAL VARIANCE FOR A RECTANGULAR PULSE OF LOW-PASS BROAD BAND NOISE WITH  $q = 1.0$ .

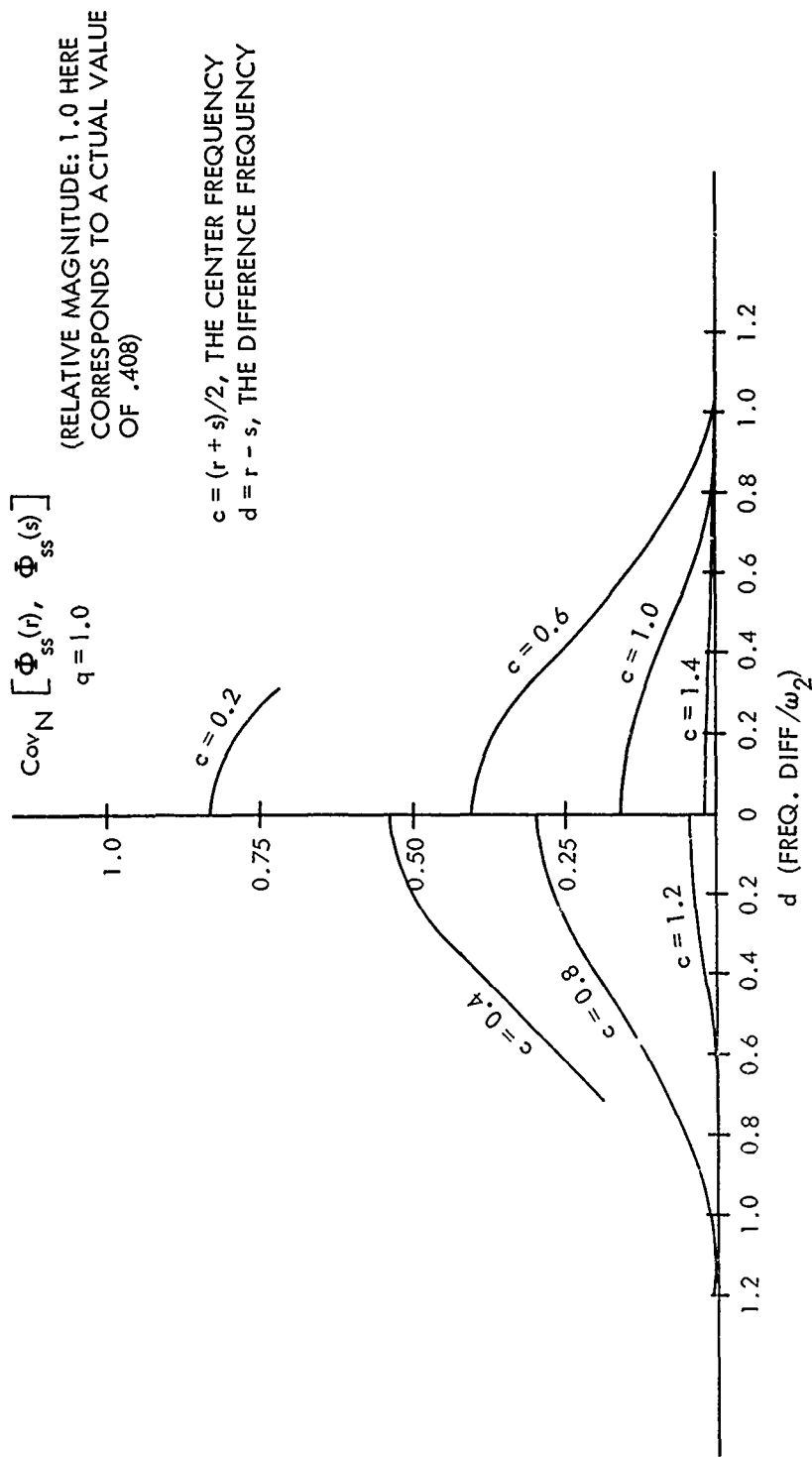


FIG. 17 SECTIONS THROUGH THE SPECTRAL COVARIANCE SURFACE FOR A RECTANGULAR PULSE OF LOW-PASS BROAD BAND NOISE WITH  $q = 1.0$ .

$$\phi_{ee}(\omega) = \frac{T^2}{2\pi} \frac{\sin^2 \frac{\omega T}{2}}{\left(\frac{\omega T}{2}\right)^2}, \quad -\infty < \omega < \infty \quad (94)$$

as was shown in reference (a), page 27. The first zero for  $\omega > 0$  occurs when the argument of the sine in the numerator equals  $\pi$ , or when

$$\omega = \frac{2\pi}{T} \quad (95)$$

This point may be taken to define the positive frequency width of the double-sided energy density spectrum of the envelope, and hence by the arguments presented above, the effective positive frequency width of the spectrum of a rectangular pulse of low-pass broad band noise can be said to be

$$W = \omega_2 + \frac{2\pi}{T} \quad (96)$$

or when normalized to the same basis as the frequency variables  $r$  and  $s$ ,

$$W_N = \frac{\omega_2}{\omega_2} + \frac{2\pi}{\omega_2 T} = 1 + 1/q \quad (97)$$

where  $q$  is defined in equation (82a). When  $q = 10$ , as for the case portrayed in Figure 7,  $W_N = 1.1$ , whereas for  $q = 1.0$ , as in Figure 13,  $W_N = 2.0$ . The size of the effective spectral width is mirrored directly in the form of the spectral covariance function. It is seen empirically that the spectral covariance, centered above the line  $r = s$ , falls to zero beyond the point  $r = s = W_N$ . In other words, the covariance between the values of the spectrum at two points will be small if either argument lies outside the region of significantly large expected value. This is well demonstrated in the  $q = 10.0$  case where the covariance surface falls sharply away for either  $r$  or  $s > 1$  (see Figures 9 and 11) and in the  $q = 1.0$  case where the surface is essentially of zero height for either  $r$  or  $s > 2$  (see Figures 15 and 16).

In seeking the width of the covariance "mound" in a direction perpendicular to its axis, one sees from Figures 12 and 17 that it is on the order of  $2/q$ . This implies immediately that the longer the random transient becomes with respect to the period of the highest noise frequency, the narrower becomes the spectral covariance function about its plane of symmetry. Thus, when  $q = 10.0$ , the width of the ridge is considerably less (by a factor of 10) than the width when  $q = 1.0$ . The peak at the origin, which arises as a consequence of equation (89) dies off for  $r, s > 1/q$ . This is especially clear in Figure 9 for the  $q = 10.0$  case.

In general, the volume lying under the covariance surface can be said to be concentrated over the  $r - s$  plane area shown in Figure 18. This region is bounded by the lines:

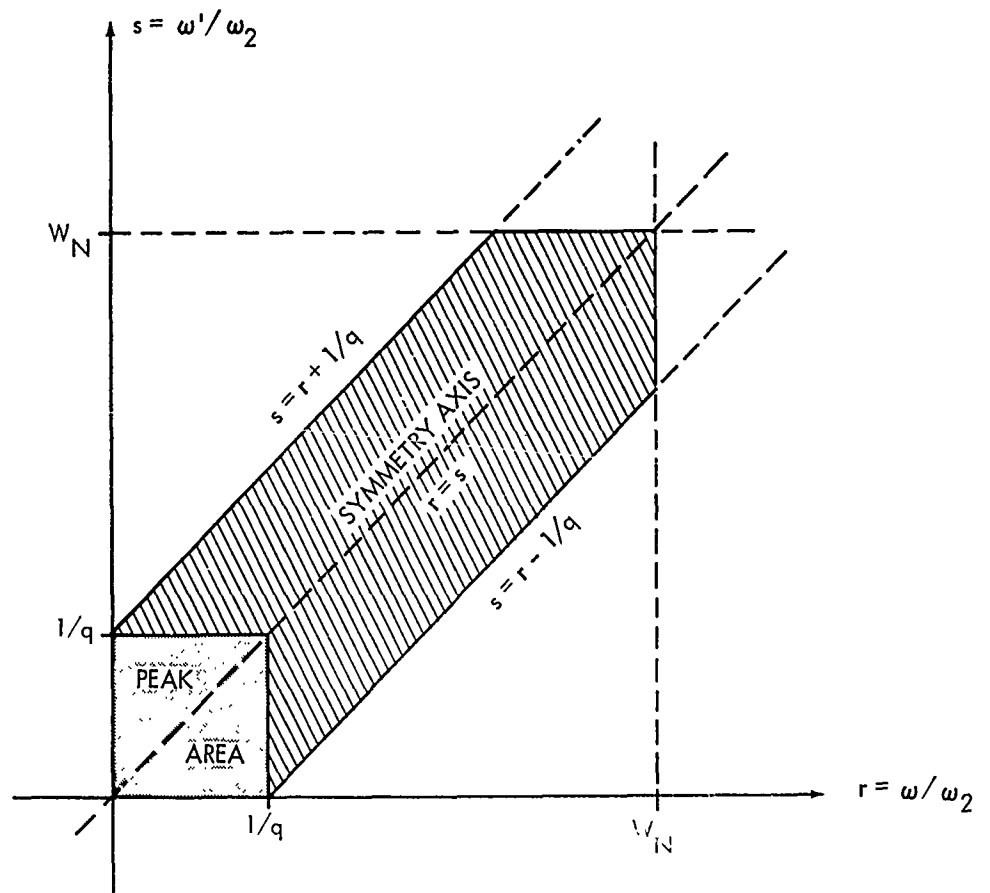


FIG. 18 THE REGION OF APPRECIABLE COVARIANCE FOR A RECTANGULAR PULSE OF LOW-PASS BROAD BAND NOISE AS DELINEATED IN THE  $r - s$  PLANE.

$$r = W_N \tag{98a}$$

$$s = W_N \tag{98b}$$

$$s = r + 1/q \tag{98c}$$

$$s = r - 1/q \tag{98d}$$

The peak at the origin lies roughly above the area bounded by the lines  $r = 1/q$  and  $s = 1/q$ .

When  $q \gg 1$ , the different sections of the covariance surface become separate and well-defined. This is shown particularly well by Figure 9. Near the origin, one finds a high narrow peak over an area roughly  $1/q$  on a side. The largest section of the surface is the narrow ridge that runs diagonally from the peak at the origin to the vicinity of the point  $r = s = 1.0$ , where it decreases sharply to insignificance. The height of the ridge is fairly constant along its length and equal to half that of the peak at the origin. This shows that for large  $q$ , the values of the empirical spectrum at two arguments do not co-vary strongly unless the arguments are close together, and conversely that spectral amplitudes for widely differing arguments are practically linearly independent.

When  $q$  is on the order of unity,  $1/q$  is of the same order as  $W_N$ , and the various regions of the covariance surface fuse together such that no separate identifications can be made. In this case, the surface becomes much more smoothly varying and spreads away from the plane  $r = s$ , as was seen in Figure 15. This implies that significant covariance exists between widely separated points on the spectrum and that a high degree of dependency is present between far removed sections of the spectrum.

The areas of non-negligible covariance delineated in Figure 18 agree well with intuition. Certainly one would expect a strong covariance between the spectral amplitudes of two points only when the expected spectral amplitudes themselves have appreciable magnitude and can be said to arise from something more than chance. The width of the ridge essentially indicates that two spectral values do not co-vary if their normalized arguments differ by more than  $\Delta r = 1/q$ . There is a well known approximate frequency resolution theorem which states that for any random time function of duration  $T$ , energy density spectrum values are statistically independent if their arguments have a difference of at least  $\Delta\omega = 2\pi/T$ . (See for example reference (f), section 6.1.1). Since by definition

$$q = \frac{\omega_2 T}{2\pi}$$

$$\frac{1}{q} = \frac{2\pi}{\omega_2 T} = \Delta r \tag{99}$$

and in terms of the unnormalized frequency variables,

$$\Delta\omega = \omega_2 \Delta r = \frac{2\pi}{T} \quad (100)$$

Thus, the form of the covariance surface bears out the prediction of this particular frequency resolution theorem.

B. Rectangular Pulse of Narrow Band Noise

We now turn to consider spectral covariance functions for narrow band random transients, again assuming a rectangular envelope function. Expressions for this noise spectrum and the corresponding autocorrelation function have already been given in equations (71) and (72). Again the various statistical measures will be presented in normalized versions in which

$$q \equiv \frac{\omega_0 T}{2\pi}, \quad \text{the number of periods of the noise center frequency contained in a pulse length.} \quad (101a)$$

$$r \equiv \frac{\omega}{\omega_0}, \quad \omega \text{ expressed as a fraction of } \omega_0. \quad (101b)$$

$$s \equiv \frac{\omega'}{\omega_0}, \quad \omega' \text{ expressed as a fraction of } \omega_0. \quad (101c)$$

$$z \equiv \frac{\Delta\omega}{\omega_0}, \quad \text{the noise bandwidth as a fraction of the center frequency.} \quad (101d)$$

The resulting expressions, obtained precisely as in the broad band case, become:

$$E_N[\phi_{SS}(r)] = 2q \int_0^1 (1-x) \frac{\sin \pi q z x}{\pi q z x} \cos 2\pi q x \cos 2\pi q r x \, dx \quad (102)$$

such that

$$\int_{-\infty}^{\infty} E_N[\phi_{SS}(r)] \, dr = 1$$

and

$$E[\phi_{SS}(\omega)] = 4N_0 T E_N[\phi_{SS}(r = \frac{\omega}{\omega_0})] \quad (103)$$

$$\text{Cov}[\phi_{ss}(r), \phi_{ss}(s)] =$$

$$4q^2 \left\{ \begin{aligned} & \left[ \int_0^1 (1-x) \frac{\sin \Pi q z x}{\Pi q z x} \cos 2\Pi q x \frac{\sin \Pi q (1-x)(r+s)}{\Pi q (1-x)(r+s)} \cos \Pi q x (r-s) dx \right]^2 \\ & + \\ & \left[ \int_0^1 (1-x) \frac{\sin \Pi q z x}{\Pi q z x} \cos 2\Pi q x \frac{\sin \Pi q (1-x)(r-s)}{\Pi q (1-x)(r-s)} \cos \Pi q x (r+s) dx \right]^2 \end{aligned} \right\} \quad (104)$$

with

$$\text{Cov}[\phi_{ss}(\omega), \phi_{ss}(\omega')] = 16N_0^2 T^2 \text{Cov}[\phi_{ss}(r = \frac{\omega}{\omega_0}), \phi_{ss}(r = \frac{\omega'}{\omega_0})] \quad (105)$$

Two examples of the rectangular pulse of narrow noise are shown in the figures to display the characteristics of the corresponding spectral covariance surfaces. In Figure 19, is shown the spectral expected value for a narrow-band random transient with  $q = 50.0$  and  $z = 0.1$ . This is to say that the length of the transient is such that 50 cycles of the center frequency can be contained therein, and that the bandwidth of the underlying noise process is 1/10 the center frequency. Using spectral convolution arguments as before, the positive frequency spectral width will be on the order of

$$W = \frac{4\Pi}{T} + 2\Delta\omega \quad (106)$$

and normalization with  $\omega_0$  as the basis yields

$$W_N = \frac{2}{q} + z \quad (107)$$

In the present example,  $W_N = .14$ , as is borne out by the graph of Figure 19. The spectral covariance surface for this case is rendered three-dimensionally in Figure 21, and in section in Figure 22. A plot of the normalized spectral variance is shown in Figure 20. It will be recalled that such a graph can be interpreted as yielding a section of the covariance surface through the plane of symmetry. Because of the relative compactness of  $E[\phi_{ss}(\omega)]$ , the covariance surface is a short, sharply peaked ridge symmetrically placed about the plane  $r = s$  and concentrated between  $r = s = 1 - z$  and  $r = s = 1 + z$ . As before, the sections of Figure 22 are taken at right angles to the axis of the ridge.

The corresponding set of figures is shown for the case where  $q = 10.0$  and  $z = 0.01$ . Here the bandwidth of  $n(t)$  is very small compared with the center

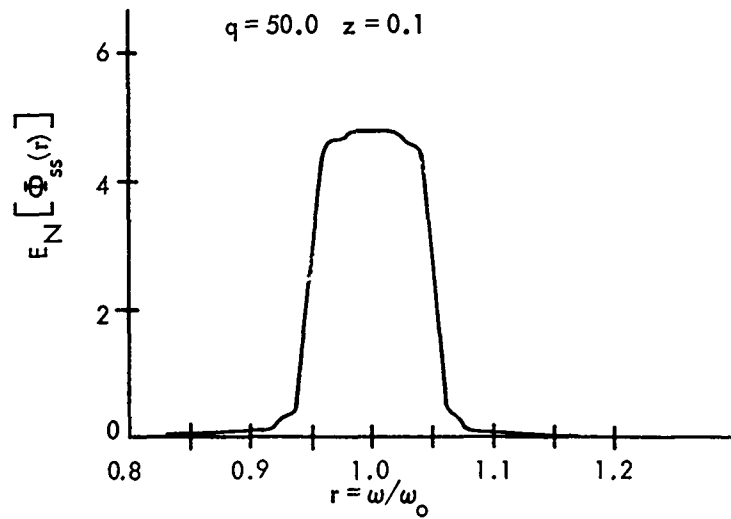


FIG. 19 NORMALIZED SPECTRAL EXPECTED VALUE FOR A RECTANGULAR BURST OF NARROW BAND NOISE WITH  $q = 50.0$  AND  $z = 0.1$ .

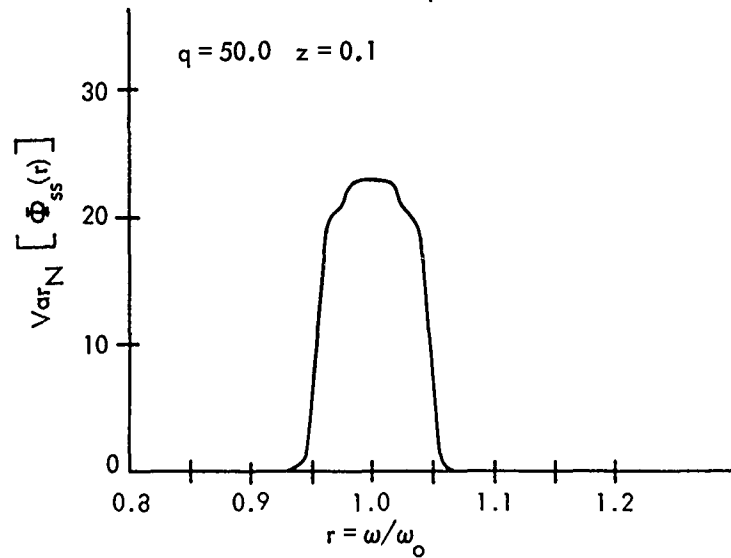


FIG. 20 NORMALIZED SPECTRAL VARIANCE FOR A RECTANGULAR BURST OF NARROW BAND NOISE WITH  $q = 50.0$  AND  $z = 0.1$ .

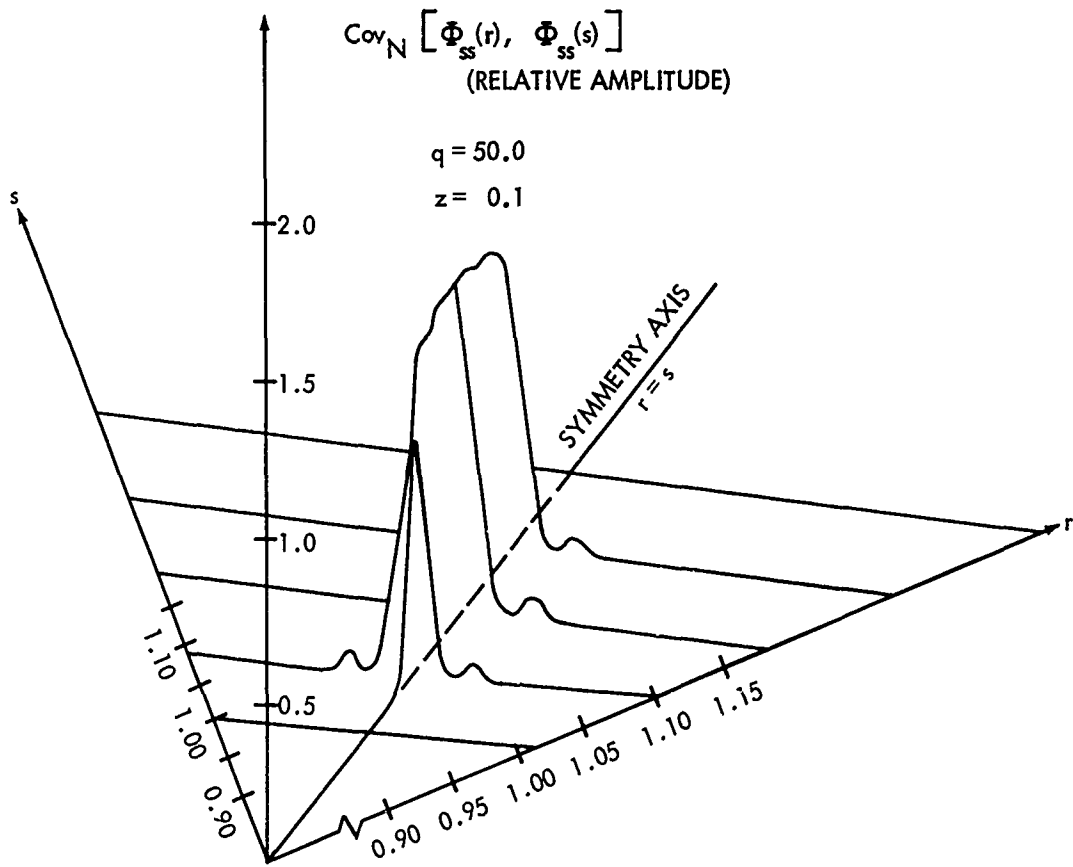


FIG.21 NORMALIZED SPECTRAL COVARIANCE SURFACE FOR A RECTANGULAR PULSE OF NARROW BAND NOISE WITH  $q = 50.0$  AND  $z = 0.1$ .

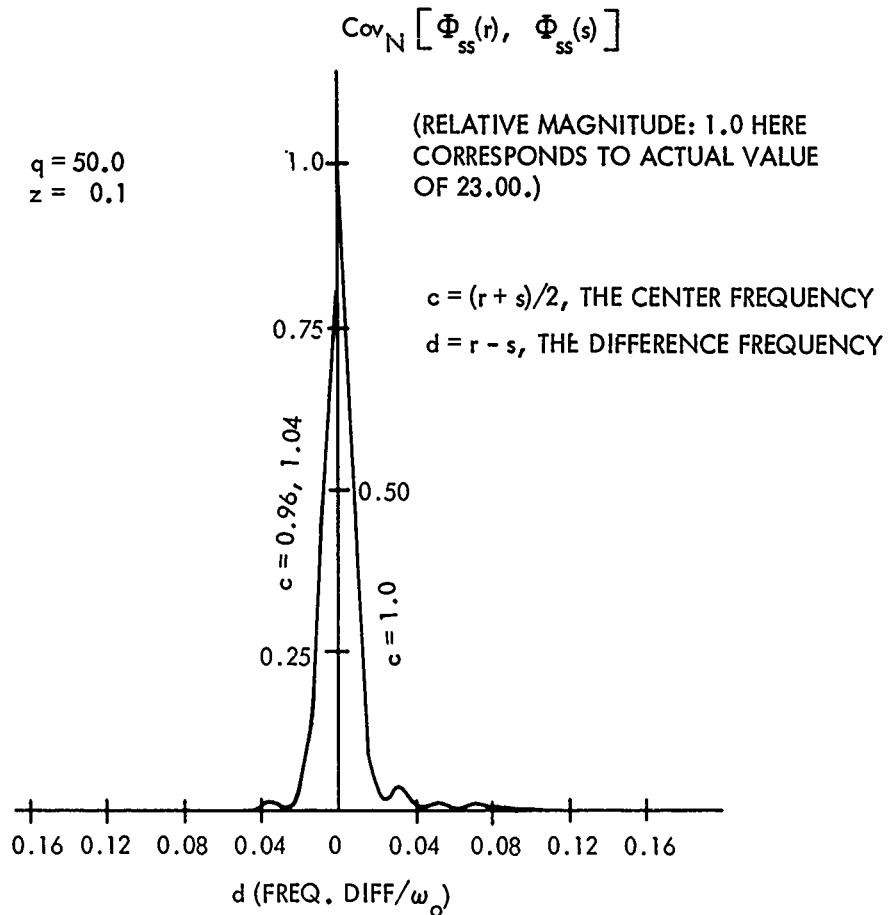


FIG. 22 SECTIONS THROUGH THE SPECTRAL COVARIANCE SURFACE FOR A RECTANGULAR PULSE OF NARROW BAND NOISE WITH  $q = 50.0$  AND  $z = 0.1$ .

frequency, and also small compared to the spectral width of the envelope function. As a result, the spectral expected value (Figure 23) is practically identical with that of the envelope (which has the familiar  $\sin^2x/x^2$  form), and in turn the covariance peak is more widely spread and smoothly rounded around the vicinity  $r = s = 1$  (see Figures 23, 25, and 26). Here the spectral width is approximately equal to  $2/q$  since  $z$  is relatively so small.

In general, it is found for the rectangular narrow band case that the covariance peak is found over an area delineated in the  $r - s$  plane by the lines

$$r = 1 + W_N/2 \quad (108a)$$

$$r = 1 - W_N/2 \quad (108b)$$

$$s = 1 + W_N/2 \quad (108c)$$

$$s = 1 - W_N/2 \quad (108d)$$

$$s = r + 1/q \quad (108e)$$

$$s = r - 1/q \quad (108f)$$

as in Figure 27. Again, this representation agrees with the interpretation offered for Figure 18 and the rectangular broad band case.

#### C. Random Transient Ensembles with Decaying Exponential Envelopes

A number of examples of  $E_N[\phi_{ss}(r)]$  and  $\text{Cov}_N[\phi_{ss}(r), \phi_{ss}(s)]$  have been computed and graphed for random transient ensembles generated with decaying exponential envelopes. In these studies, the parameter  $q$  has been defined, analogously to equations (82a) and (101a), with  $T$  now taken to represent the time constant of the exponential decay.  $q$  here represents, then, the number of periods of a typical noise frequency contained in the time constant. For a given underlying noise process, the various spectral statistics for the exponential envelope cases do not differ in any gross manner from their counterparts in the rectangular envelope cases with identical  $q$  (i.e., from those arising from rectangular random transients whose envelope length is equal to the exponential time constant). The only appreciable difference observed is that the spectral width is slightly narrower in cases where the spectral width of the envelope is a significant part of the total, and that the transverse width of the spectral covariance ridge is somewhat reduced, although it is still well approximated by  $2/q$ . These effects are demonstrated in Figures 28 and 29 which compare the results found for exponential and rectangular envelope narrow band random transients with  $q = 10.0$  and  $z = 0.1$ . These changes are not unexpected, since the energy density spectrum of a decaying exponential pulse is significantly narrower than that of a rectangular pulse whose length is set equal to the time constant. This is shown in Figure 30.

One may say, then, that the approximate delineation of the region of appreciable covariance set forth for the rectangular transients (Figures 18 and 27) applies, for most practical purposes, to the exponential envelope cases also. It may safely be concluded that the detailed shape of the envelope function is relatively unimportant for the form of the spectral statistics, and that the envelope duration - or some consistent measure thereof - is the most important envelope

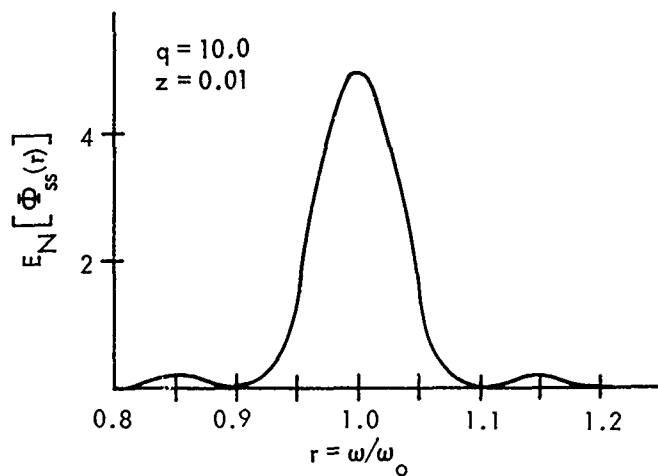


FIG. 23 NORMALIZED SPECTRAL EXPECTED VALUE FOR A RECTANGULAR BURST OF NARROW BAND NOISE WITH  $q = 10.0$  AND  $z = 0.01$  . .

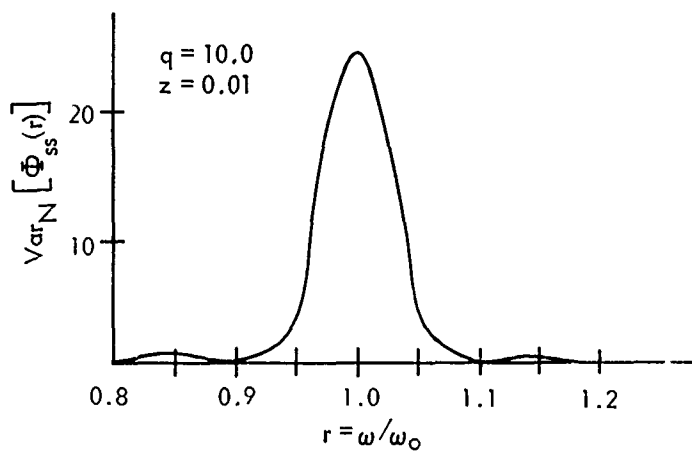


FIG. 24 NORMALIZED SPECTRAL VARIANCE FOR A RECTANGULAR BURST OF NARROW BAND NOISE WITH  $q = 10.0$  AND  $z = 0.01$  .

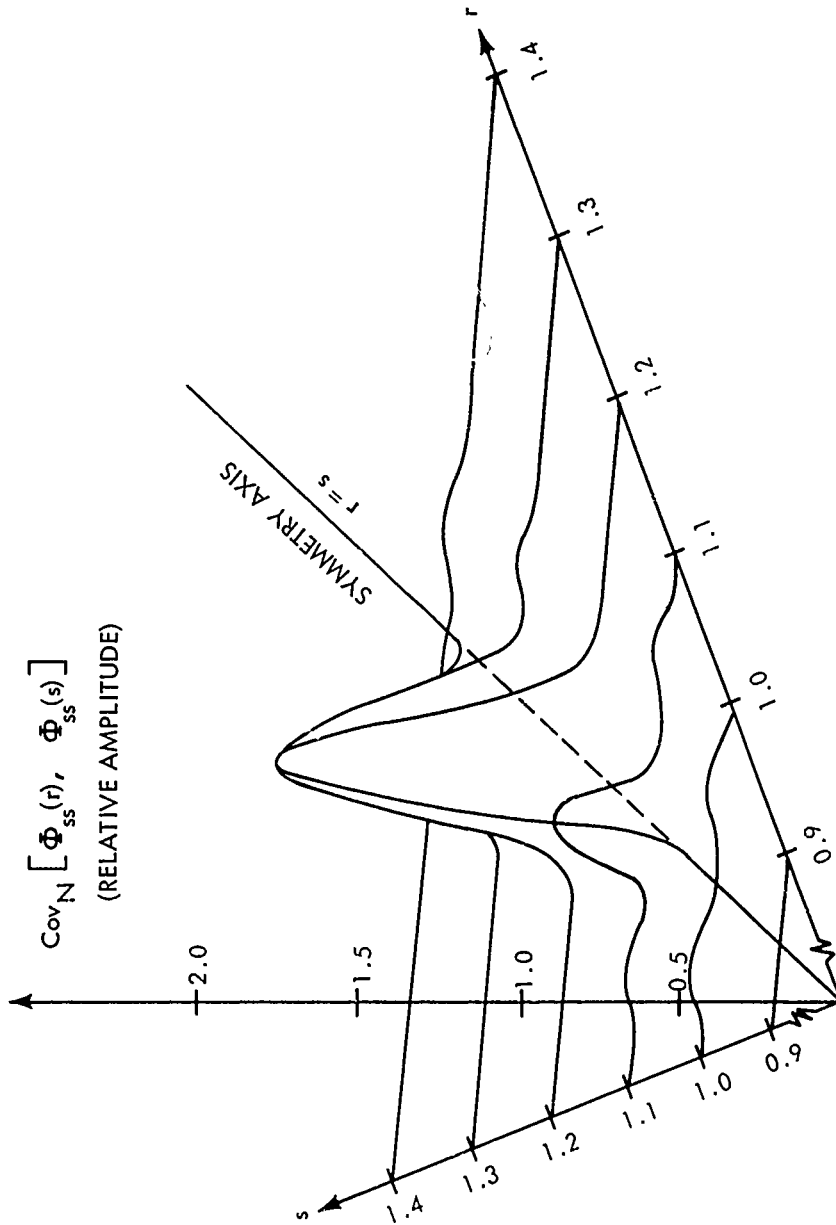


FIG. 25 NORMALIZED SPECTRAL COVARIANCE SURFACE FOR A RECTANGULAR PULSE OF NARROW BAND NOISE WITH  $q = 10.0$  AND  $z = 0.01$ .

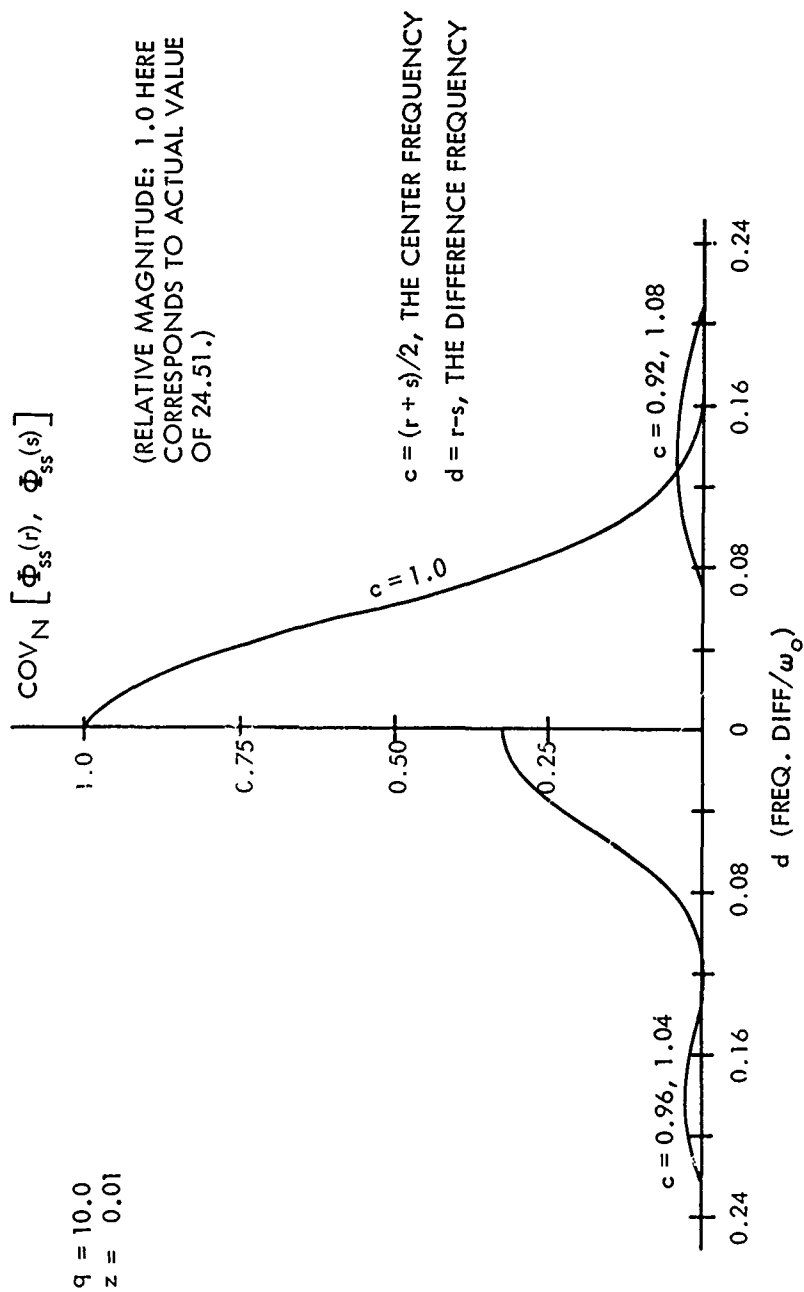


FIG. 26 SECTIONS THROUGH THE SPECTRAL COVARIANCE SURFACE FOR A RECTANGULAR PULSE OF NARROW BAND NOISE WITH  $q = 10.0$  AND  $z = 0.01$ .

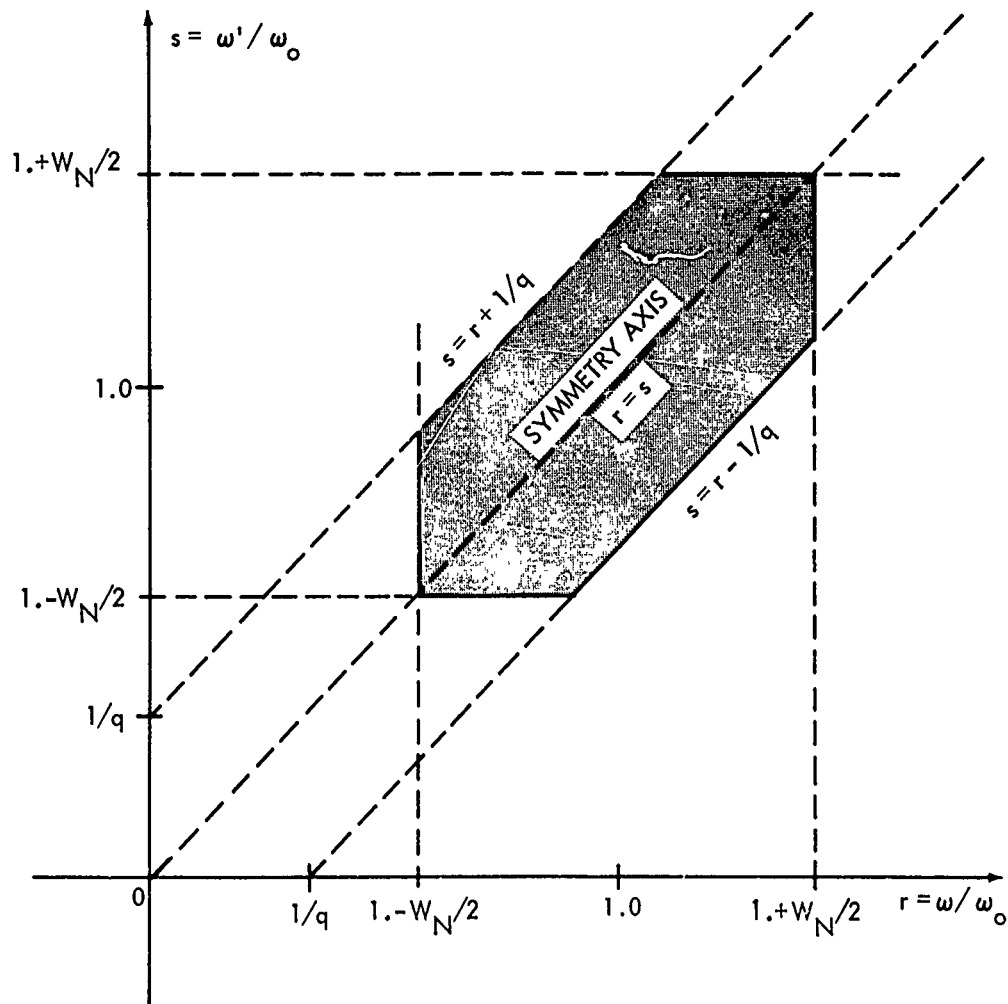


FIG. 27 THE REGION OF APPRECIABLE SPECTRAL COVARIANCE FOR A RECTANGULAR PULSE OF NARROW BAND NOISE DELINEATED IN THE  $r - s$  PLANE.

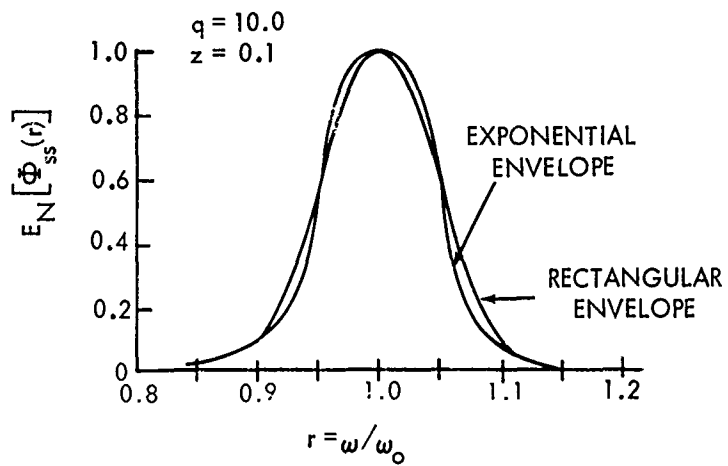


FIG.28 COMPARISON OF THE SPECTRAL EXPECTED VALUES FOR RECTANGULAR AND DECAYING EXPONENTIAL PULSES OF NARROW BAND NOISE WITH  $q = 10.0$  AND  $z = 0.1$ .

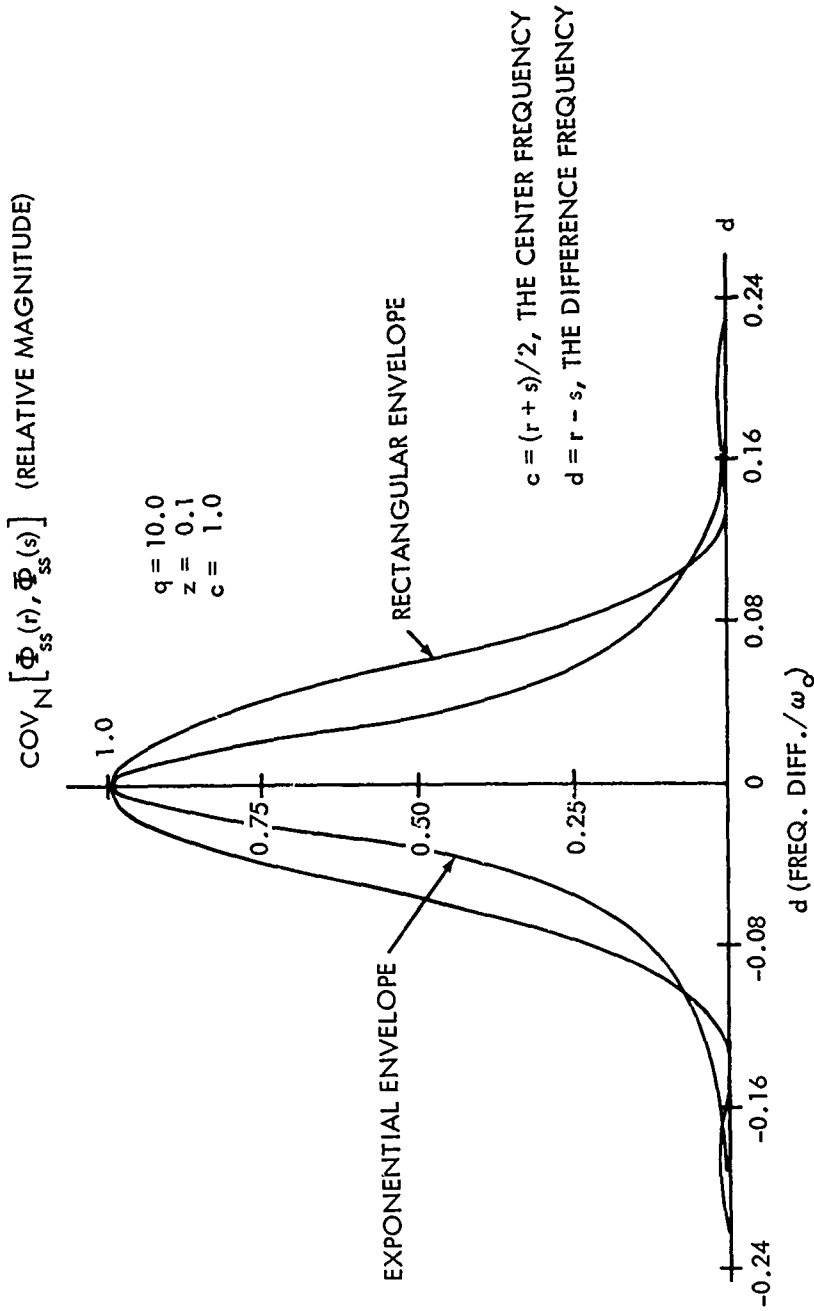


FIG. 29 COMPARISON OF SECTIONS THROUGH THE SPECTRAL COVARIANCE SURFACE FOR RECTANGULAR AND DECAYING EXPONENTIAL PULSES OF NARROW BAND NOISE FOR  $q = 10.0$  AND  $z = 0.1$ . HERE, THE CENTER FREQUENCY HAS BEEN CHOSEN EQUAL TO THE CENTER FREQUENCY OF THE UNDERLYING NOISE PROCESS.

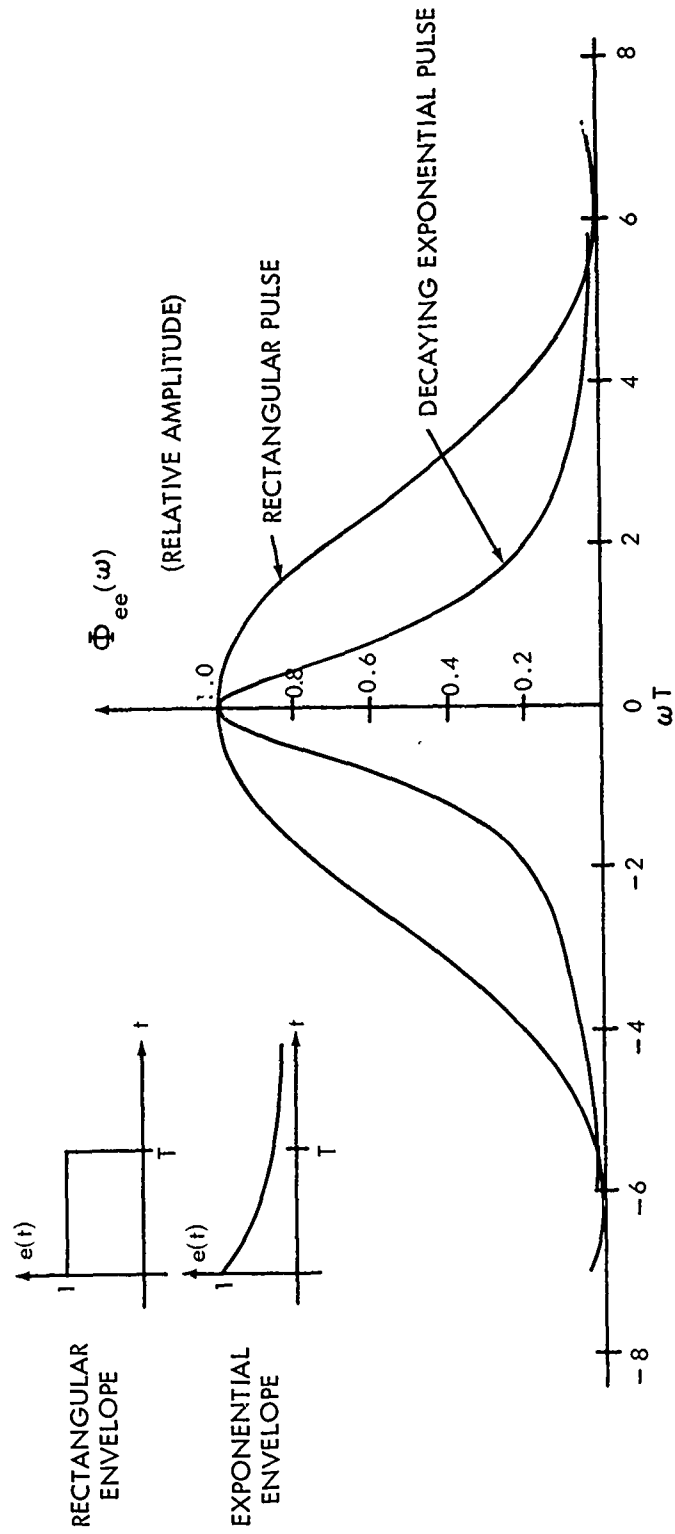


FIG.30 A COMPARISON OF THE ENERGY DENSITY SPECTRA FOR A RECTANGULAR PULSE OF LENGTH T AND A DECAYING EXPONENTIAL PULSE OF TIME CONSTANT T.

feature for the determination of the spectral character of the random transient ensemble. This is particularly true when the transient duration is such that it contains many cycles of a typical noise frequency, i.e., when the parameter  $q$  is large.

This concludes our discussion of random transient spectral covariance surfaces. It is hoped that the reader has been given sufficient grasp of the concepts involved to permit him to continue on his own to explore special cases of interest.

## Chapter IV

## IDEAL BAND PASS FILTERING OF RANDOM TRANSIENT WAVEFORMS

In this chapter will be studied the problem of passing an ensemble of random transients through an idealized narrow band filter whose system function is given by the expression

$$H(\omega) = 1, \quad \omega_c - \frac{B}{2} \leq |\omega| \leq \omega_c + \frac{B}{2} \quad (109)$$

$$= 0, \quad \text{elsewhere}$$

where  $\omega_c$  is the center frequency of the filter, and  $B$  is its bandwidth, both in radians/second.  $H(\omega)$  is portrayed in Figure 31.

A few words are in order about this filter function. First we note that such a device is physically non-realizable. The impulse response  $h(t)$  is given by the Fourier transform of  $H(\omega)$ :

$$h(t) = \frac{1}{2\pi} \int_{-\infty}^{\infty} H(\omega) e^{j\omega t} d\omega = \frac{1}{\pi} \int_{\omega_c - B/2}^{\omega_c + B/2} \cos \omega t d\omega \quad (110)$$

$$= \frac{B}{\pi} \frac{\sin \frac{B}{2} t}{\frac{B}{2} t} \cos \omega_c t, \quad -\infty < t < \infty$$

and is non-zero for  $t < 0$ , implying that the device responds before the arrival of a stimulus. This is a physical impossibility (at least in this world). Since the filter of equation (109) is unrealizable, one might wonder why it will be studied here. Of course, the honest answer is that it is mathematically tractable, but it should be pointed out that if an arbitrarily long time delay is allowed between the input and output (essentially by relaxing the specification to permit non-zero phase), such a filter function can be realizably approximated to any accuracy (see, for example, reference (g), pp 240-241). At the same time, the filter function of equation (109) is a convenient mathematical abstraction which provides a means for describing the band-wise content of a random transient spectrum and particularly the degree of variability to be expected in band-pass filtering. This will provide a strong indication of the magnitude of these effects in real world cases with realizable filter functions.

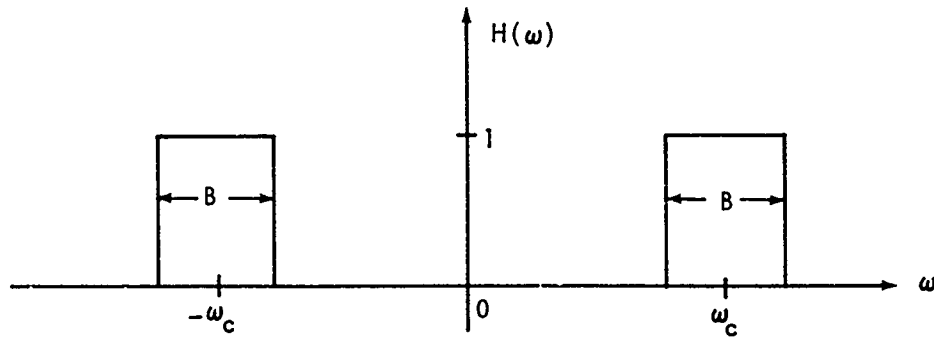


FIG.31 IDEAL NARROW-BAND FILTER FUNCTION.

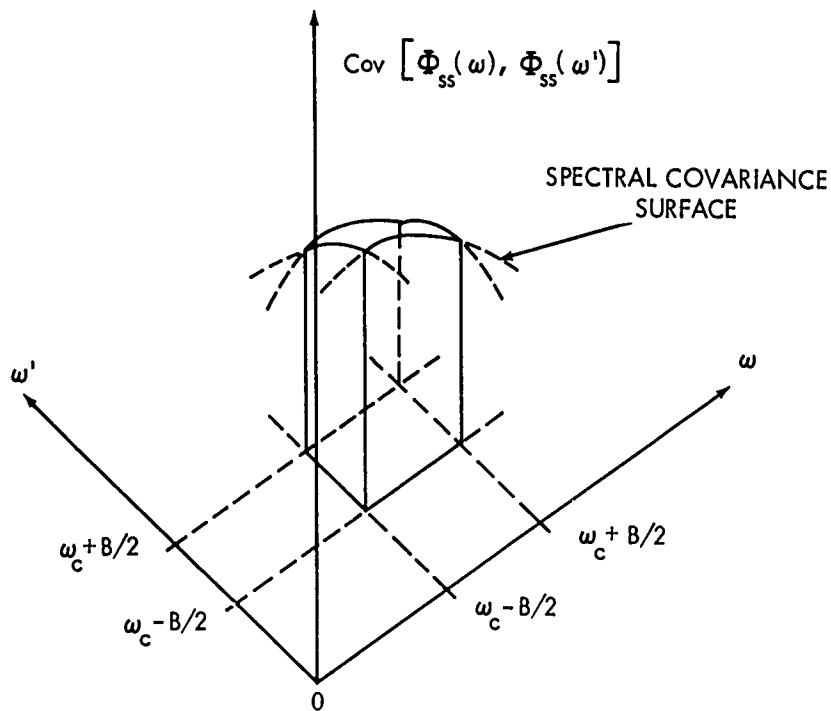


FIG.32 VAR [F(H)] PORTRAYED AS THE VOLUME OF A PRISM LYING UNDER THE SPECTRAL COVARIANCE SURFACE.

With this justification, we shall proceed. From equations (22) and (109), one may immediately find that

$$F(H) = \int_{-\omega_c - B/2}^{-\omega_c + B/2} \phi_{SS}(\omega) d\omega + \int_{\omega_c - B/2}^{\omega_c + B/2} \phi_{SS}(\omega) d\omega \quad (111)$$

and thus  $F(H)$  is indeed an expression for the area of  $\phi_{SS}(\omega)$  lying between the frequencies  $(\omega_c - B/2)$  and  $(\omega_c + B/2)$ . Since  $\phi_{SS}(\omega)$  is an even function of  $\omega$ ,

$$F(H) = 2 \int_{\omega_c - B/2}^{\omega_c + B/2} \phi_{SS}(\omega) d\omega \quad (112)$$

and further,

$$E[F(H)] = 2 \int_{\omega_c - B/2}^{\omega_c + B/2} E[\phi_{SS}(\omega)] d\omega \quad (113)$$

Similarly, from equation (30)

$$\begin{aligned} \text{Var}[F(H)] &= \int_{-\omega_c - B/2}^{-\omega_c + B/2} \int_{-\omega_c - B/2}^{-\omega_c + B/2} \text{Cov}[\phi_{SS}(\omega), \phi_{SS}(\omega')] d\omega d\omega' \\ &+ \int_{-\omega_c - B/2}^{-\omega_c + B/2} \int_{\omega_c - B/2}^{\omega_c + B/2} \text{Cov}[\phi_{SS}(\omega), \phi_{SS}(\omega')] d\omega d\omega' \\ &+ \int_{\omega_c - B/2}^{\omega_c + B/2} \int_{\omega_c - B/2}^{\omega_c + B/2} \text{Cov}[\phi_{SS}(\omega), \phi_{SS}(\omega')] d\omega d\omega' \\ &+ \int_{\omega_c - B/2}^{\omega_c + B/2} \int_{\omega_c - B/2}^{\omega_c + B/2} \text{Cov}[\phi_{SS}(\omega), \phi_{SS}(\omega')] d\omega d\omega' \end{aligned} \quad (114)$$

By the symmetry properties of the covariance function, this becomes

$$\text{Var}[E(H)] = 4 \int_{\omega_c - B/2}^{\omega_c + B/2} \int_{\omega_c - B/2}^{\omega_c + B/2} \text{Cov}[\phi_{SS}(\omega), \phi_{SS}(\omega')] d\omega d\omega' \quad (115)$$

Thus, the expected value of the output energy is given by twice the area under the curve of  $E[\phi_{SS}(\omega)]$  between  $\omega = \omega_c - B/2$  and  $\omega = \omega_c + B/2$  whereas the variance of the output energy is found to be equal to four times the volume of a prism bounded above by the covariance surface and lying over a square in the  $\omega - \omega'$  plane bounded by the lines

$$\omega = \omega_c \pm B/2 \quad (116a)$$

$$\omega' = \omega_c \pm B/2 \quad (116b)$$

as shown in Figure 32. Having arrived at an expression for  $\text{Cov}[\phi_{SS}(\omega), \phi_{SS}(\omega')]$  using the methods of the last chapter, it is straightforward, at least conceptually, to compute  $E[F(H)]$  and  $\text{Var}[F(H)]$ .

In practice, an accurate computation of the output energy expected value and variance is an exceedingly tedious business. Several attempts have been made to perform the calculation by digital computer, using multiple numerical integration. On the IBM-7090 at NOL, the computation time for a single point on a typical graph of  $\text{Var}[F(H)]$  was on the order of 30 minutes! It appears, then, that an accurate computer calculation of these measures is completely out of the question, and one is forced to the use of approximations which, while lacking accuracy, nonetheless indicate and preserve the magnitudes of the important trends in the various statistical functions. An example of such an approximate method will be detailed now.

For our example, we shall examine the ideal frequency filtering of a rectangular pulse of narrow band noise, characterized by the parameters  $q$  and  $z$  defined previously. The spectral covariance surface of such a signal has been treated in the preceding chapter, and its features portrayed in Figures 19 through 27. Of all the examples treated in this study, this is the one of most widespread interest and generality, particularly since the results retain sufficient accuracy to predict the effects of filtering any shaped pulse of narrow band noise of approximately the same duration as the rectangular pulse, in accordance with the discussion at the close of Chapter III.

In the discussion that follows, the normalized and parameterized versions of the expected values and covariances will be used. To start the present approximate approach, the spectral expected value (of Figure 19 or 23) will be represented as a rectangular function of width  $W_N$  centered at  $r = 1.0$ . The height of this function will be taken to be the maximum value of the expected value expression computed from equation (102). This maximum will be denoted  $M_F$ , and thus

$$E_A[\phi_{SS}(r)] = M_E, \quad 1 - W_N/2 \leq |r| \leq 1 + W_N/2$$

$$= 0, \quad \text{elsewhere} \quad (117)$$

where  $E_A[\phi_{SS}(r)]$  represents the approximate normalized spectral expected value.

$E[F(H)]$  is found from the expression of equation (113):

$$E[F(H)] = 2 \int_{\omega_c - B/2}^{\omega_c + B/2} E[\phi_{SS}(\omega)] d\omega$$

Using also equation (103) and defining  $\omega_c' = \omega_c/\omega_0$  and  $B' = B/\omega_0$ ,

$$E[F(H)] = 8N_0 T \int_{\omega_c - B/2}^{\omega_c + B/2} E_N[\phi_{SS}(r = \omega/\omega_0)] d\omega$$

$$= 8N_0 \omega_0 T \int_{\omega_c' - B'/2}^{\omega_c' + B'/2} E[\phi_{SS}(r)] dr \quad (118)$$

Now denoting the approximate value of  $E[F(H)]$  by  $E_A[F(H)]$ , we have that

$$E[F(H)] \approx E_A[F(H)] = k \int_{\omega_c' - B'/2}^{\omega_c' + B'/2} E_A[\phi_{SS}(r)] dr \quad (119)$$

where

$$k = 8N_0 \omega_0 T \quad (120)$$

The integral of equation (119) can be visualized as proportional to the area of overlap of two rectangular functions: one fixed - representing the random transient spectrum (equation (117)), and the other sliding - representing the tunable filter as the latter's center frequency is swept across the frequency range of interest. This is shown in Figure 33. The resulting output energy expected value expressions can be considered a function of  $\omega_c'$ , or by defining

$$\Delta = \omega_c' - 1 = \frac{\omega_c - \omega_0}{\omega_0} \quad (121)$$

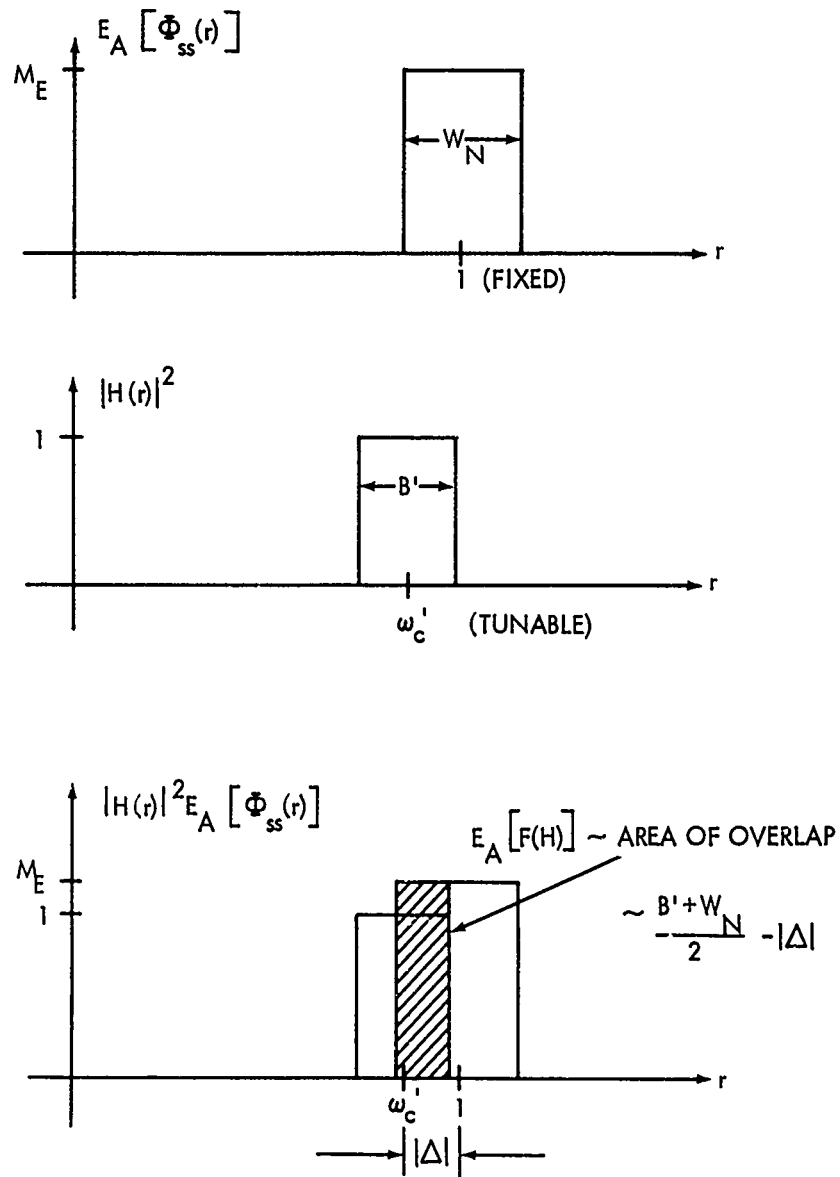


FIG. 33 AN INTERPRETATION OF THE CALCULATION OF  $E_A [F(H)]$  AS THE AREA OF OVERLAP OF TWO RECTANGULAR FUNCTIONS.

as the normalized frequency difference between the center of the filter function and that of the underlying noise spectrum, as a function of  $\Delta$ . Clearly, there are two cases to consider:

A. For  $B' \leq W_N$ ,

$$\begin{aligned} E_A[F(H)] &= M_E k B', \quad 0 \leq |\Delta| \leq \frac{W_N - B'}{2} \\ &= M_E k \left[ \frac{B' + W_N}{2} - |\Delta| \right], \quad \frac{W_N - B'}{2} \leq |\Delta| \leq \frac{W_N + B'}{2} \\ &= 0, \quad |\Delta| \geq \frac{B' + W_N}{2} \end{aligned} \quad (122)$$

B. For  $B' \geq W_N$ ,

$$\begin{aligned} E_A[F(H)] &= M_E k W_N, \quad 0 \leq |\Delta| \leq \frac{B' - W_N}{2} \\ &= M_E k \left[ \frac{B' + W_N}{2} - |\Delta| \right], \quad \frac{B' - W_N}{2} \leq |\Delta| \leq \frac{B' + W_N}{2} \\ &= 0, \quad |\Delta| \geq \frac{B' + W_N}{2} \end{aligned} \quad (123)$$

These functions are shown in Figure 34 and represent approximate expressions for the expected value of the filter output energy as a function of the filter center frequency  $\omega_c$ , when the input is a rectangular pulse of narrow band noise centered at  $\omega_0$ .

Corresponding approximate expressions involving the spectral covariance function are somewhat harder to formulate and handle. For our present needs, the spectral covariance surface can be reasonably well approximated by a right hexagonal prism erected over a base in the  $r - s$  plane delineated by the equations (108) and shown in Figure 27. The height of this prism is taken to be the maximum value of the expression of equation (104), denoted  $M_c$ . A three-dimensional rendering of the approximated surface is shown as Figure 35.

The variance of the filter output energy is expressed by means of equations (115) and (105):

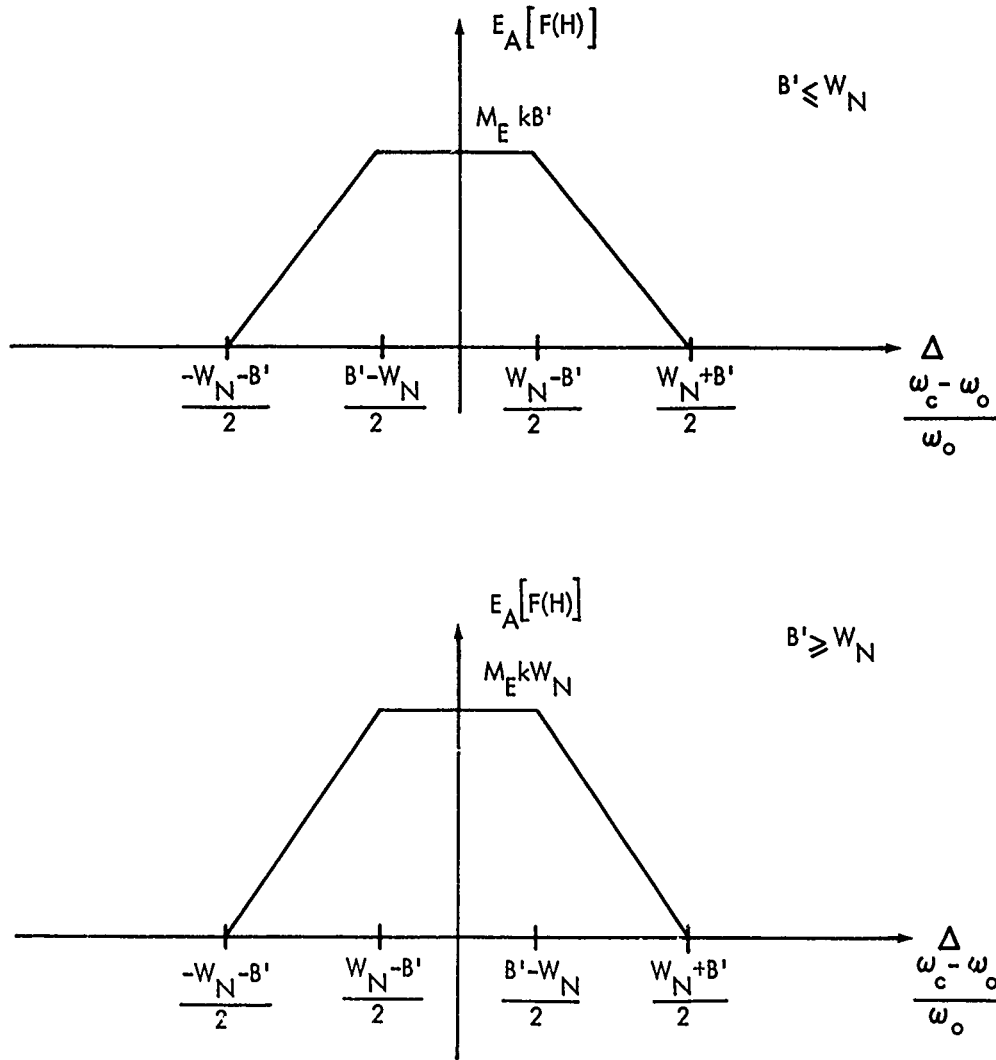


FIG.34 APPROXIMATIONS FOR THE EXPECTED VALUE OF THE OUTPUT ENERGY OF A NARROW BAND FILTER WHEN EXCITED BY A RECTANGULAR PULSE OF NARROW BAND NOISE.

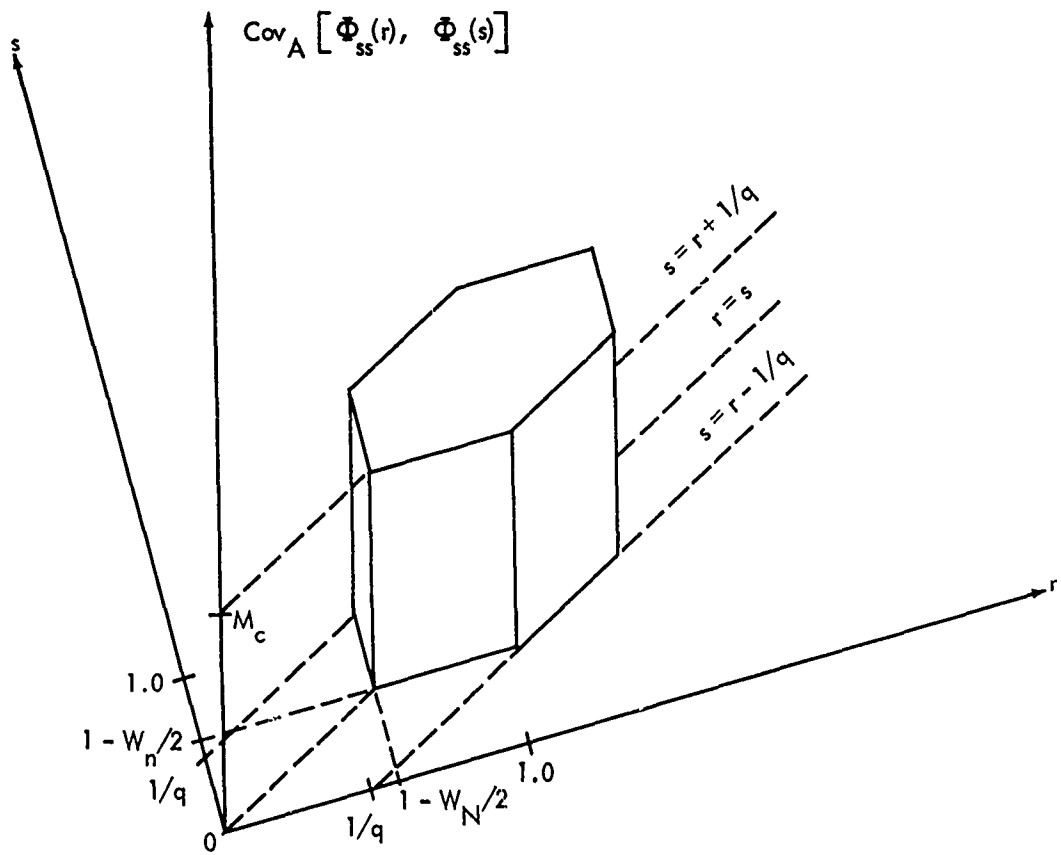


FIG. 35 AN APPROXIMATION FOR THE FORM OF THE NORMALIZED SPECTRAL COVARIANCE SURFACE FOR A RECTANGULAR PULSE OF NARROW BAND NOISE.

$$\begin{aligned}
 \text{Var}[F(H)] &= 4 \int_{\omega_c - B/2}^{\omega_c + B/2} \int_{\omega_c - B/2}^{\omega_c + B/2} \text{Cov}[\phi_{SS}(\omega), \phi_{SS}(\omega')] d\omega d\omega' \\
 &= 64 N_o^2 T^2 \int_{\omega_c - B/2}^{\omega_c + B/2} \int_{\omega_c - B/2}^{\omega_c + B/2} \text{Cov}_N[\phi_{SS}(r = \frac{\omega}{\omega_o}), \phi_{SS}(s = \frac{\omega'}{\omega_o})] d\omega d\omega' \\
 &= 64 N_o^2 T^2 \omega_o^2 \int_{\omega'_c - B'/2}^{\omega'_c + B'/2} \int_{\omega'_c - B'/2}^{\omega'_c + B'/2} \text{Cov}_N[\phi_{SS}(r), \phi_{SS}(s)] dr ds \quad (124)
 \end{aligned}$$

If we denote the approximate covariance surface as  $\text{Cov}_A[\phi_{SS}(r), \phi_{SS}(s)]$ ,

$$\text{Var}[F(H)] \approx \text{Var}_A[F(H)] = k^2 \int_{\omega'_c - B'/2}^{\omega'_c + B'/2} \int_{\omega'_c - B'/2}^{\omega'_c + B'/2} \text{Cov}_A[\phi_{SS}(r), \phi_{SS}(s)] dr ds \quad (125)$$

where  $k$  is again given by equation (12). The integral of equation (125) can be interpreted as yielding the volume under the approximate covariance surface lying above a square in the  $r - s$  plane bounded by the lines:

$$\begin{aligned}
 r &= \omega'_c \pm B'/2 \\
 s &= \omega'_c \pm B'/2
 \end{aligned} \quad (126)$$

Note that this "filter square" has the same axis of symmetry ( $r = s$ ) as the spectral covariance surface itself. A geometrical portrayal of the generation of the curve of  $\text{Var}_A[F(H)]$  versus  $\omega'_c$  is shown in Figure 36. There we see that as  $\omega_c$  changes, the filter square slides up and down the line  $r = s$ , cutting out a changing volume under the covariance surface proportional to the output energy variance. In the present approximation, where the surface is of constant height over a sharply delineated area, outside of which it is identically zero, the integral of equation (125) becomes proportional to simply the area of overlap of the filter square and the hexagon representing the base of the covariance surface. The constant of proportionality between the overlap area and the approximate variance is the height of the surface, taken here to be  $M_c$ , the maximum normalized covariance. To compute  $\text{Var}_A[F(H)]$  as a function of the filter center

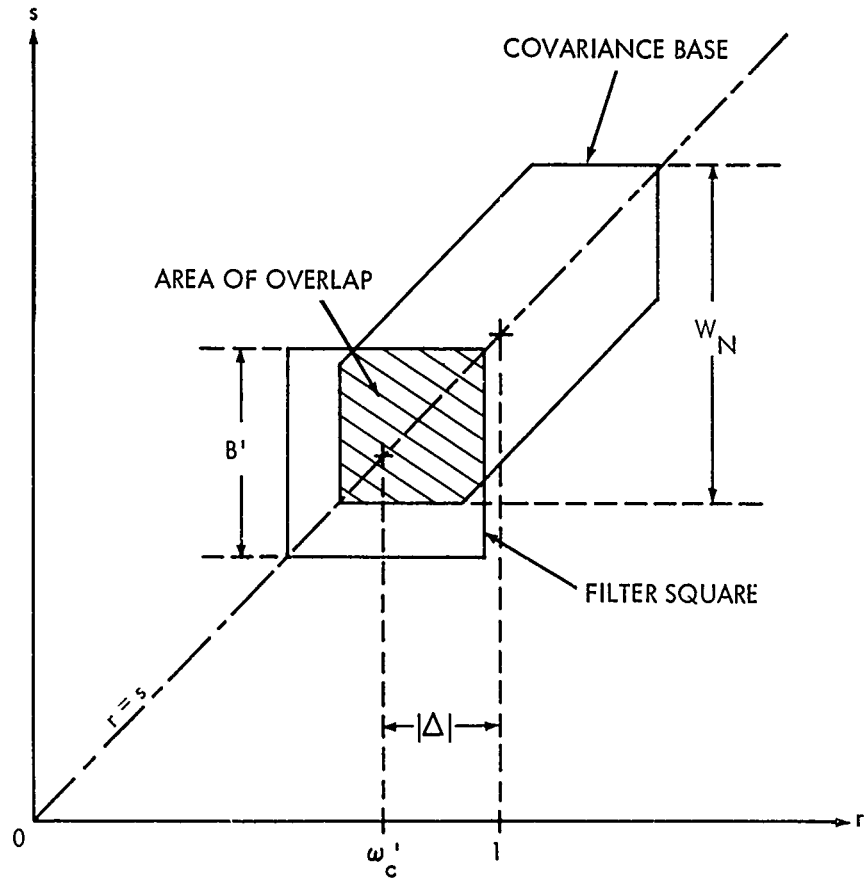


FIG.36 A GEOMETRIC INTERPRETATION OF THE APPROXIMATE OUTPUT ENERGY VARIANCE AS PROPORTIONAL TO THAT AREA OF THE "COVARIANCE HEXAGON" OVERLAPPED BY THE "FILTER SQUARE".

frequency, one lays out the covariance hexagon as a function of the random transient parameters ( $q$  and  $z$ ) and calculates the area of overlap as the filter square glides up and down the  $45^\circ$  line in the  $r - s$  plane. Since  $W_N = \frac{z}{q} + z > \frac{1}{q}$  always, the geometry of the situation leads to three distinct cases depending upon the normalized filter band-width  $B'$ :

A.  $0 \leq B' \leq 1/q$ :

$$\begin{aligned} \text{Var}_A[F(H)] &= M_c k^2 B'^2, \quad 0 \leq |\Delta| \leq \frac{W_N - B'}{2} \\ &= M_c k^2 \left[ \Delta^2 - (B' + W_N) |\Delta| + \frac{(B' + W_N)^2}{4} \right], \quad \frac{W_N - B'}{2} \leq |\Delta| \leq \frac{W_N + B'}{2} \quad (127) \\ &= 0, \quad |\Delta| \geq \frac{B' + W_N}{2} \end{aligned}$$

B.  $1/q \leq B' \leq W_N$ :

$$\begin{aligned} \text{Var}_A[F(H)] &= M_c k^2 \left[ \frac{2B'}{q} - \frac{1}{q^2} \right], \quad 0 \leq |\Delta| \leq \frac{W_N - B'}{2} \\ &= M_c k^2 \left[ \frac{B' + W_N - 2|\Delta|}{q} - \frac{1}{q^2} \right], \quad \frac{W_N - B'}{2} \leq |\Delta| \leq \frac{W_N + B'}{2} - \frac{1}{q} \quad (128) \\ &= M_c k^2 \left[ \Delta^2 - (B' + W_N) |\Delta| + \frac{(B' + W_N)^2}{4} \right], \quad \frac{W_N + B'}{2} - \frac{1}{q} \leq |\Delta| \leq \frac{W_N + B'}{2} \\ &= 0, \quad |\Delta| \geq \frac{B' + W_N}{2} \end{aligned}$$

C.  $B' \geq W_N$ :

$$\begin{aligned}
 \text{Var}_A[F(H)] &= M_c k^2 \left[ \frac{2W_N}{q} - \frac{1}{q^2} \right], \quad 0 \leq |\Delta| \leq \frac{B' - W_N}{2} \\
 &= M_c k^2 \left[ \frac{B' + W_N - 2|\Delta|}{q} - \frac{1}{q^2} \right], \quad \frac{B' - W_N}{2} \leq |\Delta| \leq \frac{B' + W_N}{2} - \frac{1}{q} \quad (129) \\
 &= M_c k^2 \left[ \Delta^2 - (B' + W_N)|\Delta| + \frac{(B' + W_N)^2}{4} \right], \quad \frac{B' + W_N}{2} - \frac{1}{q} < |\Delta| < \frac{B' + W_N}{2} \\
 &= 0, \quad |\Delta| \geq \frac{B' + W_N}{2} .
 \end{aligned}$$

The three resulting variance functions are shown in Figure (37).

In the light of practical measurement and signal processing problems, a most interesting quantity in the present context is the standard deviation of  $F(H)$  normalized by the mean. This statistic essentially indicates the spread of the probability distribution of  $F(H)$ , and hence the amount of variability to be expected in the filter output energy from sample to sample of the random transient ensemble. The approximate normalized standard deviation, here considered a function of  $B'$  and  $\Delta$ , is denoted  $R(B', \Delta)$  and is given by

$$R(B', \Delta) \equiv \frac{\sqrt{\text{Var}_A[F(H)]}}{E_A[F(H)]} \quad (130)$$

At the moment, we are almost in a position to compute this function. All of the approximate expressions for the expected value derived above can be written in the form

$$E_A[F(H)] = M_E k f_1(\Delta, B', q, z) \quad (131)$$

Similarly for the approximate energy variance,

$$\text{Var}_A[F(H)] = M_c k^2 f_2(\Delta, B', q, z) \quad (132)$$

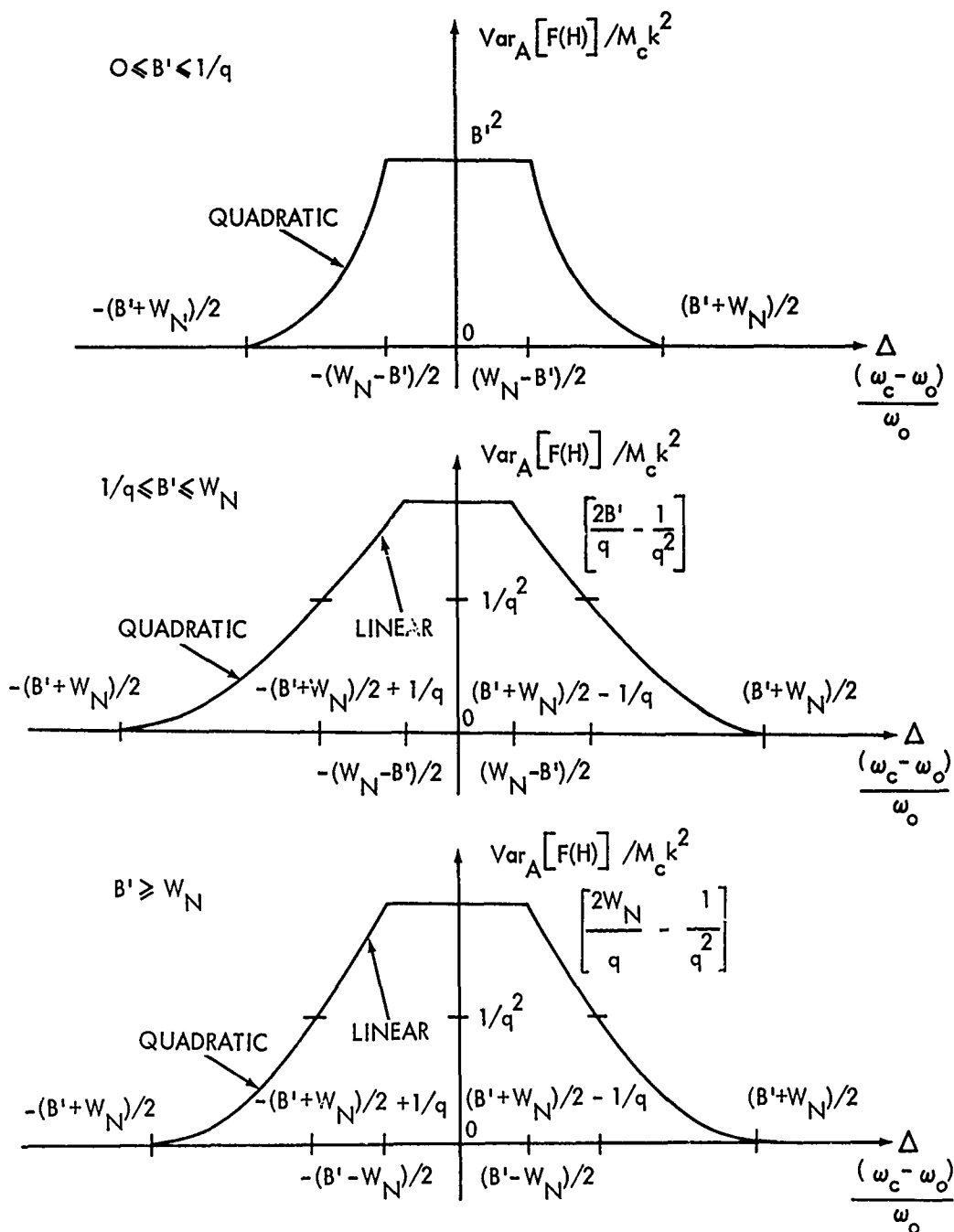


FIG. 37 APPROXIMATIONS FOR THE VARIANCE OF THE OUTPUT ENERGY OF A NARROW BAND FILTER WHEN EXCITED BY A RECTANGULAR PULSE OF NARROW BAND NOISE.

Thus,

$$R(B', \Delta) = \frac{\sqrt{M_c}}{M_E} \frac{\sqrt{f_2(\Delta, B', q, z)}}{f_1(\Delta, B', q, z)} \quad (133)$$

In the present example (i.e., that of passing a rectangular pulse of narrow band noise through the filter), it is found empirically (by direct calculations) that the maximum value of  $E_N[\phi_{SS}(r)]$  comes when  $r = 1$ . Similarly, the maximum value of  $Cov_N[\phi_{SS}(r), \phi_{SS}(s)]$  occurs when  $r = s = 1$ . Thus we may write, from equations (102) and (104), that

$$M_E = 2q \int_0^1 (1-x) \frac{\sin \pi q z x}{\pi q z x} \cos^2 2\pi q x dx \quad (134)$$

$$M_c = 4q^2 \left\{ \left[ \int_0^1 (1-x) \frac{\sin \pi q z x}{\pi q z x} \cos 2\pi q x \frac{\sin 2\pi q (1-x)}{2\pi q (1-x)} dx \right]^2 + \left[ \int_0^1 (1-x) \frac{\sin \pi q z x}{\pi q z x} \cos^2 2\pi q x dx \right]^2 \right\} \quad (135)$$

It is also found empirically that in equation (135), the first squared integral is negligible compared to the second. Thus  $M_c \approx M_E^2$ , and  $\sqrt{M_c}/M_E$  drops out of the ratio of equation (133).  $R(B', \Delta)$  may now be computed from equations (122), (123), and (127) - (129). Again, there are three cases to consider, depending upon the relative magnitude of  $B'$ :

A. For  $0 \leq B' \leq 1/q$ :

$$R(B', \Delta) = 1, \quad 0 \leq |\Delta| \leq \frac{B' + W_N}{2} \quad (136)$$

undefined elsewhere.

B. For  $1/q \leq B' \leq W_N$ :

$$R(B', \Delta) = \frac{\sqrt{2B'q-1}}{qB'}, \quad 0 \leq |\Delta| \leq \frac{W_N - B'}{2}$$

$$= \frac{2\sqrt{q(B'+W_N - 2|\Delta|)} - 1}{q(B'+W_N - 2|\Delta|)}, \quad \frac{W_N - B'}{2} \leq |\Delta| \leq \frac{W_N + B'}{2} - \frac{1}{q} \quad (137)$$

$$= 1, \quad \frac{W_N + B'}{2} - \frac{1}{q} \leq |\Delta| \leq \frac{W_N + B'}{2}$$

undefined elsewhere

C. For  $B' \geq W_N$ :

$$R(B', \Delta) = \frac{\sqrt{2W_N q - 1}}{qW_N}, \quad 0 \leq |\Delta| \leq \frac{B' - W_N}{2} \quad (138)$$

$$= \frac{2\sqrt{q(B'+W_N - 2|\Delta|)} - 1}{q(B'+W_N - 2|\Delta|)}, \quad \frac{B' - W_N}{2} \leq |\Delta| \leq \frac{B' + W_N}{2} - \frac{1}{q}$$

$$= 1, \quad \frac{B' + W_N}{2} - \frac{1}{q} \leq |\Delta| \leq \frac{B' + W_N}{2}$$

undefined elsewhere

The standard deviation ratio is shown in Figure 38 for the three cases defined above.

Another way of presenting the same data is to choose a given filter center frequency (which plays the role of a parameter) and then to study the output energy as a function of the filter bandwidth for a random transient ensemble of given parameters. In the present example, if we center the filter on  $\omega_0$  (i.e.,  $\omega_c = \omega_0$ ),  $\Delta$  becomes zero, and the normalized standard deviation as a function of  $B'$  becomes

$$\begin{aligned} R(B', 0) &= 1, \quad 0 \leq B' \leq 1/q \\ &= \frac{\sqrt{2B' q - 1}}{B' q}, \quad \frac{1}{q} \leq B' \leq W_N \\ &= \frac{\sqrt{2W_N q - 1}}{W_N q}, \quad B' \geq W_N \end{aligned} \quad (139)$$

This function is plotted as Figure 39.

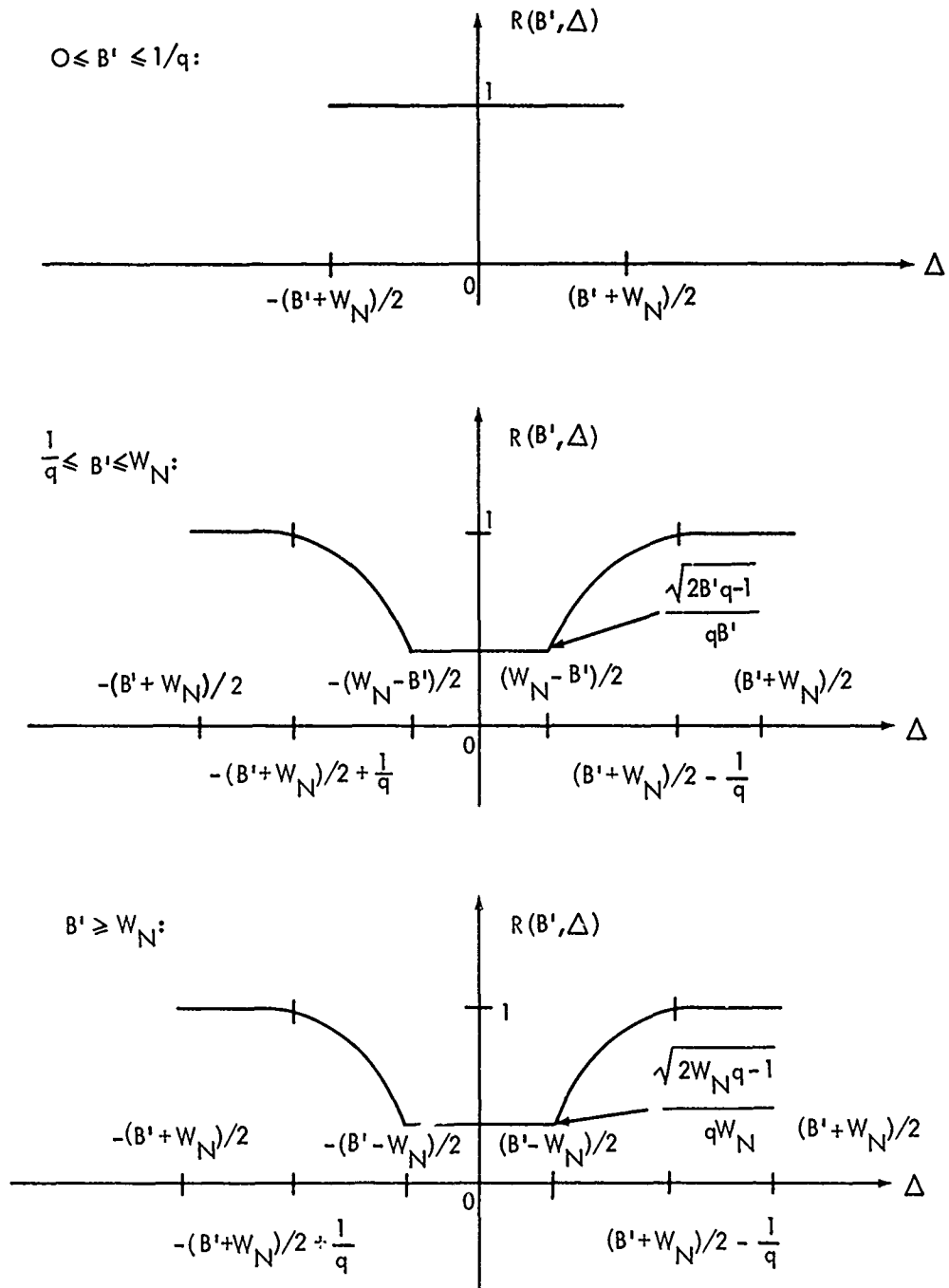


FIG. 38 APPROXIMATIONS FOR THE NORMALIZED STANDARD DEVIATION OF THE ENERGY OUT OF A NARROW BAND FILTER WHEN EXCITED BY A RECTANGULAR PULSE OF NARROW BAND NOISE.

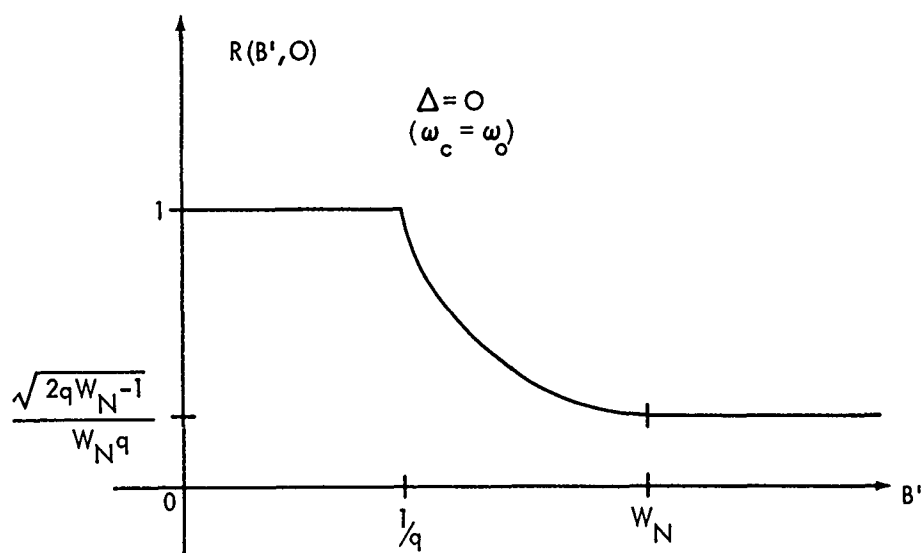


FIG.39 THE NORMALIZED STANDARD DEVIATION OF THE ENERGY OUT OF A NARROW BAND FILTER AS A FUNCTION OF NORMALIZED FILTER BANDWIDTH WHEN THE FILTER IS CENTERED ON THE CENTER FREQUENCY OF THE UNDERLYING INPUT NOISE PROCESS.

The expressions presented above for  $E_A[F(H)]$ ,  $\text{Var}_A[F(H)]$ , and  $R(B', \Delta)$  only roughly represent the actual functions, and one naturally inquires about the accuracy of these approximations. It appears that  $E_A[F(H)]$  and  $\text{Var}_A[F(H)]$  are useful principally for their portrayal of the rough functional dependence of the output energy mean and variance on the filter band-width and center frequency and the random transient parameters. Hence, a fairly good idea of the effects of parameter changes can be gained from the treatment given above, but not too much reliance should be placed on the exact functional form derived nor on the absolute magnitudes arrived at for the energy mean and variance. For  $R(B', \Delta)$ , on the other hand, which is probably the function of most interest, several of the uncertain factors cancel each other out, and the approximation well represents the actual state of affairs in both magnitude and rough functional form. The author feels that the approximation presented for  $R(B', \Delta)$  is correct to within 20% of its actual value, with higher accuracies for small  $\Delta$  and cases where  $q$  is much larger than unity. The basis for this estimate is a comparison of the approximate results with the values found for several points by an accurate numerical integration (at an enormous expense in computer time). These agreed to within 10%. Naturally, by devising more elaborate approximations for the spectral covariance surface, one could achieve any degree of accuracy required in the final result. For a wide variety of purposes, the present degree of complexity is adequate to provide considerable insight into the frequency filtering of random transient waveforms. At the very least, these results provide order of magnitude estimates for the statistical uncertainty of the filter output energies, and they thus pave the way for the preparation of adequate measurement programs and monopulse processing studies. If greater precision is required, the methodology for achieving it is clear from the above treatment.

What, then, have we found? Given a random transient generated by multiplying a narrow band Gaussian process by a square-integrable deterministic envelope, the results gained here enable one to estimate with reasonable accuracy the amount of variation from sample to sample in the output energy of narrow band filters to whose inputs such random transients are applied. The results presented have been derived in particular for rectangular envelopes, but as the discussion at the end of the last chapter indicates, they apply also to any envelope function of approximately the same length, the detailed structure of the envelope playing little role in the final outcome.

The collected results can be placed in best perspective by considering the inter-relationships of the three band-widths which arise in treating the problem. These are:

1. The band-width of the underlying noise process,  $2\Delta\omega$ . In its normalized version, this has been denoted  $z$  ( $z \equiv \frac{2\Delta\omega}{\omega_0}$ ).
2. The band-width associated with the envelope spectrum. If the nominal length of the envelope function is  $T$ , this is on the order of  $4\pi/T$ , or when normalized,  $2/q$  (since  $q = \frac{\omega_0 T}{2\pi}$ ).
3. The filter band-width  $B$ , or in its normalized version  $B' = B/\omega_0$ .

As we have noted above, the normalized approximate average spectral width for a random transient ensemble is given by

$$W_N = \frac{2}{q} + z,$$

i.e., the sum of the normalized noise and envelope spectral width. The  $r - s$  plane area of significant covariance changes its shape in accordance with the relative magnitudes of  $2/q$  and  $z$ . If  $z$  is small compared to  $2/q$ ,  $W_N \approx 2/q$ , and the transverse width of the covariance peak becomes comparable to its length, as in Figure 25 (where  $z = 0.1$  and  $q = 10.0$ ). For larger  $z$ , the width of the ridge becomes narrow compared to its length, implying that  $\phi_{SS}(\omega)$  and  $\phi_{SS}(\omega')$  covary strongly only when  $\omega \approx \omega'$ . Such a case is shown in Figure 21 (where  $z = 0.1$  and  $q = 50.0$ ). As noted above, the variance of the filter output energy can be visualized as the area of overlap between the "filter square", whose side is length  $B'$ , and the covariance area referred to above (see Figure 36). In situations where  $2/q \ll z$  and  $W_N \approx z$ , it is evident that this variance decreases as  $q$  increases, i.e., as the transient lengthens in terms of a typical noise period, since the width of the ridge goes as  $1/q$  while its length, proportional to  $W_N$ , remains constant.

The square of the output energy mean,  $E_A^2[F(H)]$ , can be interpreted in turn as being proportional to the overlap area of the filter square and a square whose side is of length  $W_N$ , as shown in Figure 40. (This emerges from equation (119) and Figure 33). Thus,  $R^2(B', \Delta)$  can be interpreted as the ratio of two areas overlapped by the filter square - that overlapped on the covariance hexagon, and that overlapped on the "expected value square". (See also Figure 40.) From this viewpoint, it becomes immediately obvious what degree of statistical reliability can be expected from measurements on random transients represented in the  $r - s$  plane as covariance hexagons. We see, for example, that  $R(B', \Delta)$  can never exceed unity since the covariance hexagon is contained entirely within the expected value square. Furthermore, when  $B' \leq 1/q$ , the filter square can be contained entirely within the covariance area, and  $R(B', \Delta)$  must always be unity, as shown by equation (136) or Figure 39. This immediately implies a very significant fact: that it is completely impossible to obtain consistent, i.e., repeatable, filter output energies for an arbitrarily narrow filter band-width. For high spectral resolution, naturally  $B'$  should be as narrow as possible, but this very narrowness destroys the stability of the measurement, and a trade-off becomes decidedly necessary. An uncertainty principle is at work here: the more narrowly we try to isolate the amount of spectral energy in a given frequency band, the less precise the estimate becomes in a statistical sense.

At the cost of spectral resolution, more stable estimates can be produced by increasing  $B'$ , i.e., the band-width of the analyzing filter. This is precisely demonstrated in Figure 39 for the special case of  $\omega'_c = 1$  ( $\Delta = 0$ ). For given  $q$  and  $W_N$ , however, there is a lower limit to the normalized standard deviation, given by

$$R_{\min}(B', \Delta) = \frac{\sqrt{2qW_N-1}}{W_Nq} = \frac{\sqrt{2qz+3}}{qz+2} = \frac{\sqrt{\pi} \sqrt{2T\Delta\omega+3\pi}}{T\Delta\omega+2\pi} \quad (140)$$

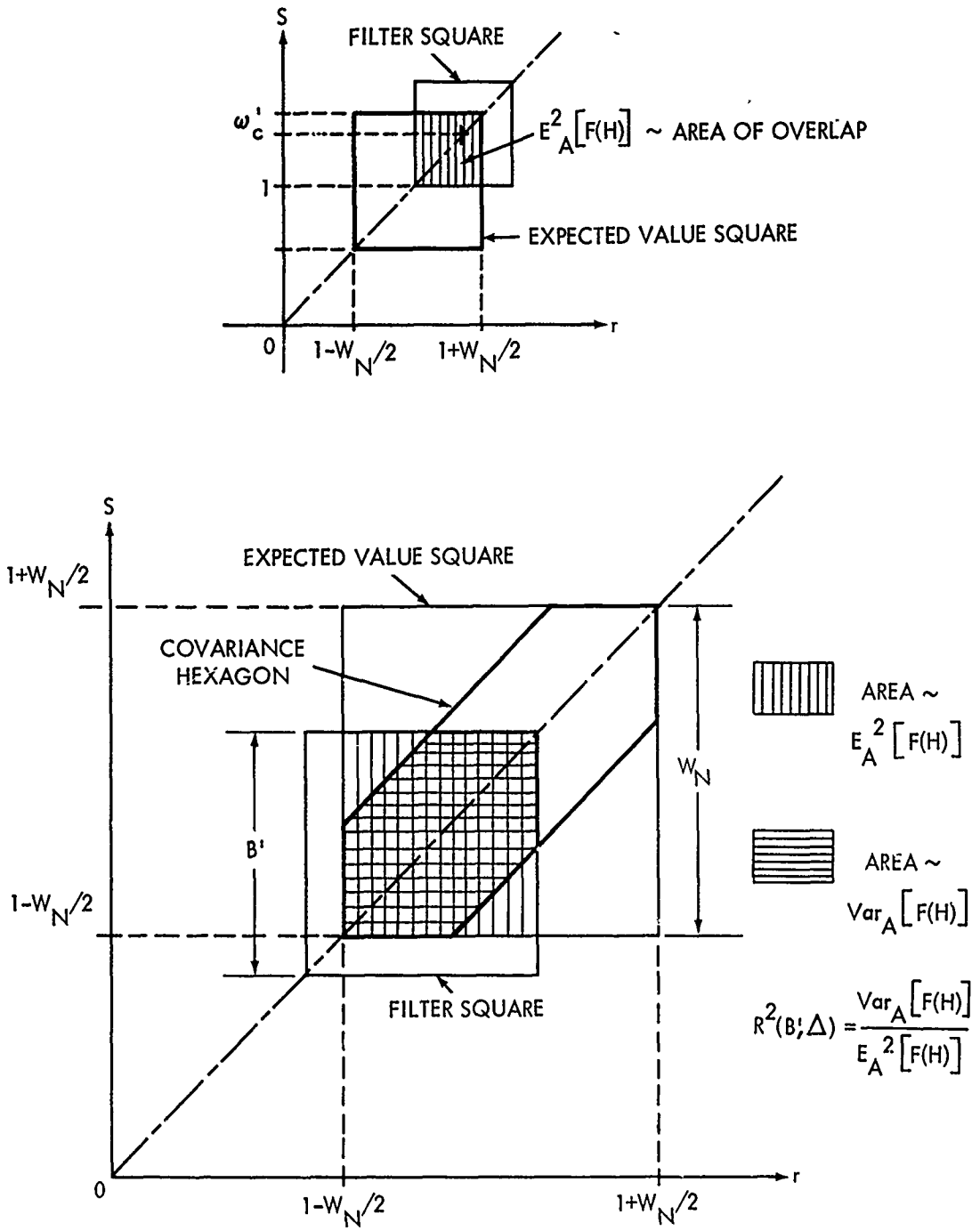


FIG. 40 A GRAPHICAL INTERPRETATION OF THE DETERMINATION OF  $R^2(B', \Delta)$  AS THE RATIO OF TWO AREAS OVERLAPPED BY THE FILTER SQUARE.

reached when  $B' = W_N$ . In Figure 40, this is when the filter square becomes the same size as the expected value square. Note that at this point virtually all spectral resolution has been sacrificed, and still the spectral estimate cannot be made arbitrarily precise. This is a direct consequence of dealing with random functions of finite length.

For given  $q$  and with  $B' < W_N$  (in an attempt to salvage some spectral resolution) the minimum value of normalized standard deviation achievable is given by

$$R_{\min}(B', \Delta) = \frac{\sqrt{2B'q-1}}{qB'} , \quad B' \leq W_N \quad (141)$$

Note that from our parameter definitions,

$$B'q = \frac{B}{\omega_0} \times \frac{\omega_0 T}{2\pi} = \frac{BT}{2\pi} \quad (142)$$

Thus, for large  $B'q$  products,

$$R_{\min}(B', \Delta) \approx \frac{\sqrt{2}}{\sqrt{qB'}} = \frac{\sqrt{4\pi}}{\sqrt{BT}} , \quad B' \leq W_N \quad (143)$$

which is essentially the result found in reference (h), section 5.4.5, for the normalized standard deviation of a spectral measurement performed with the bandwidth of the analyzing filter ( $B$ ) small compared with the bandwidth of the process, when the filter output is observed and averaged for  $T$  seconds. An alternative approach for this special case is presented in Appendix C, Equation (143) is a theoretical confirmation of the rule-of-thumb frequently quoted in spectral analysis that a large band-width-time product is necessary for statistical accuracy.

The uncertainty principle referred to above may be stated explicitly as follows: if the bandwidth of the analyzing filter is less than the effective spectral width of the ensemble, i.e., if  $B' < W_N$ , the minimum normalized output energy standard deviation is given by equation (141). We have also seen that for large  $B'q$  products that

$$R_{\min}(B', \Delta) \approx \frac{\sqrt{4\pi}}{\sqrt{BT}} , \quad B' \leq W_N$$

which implies immediately that

$$R^2(B', \Delta) > \frac{4\pi}{BT} , \quad B' \leq W_N \quad (144)$$

If  $T$  is considered a constant of the situation, then we may say that

$$BR^2(B', \Delta) > \frac{4\pi}{T}, \quad B' < W_N \quad \text{and} \quad B'q > > 1 \quad (145)$$

that is, that the product of the analyzing bandwidth and the square of the normalized energy standard deviation (the normalized energy variance) will always be greater than  $4\pi/T$  (which may be identified, as in equation (106), as the effective double-sided spectral width of a square pulse of length  $T$ ).  $R^2(B', \Delta)$  can be interpreted as a measure of the precision with which the total energy in the band of interest can be specified, since it represents the variance of the probability distribution for the energy in the band. The smaller this variance becomes, the less variation is found in the band-wise energy content of different samples, and thus the more precisely this energy can be predicted before the event. Similarly,  $B$  reflects the extent to which the fine structure of the ensemble spectrum can be resolved by the filter, since this is the bandwidth over which the spectrum will be smoothed or averaged. Naturally, spectral details of width  $B$  or smaller will not be distinguished by a filter of that band-width, but the smaller that  $B$  becomes, the higher becomes the spectral resolution obtainable. We of course would like  $B$  and  $R^2(B', \Delta)$  to be simultaneously as small as possible so that spectral resolution and amplitude stability are both high. Equation (145) demonstrates immediately, however, that it is impossible to attain arbitrarily high precision in both resolution and amplitude at the same time since the product of the frequency and amplitude "uncertainties" must always exceed  $4\pi/T$ . Thus, a decrease in the uncertainty of the spectral amplitude comes at the expense of a concomitant increase in the averaging band and thus a decrease in spectral resolution. The single parameter that determines the lower limit of the uncertainty product is the effective length of the envelope function  $T$ , and in general, the simultaneous uncertainty varies in inverse proportion to this quantity.

It is also seen above that there is a definite lower limit to the normalized standard deviation for an ensemble of given parameters, and this is reached when  $B' = W_N$ . This lower limit is precisely the standard deviation of the total energy of an ensemble member and, our uncertainty principle notwithstanding, cannot be reduced by further sacrifices of frequency resolution, since indeed there is none left to sacrifice. The situation here is such that the uncertainty relation stated is not unrestricted, and that not only are we prevented from attaining arbitrarily high amplitude precision and frequency resolution simultaneously, but there is even a limit on the extent to which the latter can be traded for the former. This limit is given as a function of the ensemble parameters in equation (140).

The foregoing should provide the interested reader with at least some insight into the spectral distribution of energy in narrow band random transients. The extension to the broad band case is straightforward and leads to the same basic principle - that a trade-off between spectral resolution and statistical reliability is always necessary, and that there is a certain lower limit to the normalized energy standard deviation which is determined by the parameters of the random transient ensemble, and which cannot be avoided no matter what kind of filtering is employed. In all cases, as  $B' \rightarrow 0$ , the filter output energy approximates the so-called periodogram for  $\phi_{SS}(\omega)$ , for which it can be shown that  $R(B', \Delta) \geq 1$ , making it an inconsistent estimate of  $\phi_{SE}(\omega)$  in the statistical sense (see reference (c), pp 107-108).

## Chapter V

## CONCLUSIONS AND SUGGESTIONS FOR FUTURE RESEARCH

The theory set forth in the present report is a logical extension of the methods outlined in its predecessor (reference (a)), and the treatment of random transient frequency filtering given here has wide application in areas of present interest. These fall into two broad classes: spectral analysis of transient random waveforms; and monopulse signal processing applications where the effects of sample-to-sample variations are important. These will be treated separately.

One of the central problems of traditional spectral analysis is the empirical estimation of the power spectrum of a continuing stationary process, given a sample record of some finite length  $T$ . The "intuitive" approach of computing the squared magnitude of the empirical Fourier transform of the sample record and dividing by  $T$  provides the so-called periodogram of the record. Unfortunately, the periodogram is a random variable for every value of  $\omega$  which has at all points a standard deviation at least as large as the mean, no matter how long the sample record is taken. Contrary to intuition, then, the periodogram is not a consistent estimator of the power spectrum as  $T$  increases without limit. For this reason, a number of alternative methods have been devised which provide power spectral estimates averaged over a band of frequencies as opposed to attempting a point estimate. In the well-known work of Blackman and Tukey (reference (i)), these estimates are obtained by weighting the empirical autocorrelation function, before it is Fourier transformed, to yield band-integrated power spectrum estimates of high statistical reliability. Similarly, Bendat and Piersol (reference (h)) provide a rough description of the use of narrow band filters for empirical spectrum measurement. In both approaches, it is found that the price paid for higher statistical reliability is longer sample lengths, or decreased spectral resolution, or both. For resolving the spectral fine structure of the process of interest, the analyzing band-width should be as narrow as possible. Unfortunately, the narrower this bandwidth, the less precise the estimate becomes. For ease of computation and data handling, the sample length should be as short as possible. Unfortunately, the shorter the sample taken, the larger becomes the standard deviation of the estimate. Indeed, as noted above at the close of Chapter IV, this standard deviation, as a percentage of the mean, is on the order of  $1/\sqrt{BT}$ , and for arbitrary accuracy, a trade-off between the two factors is necessary.

Many of these same considerations apply to the analysis of energy spectra for random transient waveforms, and indeed the estimation of a process spectrum from a sample function of length  $T$  can be considered a special case of the transient spectral problem: that in which a rectangular envelope function of length  $T$  is selected, and one seeks from the separate realizations of the resulting random transient ensemble to estimate  $\Psi_{nn}(\omega)$  for the underlying noise process. There is, however, a difference in emphasis. In the case of random transient spectral analysis, one has no control over  $T$ , or the effective length of the signal, and is faced with the task of making the best of the situation in

deriving a meaningful spectral description. In a theoretical approach, where there are reasonable grounds for assuming the form of  $e(t)$  and  $\psi_{nn}(\omega)$ , the present theory provides expressions for the expected value of the random transient spectrum at a point and also its variance. As we have seen, this variance is rather large, no matter what the effective length of the transient. We have thus learned very little about the spectrum of a single sample since the probability distribution for the spectrum at a point is so widely spread. One way out is to formulate predictions of the spectral energy lying in non-zero bands, since for these the normalized standard deviation will be on the order of  $1/\sqrt{BT}$ , where  $B$  is the analyzing bandwidth (here in hertz). Naturally, spectral resolution is sacrificed in this approach, but this is the price that must be paid for statistical consistency. In this world, one never gets something for nothing.

In an experimental approach, where one is given a collection of realizations of the random transient process, and the problem at hand is to determine the spectral character with no a priori knowledge about the source, filtering to an arbitrarily narrow frequency band destroys the repeatability of the results from sample to sample, and an average value may or may not constitute a reasonable prediction for the result to be found in dealing with an individual sample. Probably the best course of action here is to calculate the empirical means and variances as a means to estimating limits on the sample-to-sample variations. It must always be kept in mind that it is simply impossible to predict the energy density spectrum of a single transient with simultaneous arbitrary precision in spectral resolution and amplitude. This is particularly true in cases where the effective width of the envelope spectrum is significantly larger than that of the noise process, since increasing the analysis bandwidth does not produce a decrease in the standard deviation of the results until this bandwidth becomes commensurate with the effective spectral width of the transient itself.

In monopulse signal processing situations where either the signal of interest, or the interfering noise, can be modeled as a random transient of the type assumed in this work, the results found here predict the extent to which filter output energies vary from pulse to pulse. Admittedly, narrow band filtering represents but one of many processing techniques that might be employed. Still, it is probably the most basic and indicates the kind of effect to be expected in more general situations. In predicting the signal-to-noise ratio at the output of a narrow band filter, or in predicting the results of thresholding operations following such filtering, the statistical deviation from sample to sample must be considered. If the system is tailored too closely to the expected value of the output energies, it may well malfunction when those samples arrive, which, because of the inherent statistical nature of the ensemble, yield output energies significantly different from the mean. Obviously, this difficulty can be alleviated by increasing the filter bandwidth and thus decreasing the statistical spread, but often this deteriorates the signal-to-noise ratio out of the device, and another difficult problem of trade-offs appears. For reasonable statistical stability, the product of the effective pulse duration and analyzing bandwidth should be appreciably greater than unity, but admittedly this may not always be possible. It should be noted that the absolute lower limit for the output energy standard deviation as a percentage of the mean is on the order of  $1/\sqrt{TW_N}$  no matter what filter bandwidth is used. For certain random transient ensembles, therefore, particularly those whose effective spectral width is controlled by the envelope spectrum (and thus is on the order of  $1/T$ ), the output standard deviation will always be large, no matter how it is analyzed. Ultimately, the use of narrow band filtering must be approached with care in monopulse processing systems with

particular attention to the opposing demands of finer resolution (and enhanced signal-to-noise ratio) and statistical stability. This study provides some insight and theoretical guidance in seeking an intelligent compromise.

### Suggestions for Future Research

There are several avenues of future research in both theoretical and experimental directions that can be proposed at the present time. In the latter area, it would be of great interest to generate an experimental ensemble of random transients and to subject representative sample functions to narrow band filtering in an attempt to test the predictions of the present theory. These experiments could be very efficiently performed using digital computer signal processing techniques. In particular, after producing a suitable random transient ensemble and recording its members on magnetic tape, it would be straightforward to sample and digitize the sample functions for computer analysis using digital filtering and Fast Fourier transform techniques. This would provide an immediate check on the appropriateness of the assumptions and simplifications used throughout and would lend a good deal of insight to the practical implications of sample-to-sample variations. Ultimately, these methods could be used to study the statistical/spectral properties of transient noise phenomena from the real world, such as EER returns and sonar reverberation. This would help in evaluating the model chosen and in selecting appropriate parameters for characterizing the signals of interest. It should be added that it may well be feasible to generate random transient sample functions entirely within the computer, using digital filtering techniques on a table of random numbers, and thus doing away with any "analog" portions of the experiment altogether. It remains to be seen which approach will be the most effective.

Many interesting questions have been raised on the theoretical front. As the reader has certainly noticed, the final results of the study have come out of a gross simplification of the spectral covariance surface. The proposed experimental study may well show that this approximation is inadequate, and in that event, a better characterization will be necessary. One is faced with the problem of devising expressions for the form of the surface which retain satisfactory accuracy while remaining in the realm of mathematical tractability. Perhaps an approach along the lines of an expansion in orthogonal functions would be appropriate here.

The narrow band filter is but one example of a linear system, albeit one of great practical and theoretical importance. It would be desirable to extend the present theory to embrace more general linear systems with transient random inputs. In particular, the correlation properties of the input and output of such systems and the notion of optimum linear filtering when signal or noise or both are random transients are of both practical and academic interest. The application of double-frequency Fourier transforms (see reference (h), Chapter 9 and reference (m), Chapter 12) is another area that bears study since there is a strong resemblance between that body of techniques and those developed here.

The study reported above has attempted to illuminate certain aspects of the behavior of transient random signals. In particular, it has concentrated on the problems that arise, due to the pulse nature of the waveforms, in seeking to formulate a meaningful description of the energy density spectrum of such signals. Among the most interesting findings have been the uncertainty relations that exist between spectral amplitude and frequency resolution and their implications, in

practical measurement and processing situations. This is but one aspect of a very general problem in scientific research; that of defining and coping with the inherent uncertainties and imprecision of scientific measurements. Certainly the realization that there are definite limits on our ability to resolve the detailed properties of natural phenomena has been one of the touch-stones of modern science, leading to overall average statistical descriptions. For this reason, it is not inappropriate to close with these perceptive words of Max Born (reference (j)):

"The concept of chance enters into the very first steps of scientific activity in virtue of the fact that no observation is absolutely correct. I think chance is a more fundamental conception than causality; for whether in a concrete case a cause-effect relation holds or not can only be judged by applying the laws of chance to observations."

EDWARD C. WHITMAN  
Magnetics and Electrical Division

APPENDIX A

The Spectral Normalization Problem

As noted in the main text, the purpose of the spectral normalization is to divorce the results of the analysis from specific parameter values, insofar as this is possible. For this reason, frequency variables have been expressed as ratios of actual frequency to the "typical" frequency of the underlying noise process ( $\omega_2$  in the broad band case;  $\omega_0$  in the narrow), and the length of the envelope has been expressed in terms of the number of "typical" noise periods contained in it. Where needed, time variables are normalized by division by the envelope length  $T$ . As an example, consider the rectangular pulse of broad band noise for which

$$E[\phi_{SS}(\tau)] = 2N_0 \omega_2 T \left(1 - \frac{|\tau|}{T}\right) \frac{\sin \omega_2 \tau}{\omega_2 \tau}, \quad -T \leq \tau \leq T \quad (A-1)$$

$$= 0, \text{ elsewhere}$$

By Fourier transformation,

$$E[\phi_{SS}(\omega)] = \frac{2N_0 \omega_2 T}{\pi} \int_0^T \left(1 - \frac{\tau}{T}\right) \frac{\sin \omega_2 \tau}{\omega_2 \tau} \cos \omega \tau \, d\tau \quad (A-2)$$

From Parseval's Theorem it is known that

$$\int_{-\infty}^{\infty} E[\phi_{SS}(\omega)] \, d\omega = E[\phi_{SS}(0)] = 2N_0 \omega_2 T, \quad (A-3)$$

which is the average total energy. Now introducing the parameters

$$x = \frac{\tau}{T} \quad (A-4a)$$

$$q = \frac{\omega_2 T}{2\pi} \quad (A-4b)$$

$$r = \frac{\omega}{\omega_2} \quad (A-4c)$$

and substituting these into equation (A-2) yields a function of  $r$ :

$$E[\phi'_{ss}(r)] = \frac{2N_o \omega_2 T^2}{\Pi} \int_0^1 (1-x) \frac{\sin 2\Pi qx}{2\Pi qx} \cos 2\Pi qxr \, dx \quad (A-5)$$

such that  $E[\phi_{ss}(\omega)] = E\left[\phi'_{ss}\left(r = \frac{\omega}{\omega_2}\right)\right]$

Now from equation (A-3) we know that

$$\int_{-\infty}^{\infty} E[\phi_{ss}(\omega)] \, d\omega = \int_{-\infty}^{\infty} E\left[\phi'_{ss}\left(r = \frac{\omega}{\omega_2}\right)\right] \, d\omega = 2N_o \omega_2 T \quad (A-6)$$

Making a change of variables in the second integral yields

$$\int_{-\infty}^{\infty} E\left[\phi'_{ss}\left(r = \frac{\omega}{\omega_2}\right)\right] \, d\omega = \int_{-\infty}^{\infty} \omega_2 E[\phi'_{ss}(r)] \, dr = 2N_o \omega_2 T \quad (A-7)$$

Thus,

$$\int_{-\infty}^{\infty} E[\phi'_{ss}(r)] \, dr = 2N_o T \quad (A-8)$$

For convenience, we ask that the normalized average total energy be unity. Evidently this is attained for the function

$$E_N[\phi_{ss}(r)] = \frac{1}{2N_o T} E[\phi'_{ss}(r)] \quad (A-9)$$

which gives

$$E_N[\phi_{ss}(r)] = \frac{\omega_2 T}{\Pi} \int_0^1 (1-x) \frac{\sin 2\Pi qx}{2\Pi qx} \cos 2\Pi qxr \, dx \quad (A-10)$$

or since  $q = \frac{\omega_2 T}{2\Pi}$ ,

$$E_N[\phi_{ss}(r)] = 2q \int_0^1 (1-x) \frac{\sin 2\Pi qx}{2\Pi qx} \cos 2\Pi qxr \, dx \quad (A-11)$$

It is easily seen from above that

$$\int_{-\infty}^{\infty} E_N[\phi_{SS}(r)] dr = 1 \quad (A-12)$$

and that

$$E[\phi_{SS}(\omega)] = 2N_o T E_N\left[\phi_{SS}\left(r = \frac{\omega}{\omega_2}\right)\right] \quad (A-13)$$

The extension of this normalization to the covariance expressions is straightforward and results in a definition of  $Cov_N[\phi_{SS}(r), \phi_{SS}(s)]$  such that

$$Cov[\phi_{SS}(\omega), \phi_{SS}(\omega')] = 4N_o^2 T^2 Cov_N\left[\phi_{SS}\left(r = \frac{\omega}{\omega_2}\right), \phi_{SS}\left(s = \frac{\omega'}{\omega_2}\right)\right] \quad (A-14)$$

One goes through a similar procedure to obtain the analogous expressions for the narrow band cases.

There is one disadvantage to the present normalization which may mislead the unwary unless it is pointed out. We know that  $E[\phi_{SS}(\omega)]$  is the Fourier transform of  $E[\phi_{SS}(\tau)]$  and vice-versa. What can be said of the Fourier transform of  $E_N[\phi_{SS}(r)]$ ? From equation (A-11) one can see that

$$\begin{aligned} E_N[\phi_{SS}(r)] &= \frac{1}{q} \int_{-1}^1 (1-|x|) \frac{\sin 2\pi qx}{2\pi qx} e^{-j2\pi qrx} dx \\ &= \frac{1}{2\pi} \int_{-2\pi q}^{2\pi q} \left(1 - \frac{|x|}{2\pi q}\right) \frac{\sin x}{x} e^{-jxr} dx \end{aligned} \quad (A-15)$$

Thus  $E_N[\phi_{SS}(r)]$  and the function

$$\begin{aligned} \phi'(x) &= \left(1 - \frac{|x|}{2\pi q}\right) \frac{\sin x}{x}, \quad -2\pi q \leq x \leq 2\pi q \\ &= 0, \quad \text{elsewhere} \end{aligned} \quad (A-16)$$

are a Fourier transform pair. This is not the expression one gets from equation (A-1) by setting  $2N_0\omega_2T = 1$  and substituting the parameters of equations (A-4). As a matter of fact, under these conditions, equation (A-1) becomes

$$E[\phi_{ss}(x)] = (1 - |x|) \frac{\sin 2\pi qx}{2\pi qx}, \quad -1 \leq x \leq 1 \quad (\text{A-17})$$

$$= 0, \quad \text{elsewhere}$$

and thus is not the Fourier transform of  $E_N[\phi_{ss}(r)]$ .

## APPENDIX B

## THE "WIDTH" OF THE CONVOLUTION OF TWO FUNCTIONS

In the main body is made the statement that in an approximate sense, "the width of the convolution of two even functions is equal to the sum of the widths of the functions themselves." This approximation sees constant use in practical treatments of modulation, transient analysis, and sampling theory. This appendix gives explicit justification for the cases of major interest in this report.

If  $f(x)$  and  $g(x)$  are two real functions, their convolution, subject to certain existence conditions, is given by

$$c(x) = f(x) \otimes g(x) = \int_{-\infty}^{\infty} f(u) g(x-u) du = \int_{-\infty}^{\infty} g(u) f(x-u) du \quad (\text{B-1})$$

If  $f(x)$  and  $g(x)$  are both even functions, then

$$g(x-u) = g(u-x) \quad (\text{B-2a})$$

and

$$f(x-u) = f(u-x) \quad (\text{B-2b})$$

and thus

$$c(x) = \int_{-\infty}^{\infty} f(u) g(u-x) du = \int_{-\infty}^{\infty} g(u) f(u-x) du = \phi_{fg}(-x) \quad (\text{B-3})$$

where  $\phi_{fg}(x)$  is the cross-correlation function of  $f(x)$  and  $g(x)$  defined as

$$\phi_{fg}(x) \equiv \int_{-\infty}^{\infty} f(u) g(u+x) du \quad (\text{B-4})$$

Furthermore, when both functions are even,  $\phi_{fg}(x) = \phi_{fg}(-x)$  and thus

$$c(x) = \phi_{fg}(x) \quad (\text{B-5})$$

which is to say that the convolution of  $f(x)$  and  $g(x)$  is the same as their cross-correlation function. In the present application, we deal with power and energy density spectra, which are indeed real, even functions, integrable over the whole real line. In the low pass cases, these functions are concentrated at the origin and tend to zero as their arguments approach  $+\infty$  or  $-\infty$ . One can thus define a spectral half width  $W$  which represents the positive frequency range for which the spectral amplitude differs significantly from zero. In band pass situations, a spectral width can similarly be defined for the spectral concentration around the center frequency. Admittedly, the criteria one uses to define the spectral width are arbitrary and subject to question, but if it is consistently defined in the problem of interest, the interpretation should be unambiguous.

As an example, consider the case where both convolved functions are rectangular pulses of unit amplitude, entered at the origin:

$$f(x) = 1, \quad -A \leq x \leq A \quad (B-6)$$

$$= 0, \quad \text{elsewhere}$$

$$g(x) = 1, \quad -B \leq x \leq B \quad (B-7)$$

$$= 0, \quad \text{elsewhere}$$

Assuming that  $A \geq B$  and using equation (B-3), we find that

$$\begin{aligned} c(x) &= f(x) \otimes g(x) = x + A + B, \quad -A - B \leq x \leq -A + B \\ &= 2B, \quad -A + B \leq x \leq A - B \quad (B-8) \\ &= A + B - x, \quad A - B \leq x \leq A + B \\ &= 0, \quad |x| > A + B \end{aligned}$$

This is shown graphically in Figure B-1. If the function half-widths are defined as the positive frequency spread for which they are non-zero, it is evident that

$$W_f = A \quad (B-9a)$$

$$W_g = B \quad (B-9b)$$

and that

$$W_c = A + B = W_f + W_g \quad (B-10)$$

which confirms the result. This is a very important special case, since in practice one often approximates spectra of arbitrary shape as rectangular idealizations whose amplitude is set equal to the maximum value of the spectrum of interest and whose "equivalent width" is chosen to set the area under the approximation equal to that under the actual curve.

Another example of interest is that where  $f(x)$  and  $g(x)$  are both double sided decaying exponentials:

$$f(x) = e^{-|x|/A}, \quad -\infty < x < \infty \quad (B-11)$$

$$g(x) = e^{-|x|/B}, \quad -\infty < x < \infty \quad (B-12)$$

with  $A > B$ . A reasonable measure of the function half-width in this case is that point where the function amplitude falls to  $1/e$  times its value at the origin. This gives

$$W_f = A \quad (B-13a)$$

$$W_g = B \quad (B-13b)$$

From equation (B-3), we find that

$$c(x) = f(x) \otimes g(x) = \frac{AB}{A+B} \left( e^{-|x|/A} + e^{-|x|/B} \right) + \frac{AB}{A-B} \left( e^{-|x|/A} - e^{-|x|/B} \right), \quad (B-13)$$

$$-\infty < x < \infty$$

The constituent functions and the resulting convolution are shown for two cases in Figure B-2. If the half-width of the convolution is taken as the argument for which the amplitude falls to  $1/e$  times its value at the origin, the following table of computed results can be derived using equation (B-13):

$W_f = A$	$W_g = B$	$W_f + W_g$	$W_c = c^{-1}(1/e)$
1.0	0.9	1.9	2.06
1.0	0.5	1.5	1.59
1.0	0.25	1.25	1.29
1.0	0.1	1.1	1.11

One again concludes that  $W_c \approx W_f + W_g$  with the approximation becoming better and better as  $g(x)$  becomes increasingly narrow with respect to  $f(x)$ .

The generality of this conclusion is made even more plausible by those interpretations of the convolution integral which treat  $g(-s)$  as a "scanning function" which slides along  $f(x)$  to generate a smoothed version of the latter (see reference (k), p 323, and reference (l), p 71). Naturally, the wider  $g(x)$  becomes, the more broadly will  $f(x)$  be smoothed out, and the width of the smoothed version will be proportional to the sum of the widths of  $f(x)$  and  $g(x)$ .

It is easily seen in this graphical interpretation that in cases where one of the two convolved functions is of band pass nature and the other of low pass character, the resulting convolution will yield a smoothed (broadened) version of the former centered at the original center frequency with an equivalent width approximately equal to the sum of the double sided width of the two constituents. This is precisely what is done in the familiar spectral interpretation of amplitude modulation.

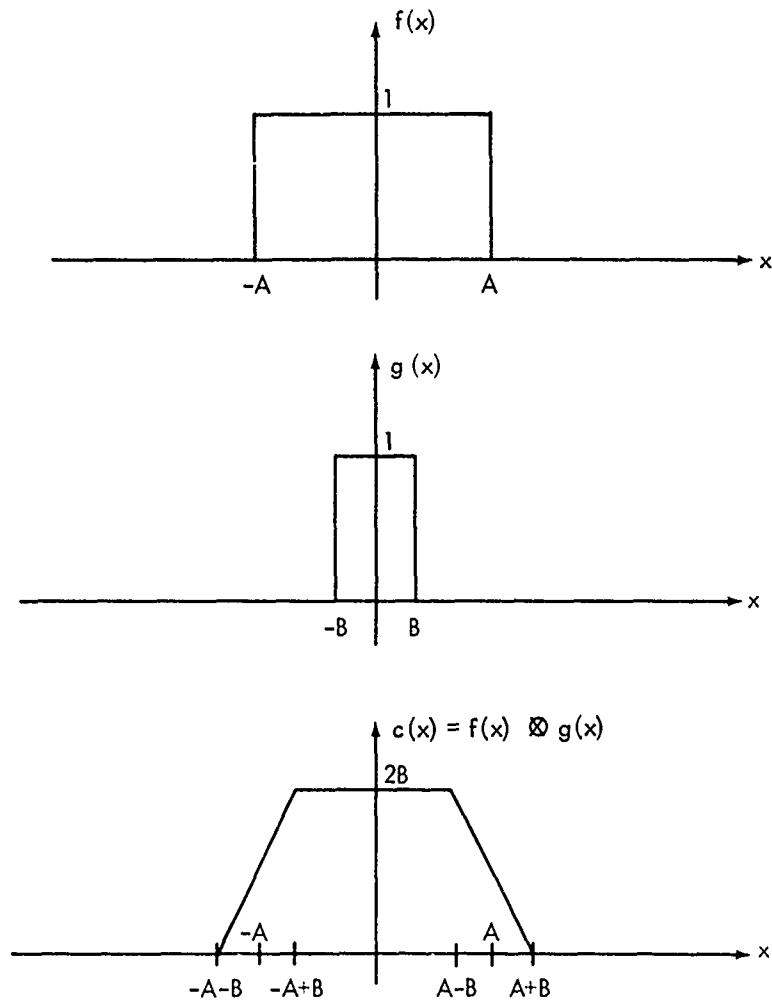


FIG. B-1 THE CONVOLUTION OF TWO RECTANGULAR PULSES.

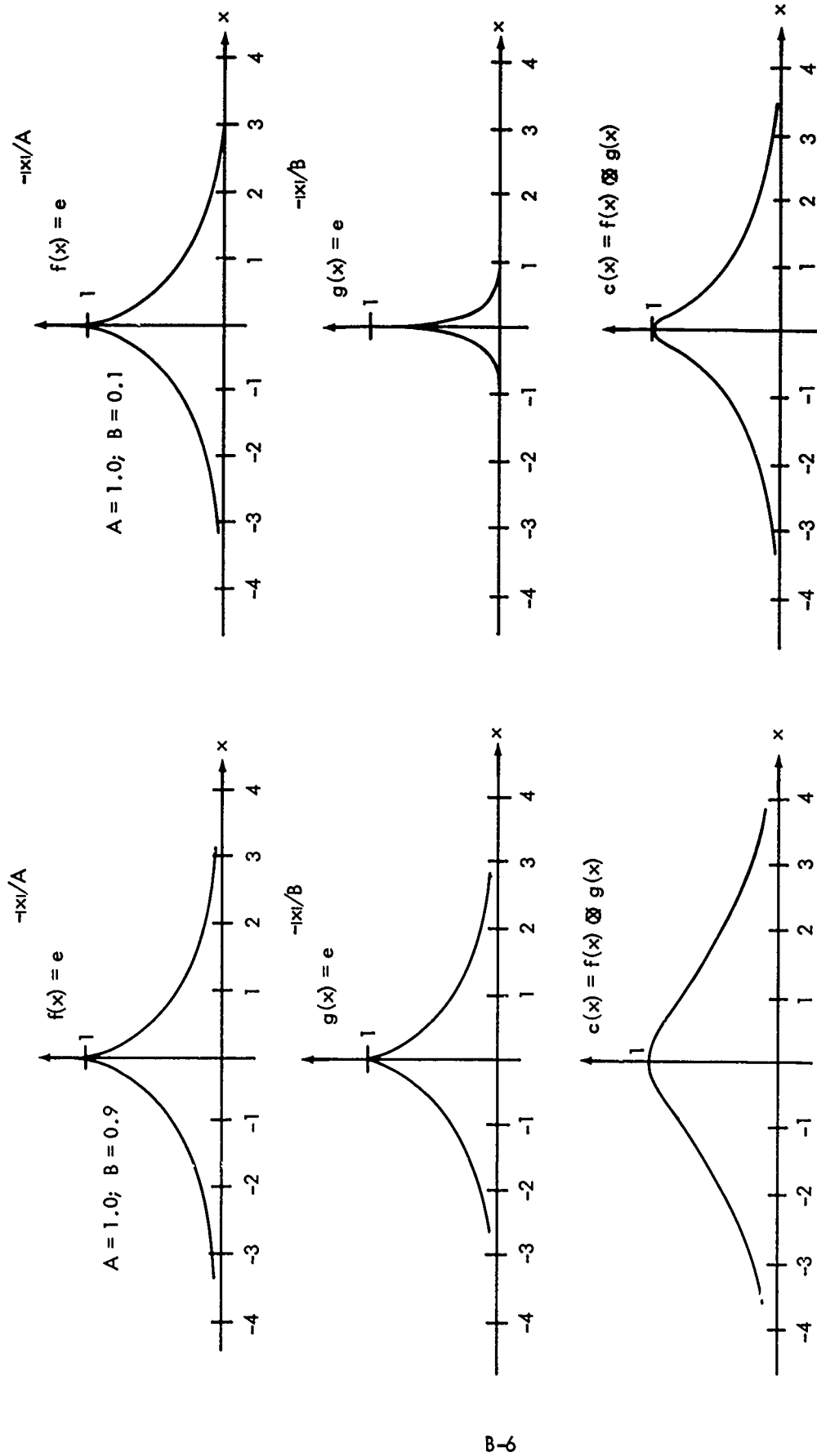


FIG. B-2 CONVOLUTION OF DOUBLE-SIDED DECAYING EXPONENTIAL PULSES FOR TWO SETS OF PARAMETER VALUES. ALL AMPLITUDES HAVE BEEN NORMALIZED TO UNITY AT THE ORIGIN.

APPENDIX C

An Alternative Approach to the Narrow Band Filtering Problem  
with a Solution for an Important Special Case

Consider passing a random transient ensemble through the narrow band filter given by equation (109) and Figure 31. By equation (113),

$$E[F(H)] = \frac{1}{2} \int_{\omega_c - B/2}^{\omega_c + B/2} E[\phi_{SS}(\omega)] d\omega \quad (C-1)$$

Now by equation (8) this is

$$E[F(H)] = \frac{1}{\pi} \int_{\omega_c - B/2}^{\omega_c + B/2} \int_{-\infty}^{\infty} \psi_{nn}(x) \phi_{ee}(x) e^{-j\omega x} dx d\omega \quad (C-2)$$

Interchanging the order of integration yields

$$\begin{aligned} E[F(H)] &= \frac{1}{\pi} \int_{-\infty}^{\infty} \psi_{nn}(x) \phi_{ee}(x) \int_{\omega_c - B/2}^{\omega_c + B/2} e^{-j\omega x} d\omega dx \\ &= \frac{B}{\pi} \int_{-\infty}^{\infty} \psi_{nn}(x) \phi_{ee}(x) \frac{\sin \frac{x B}{2}}{\frac{x B}{2}} e^{-j\omega_c x} dx \end{aligned} \quad (C-3)$$

since  $\psi_{nn}(x)$  and  $\phi_{ee}(x)$  are both even functions of  $x$ .

From equation (115), we know that

$$\text{Var}[F(H)] = 4 \int_{\omega_c - B/2}^{\omega_c + B/2} \int_{\omega_c - B/2}^{\omega_c + B/2} \text{Cov}[\phi_{SS}(\omega), \phi_{SS}(\omega')] d\omega d\omega' \quad (C-4)$$

where  $\text{Cov}[\phi_{SS}(\omega), \phi_{SS}(\omega')]$  is given by equations (41) and (44) as

$$\text{Cov}[\phi_{SS}(\omega), \phi_{SS}(\omega')] = \tag{C-5}$$

$$\frac{1}{4\pi^2} \int_0^\infty \int_0^\infty \int_0^\infty \int_0^\infty e(t)e(x)e(u)e(v)\psi_{nn}(t-u)\psi_{nn}(x-v)e^{-j\omega(t-x)}e^{-j\omega'(u-v)} dt dx du dv$$

$$+ \frac{1}{4\pi^2} \int_0^\infty \int_0^\infty \int_0^\infty \int_0^\infty e(t)e(x)e(u)e(v)\psi_{nn}(t-v)\psi_{nn}(x-u)e^{-j\omega(t-x)}e^{-j\omega'(u-v)} dt dx du dv$$

When equation (C-5) is used in equation (C-4), some judicious manipulation makes it possible to perform the integrations on  $\omega$  and  $\omega'$ . The following expression emerges:

$$\text{Var}[F(H)] = \frac{1}{\pi^2} \int_{-\infty}^\infty \int_{-\infty}^\infty \int_0^\infty \int_0^\infty e(t)e(t-a)e(u)e(u-b) \tag{C-6}$$

$$[\psi_{nn}(t-u)\psi_{nn}(t-a-u+b) + \psi_{nn}(t-u+b)\psi_{nn}(t-u-a)]$$

$$\frac{\sin aB/2}{aB/2} \frac{\sin bB/2}{bB/2} e^{-j\omega_0(a-b)} dt du da db$$

Now let us consider the special case where the effective noise bandwidth is much larger than the analyzing filter bandwidth, which in turn is much larger than the effective bandwidth of the envelope function. This implies that  $\psi_{nn}(x)$  is very much narrower than  $\frac{\sin Ba/2}{Ba/2}$ , which in turn is much narrower than the envelope autocorrelation functions. An approximate solution for this case is found by assuming that the noise correlation function can be well represented by the Dirac delta function:

$$\psi_{nn}(\tau) \approx N_0\mu_0(\tau) \tag{C-7}$$

Then, from equation (B-3),

$$E[F(H)] \approx \frac{B}{\Pi} \int_{-\infty}^{\infty} N_0 \mu_0(x) \phi_{ee}(x) \frac{\sin xB/2}{xB/2} e^{-j\omega_c x} dx \quad (C-8)$$

$$E[F(H)] \approx \frac{BN_0}{\Pi} \phi_{ee}(0) = \frac{BN_0}{\Pi} \int_0^{\infty} e^2(t) dt$$

Substituting equation (C-7) into equation (C-6) yields:

$$\text{Var}[F(H)] \approx \frac{N_0^2 B^2}{\Pi^2} \int_{-\infty}^{\infty} \int_{-\infty}^{\infty} \int_0^{\infty} \int_0^{\infty} e(t)e(t-a)e(u)e(u-b)\mu_0(t-u)\mu_0(t-a-u+b) \frac{\sin aB/2}{aB/2} \frac{\sin bB/2}{bB/2} e^{-j\omega_0(a-b)} dt du da db \quad (C-9)$$

$$+ \frac{B^2 N_0^2}{\Pi^2} \int_{-\infty}^{\infty} \int_{-\infty}^{\infty} \int_0^{\infty} \int_0^{\infty} e(t)e(t-a)e(u)e(u-b)\mu_0(t-u+b)\mu_0(t-u-a) \frac{\sin aB/2}{aB/2} \frac{\sin bB/2}{bB/2} e^{-j\omega_0(a-b)} dt du da db$$

The integrand of the first integral is zero except where

$$t - u = t - a - u + b = 0 \quad (C10a)$$

and that of the second is zero except where

$$t - u + b = t - u - a = 0 \quad (C10b)$$

This implies in both cases that  $a = b$ . Thus, integrating on  $u$  and  $a$  yields

$$\text{Var}[F(H)] \approx \frac{2N_0^2 B^2}{\Pi^2} \int_{-\infty}^{\infty} \int_0^{\infty} e^2(t)e^2(t-b) \frac{\sin^2 bB/2}{(bB/2)^2} dt db \quad (C-11)$$

where we have used the integral properties of the Dirac delta function. Now define the autocorrelation function of the square of the envelope function:

$$\phi_{e^2e^2}(\tau) \equiv \int_0^{\infty} e^2(t)e^2(t-\tau) dt \quad (C-12)$$

and with this at hand,

$$\text{Var}[F(H)] \approx \frac{4N_o^2B^2}{\Pi^2} \int_0^{\infty} \phi_{e^2e^2}(b) \frac{\sin^2 bB/2}{(bB/2)^2} db \quad (C-13)$$

Now recalling that  $\frac{\sin bB/2}{bB/2}$  has been assumed to be much narrower than the envelope autocorrelation function,

$$\text{Var}[F(H)] \approx \frac{4N_o^2B^2}{\Pi^2} \phi_{e^2e^2}(0) \int_0^{\infty} \frac{\sin^2 bB/2}{(bB/2)^2} db \quad (C-14)$$

Consulting a table of integrals then yields

$$\text{Var}[F(H)] \approx \frac{4N_o^2B}{\Pi} \phi_{e^2e^2}(0) = \frac{4N_o^2B}{\Pi} \int_0^{\infty} e^4(t) dt \quad (C-15)$$

Finally, forming the ratio

$$R(H) \equiv \frac{\sqrt{\text{Var } F(H)}}{E[F(H)]} \quad (C-16)$$

which is the normalized standard derivation of the output energy for this case, we find that

$$R(H) = \frac{2\sqrt{\Pi}}{\sqrt{B}} \frac{\sqrt{\int_0^{\infty} e^4(t) dt}}{\int_0^{\infty} e^2(t) dt} \quad (C-17)$$

When  $e(t)$  is a rectangular pulse of length  $T$ , the ratio of integrals becomes merely  $1/\sqrt{T}$ . Thus for this case,

$$R(H) = \frac{2\sqrt{\Pi}}{\sqrt{BT}} \quad (C-18)$$

which is exactly the expression found using the method of spectral covariance surfaces (see equation (143)) and which is quoted in reference (h) as arising in a "well-resolved" spectrum analysis. Of course, all of the above derivation after equation (C-6) is heuristic rather than rigorous, but it provides an interesting confirmation of a previous result and demonstrates the importance of considering the relative size of the several bandwidths involved.

## DISTRIBUTION

	Copies
Commander Naval Ordnance Systems Command Washington, D. C. 20360 Code 034 Code 0521	1 1
Commander Naval Ship Systems Command Washington, D. C. 20360 Code NAVSEC 6454	1
Chief of Naval Material Washington, D. C. 20360 MAT-03L	2
Chief, Office of Naval Research Washington, D. C. 20360 Code 468 Code 466	1 1
Manager, Antisubmarine Warfare Systems Project Office Department of the Navy Washington, D. C. 20360 Code ASW-P1 Code ASW-2212 Code ASW-221	1 1 1
NASA Scientific and Technical Information Facility P. O. Box 5700 Bethesda, Maryland 20546	1
Commander Naval Undersea Warfare Center 3202 E. Foothill Boulevard Pasadena, California 91107	1
Commander Naval Command Control Communications Laboratory Center San Diego, California 92152	1
Commanding Officer and Director Naval Research Laboratory Washington, D. C. 20390	1
Commanding Officer U. S. Naval Air Development Center Johnsville, Pennsylvania 18974	1

## DISTRIBUTION

	Copies
Commanding Officer and Director Navy Underwater Sound Laboratory Fort Trumball New London, Connecticut 06320	1
Ordnance Research Laboratory Pennsylvania State University State College, Pennsylvania 16801	1
Defense Research Laboratory University of Texas Austin, Texas 78712 Mr. M. Mechler	1
Commanding Officer U.S. Naval Underwater Weapons Research and Engineering Station Newport, Rhode Island 02840	1
Clevite Corporation, Ordnance Division 18901 Euclid Avenue Cleveland, Ohio 44117 Mr. B. W. Abrams	2
Westinghouse Corporation Underseas Division 3601 Washington Boulevard Baltimore, Maryland 21227	1
General Electric Company Ordnance Department 100 Plastics Avenue Pittsfield, Massachusetts 01201	1
General Dynamics/Electric Boat Groton, Connecticut 06340	1
Honeywell, Incorporated Seattle Development Laboratory 5303 Shilshole Avenue, N. W. Seattle, Washington 98107	1
Defense Documentation Center Cameron Station Alexandria, Virginia 22314	20

UNCLASSIFIED

Security Classification

DOCUMENT CONTROL DATA - R & D

(Security classification of title, body of abstract and indexing annotation must be entered when the overall report is classified)

1. ORIGINATING ACTIVITY (Corporate author)  U. S. NAVAL ORDNANCE LABORATORY WHITE OAK, SILVER SPRING, MARYLAND 20910		2a. REPORT SECURITY CLASSIFICATION <b>UNCLASSIFIED</b>	
		2b. GROUP	
3. REPORT TITLE  ON THE FREQUENCY FILTERING OF TRANSIENT NOISE SIGNALS			
4. DESCRIPTIVE NOTES (Type of report and inclusive dates)			
5. AUTHOR(S) (First name, middle initial, last name)  EDWARD C. WHITMAN			
6. REPORT DATE 26 JUNE 1968		7a. TOTAL NO. OF PAGES 102	7b. NO. OF REFS 13
8a. CONTRACT OR GRANT NO.  b. PROJECT NO. MAT-03L-000/F008-98-01, Proj 009 c. d.		9a. ORIGINATOR'S REPORT NUMBER(S)  NOLTR 68-124	
		9b. OTHER REPORT NO(S) (Any other numbers that may be assigned this report)	
10. DISTRIBUTION STATEMENT  This document is subject to special export controls and each transmittal to foreign governments may be made only with prior approval of NOL(WO).			
11. SUPPLEMENTARY NOTES		12. SPONSORING MILITARY ACTIVITY  Naval Ordnance Systems Command	
13. ABSTRACT  A class of transient random signals is modeled as the product of a deterministic, square integrable envelope function and a Gaussian random process having a well-defined power spectrum. The passage of an ensemble of such random signals through a linear filter is studied with particular emphasis on the mean and variance of the total output energy. It is found that an important role is played in these considerations by the covariance function between values of the energy density spectrum of a sample function evaluated at different frequency arguments. Accordingly, the form of this function is derived and portrayed as a surface lying above a two-dimensional frequency plane. Examples of these spectral covariance surfaces are presented and discussed for both rectangular and decaying exponential pulses of both broad and narrow band Gaussian noise, and their general characteristics are identified. Finally, the problem of idealized narrow band filtering is specifically approached and approximate expressions derived for the mean, variance, and normalized standard deviation of the output energy of a narrow band filter excited by rectangular pulses of narrow band Gaussian noise. The approximate relationships of the filter bandwidth, pulse duration, and underlying noise spectrum are explored for their effects on spectral resolution and statistical stability, leading to an uncertainty principle. The implications of these findings for spectral analysis and monopulse signal processing are discussed in the light of this uncertainty principle and the limitations it imposes on the simultaneous precision of frequency resolution and spectral amplitude.			

UNCLASSIFIED

Security Classification

14. KEY WORDS	LINK A		LINK B		LINK C	
	ROLE	WT	ROLE	WT	ROLE	WT
TRANSIENT NOISE SIGNALS						
ENERGY DENSITY SPECTRA						
SPECTRUM ANALYSIS						
SIGNAL PROCESSING						
FREQUENCY FILTERING						

UNCLASSIFIED

Security Classification

<p>1. Sound, Underwater Signals, Acoustic Sonar - Interference Title</p> <p>II. Whitman, Edward C.</p> <p>III. Project</p>	<p>Naval Ordnance Laboratory, White Oak, Md. (NOL technical report 68-124). ON THE FREQUENCY FILTERING OF TRANSIENT NOISE SIGNALS, by Edward C. Whitman. 26 June 1968. v.p. charts, tables. CRM task MAT- 03L-000/FOG8-98-01.</p> <p>UNCLASSIFIED</p> <p>A class of transient random signals is modeled as the product of a deterministic envelope and a Gaussian random process. The linear filtering of such signals is studied, emphasizing the mean and variance of the total output energy. The "spectral covariance surface" of the ensemble plays an important role and this is derived and discussed for typical situations. We discuss the problem of ideal narrow band filtering, and draw implications for spectral analysis and monopulse signal processing.</p>	<p>1. Sound, Underwater Signals, Acoustic Sonar - Interference Title</p> <p>II. Whitman, Edward C.</p> <p>III. Project</p>	<p>Naval Ordnance Laboratory, White Oak, Md. (NOL technical report 68-124). ON THE FREQUENCY FILTERING OF TRANSIENT NOISE SIGNALS, by Edward C. Whitman. 26 June 1968. v.p. charts, tables. CRM task MAT- 03L-000/FOG8-98-01.</p> <p>UNCLASSIFIED</p> <p>A class of transient random signals is modeled as the product of a deterministic envelope and a Gaussian random process. The linear filtering of such signals is studied, emphasizing the mean and variance of the total output energy. The "spectral covariance surface" of the ensemble plays an important role and this is derived and discussed for typical situations. We discuss the problem of ideal narrow band filtering, and draw implications for spectral analysis and monopulse signal processing.</p>
<p>1. Sound, Underwater Signals, Acoustic Sonar - Interference Title</p> <p>II. Whitman, Edward C.</p> <p>III. Project</p>	<p>Naval Ordnance Laboratory, White Oak, Md. (NOL technical report 68-124). ON THE FREQUENCY FILTERING OF TRANSIENT NOISE SIGNALS, by Edward C. Whitman. 26 June 1968. v.p. charts, tables. CRM task MAT- 03L-000/FOG8-98-01.</p> <p>UNCLASSIFIED</p> <p>A class of transient random signals is modeled as the product of a deterministic envelope and a Gaussian random process. The linear filtering of such signals is studied, emphasizing the mean and variance of the total output energy. The "spectral covariance surface" of the ensemble plays an important role and this is derived and discussed for typical situations. We discuss the problem of ideal narrow band filtering, and draw implications for spectral analysis and monopulse signal processing.</p>	<p>1. Sound, Underwater Signals, Acoustic Sonar - Interference Title</p> <p>II. Whitman, Edward C.</p> <p>III. Project</p>	<p>Naval Ordnance Laboratory, White Oak, Md. (NOL technical report 68-124). ON THE FREQUENCY FILTERING OF TRANSIENT NOISE SIGNALS, by Edward C. Whitman. 26 June 1968. v.p. charts, tables. CRM task MAT- 03L-000/FOG8-98-01.</p> <p>UNCLASSIFIED</p> <p>A class of transient random signals is modeled as the product of a deterministic envelope and a Gaussian random process. The linear filtering of such signals is studied, emphasizing the mean and variance of the total output energy. The "spectral covariance surface" of the ensemble plays an important role and this is derived and discussed for typical situations. We discuss the problem of ideal narrow band filtering, and draw implications for spectral analysis and monopulse signal processing.</p>

Naval Ordnance Laboratory, White Oak, Md.  
(NOL technical report 68-124).  
ON THE FREQUENCY FILTERING OF TRANSIENT  
NOISE SIGNALS, by Edward C. Whitman. 26 June  
1968. v.p. charts, tables. CAM task MAT-  
03L-000/FOCS-98-01.

UNCLASSIFIED  
A class of transient random signals is modeled as the product of a deterministic envelope and a Gaussian random process. The linear filtering of such signals is studied, emphasizing the mean and variance of the total output energy. The "spectral covariance surface" of the ensemble plays an important role and this is derived and discussed for typical situations. We discuss the problem of ideal narrow band filtering, and draw implications for spectral analysis and monopulse signal processing.

1. Sound, Underwater Signals, Acoustic Sonar - Interference
- I. Title
- II. Whitman, Edward C.
- III. Project

1. Sound, Underwater Signals, Acoustic Sonar - Interference
- I. Title
- II. Whitman, Edward C.
- III. Project

Naval Ordnance Laboratory, White Oak, Md.  
(NOL technical report 68-124).  
ON THE FREQUENCY FILTERING OF TRANSIENT  
NOISE SIGNALS, by Edward C. Whitman. 26 June  
1968. v.p. charts, tables. CAM task MAT-  
03L-000/FOCS-98-01.

UNCLASSIFIED  
A class of transient random signals is modeled as the product of a deterministic envelope and a Gaussian random process. The linear filtering of such signals is studied, emphasizing the mean and variance of the total output energy. The "spectral covariance surface" of the ensemble plays an important role and this is derived and discussed for typical situations. We discuss the problem of ideal narrow band filtering, and draw implications for spectral analysis and monopulse signal processing.

Naval Ordnance Laboratory, White Oak, Md.  
(NOL technical report 68-124).  
ON THE FREQUENCY FILTERING OF TRANSIENT  
NOISE SIGNALS, by Edward C. Whitman. 26 June  
1968. v.p. charts, tables. CAM task MAT-  
03L-000/FOCS-98-01.

UNCLASSIFIED  
A class of transient random signals is modeled as the product of a deterministic envelope and a Gaussian random process. The linear filtering of such signals is studied, emphasizing the mean and variance of the total output energy. The "spectral covariance surface" of the ensemble plays an important role and this is derived and discussed for typical situations. We discuss the problem of ideal narrow band filtering, and draw implications for spectral analysis and monopulse signal processing.

1. Sound, Underwater Signals, Acoustic Sonar - Interference
- I. Title
- II. Whitman, Edward C.
- III. Project

1. Sound, Underwater Signals, Acoustic Sonar - Interference
- I. Title
- II. Whitman, Edward C.
- III. Project

Naval Ordnance Laboratory, White Oak, Md.  
(NOL technical report 68-124).  
ON THE FREQUENCY FILTERING OF TRANSIENT  
NOISE SIGNALS, by Edward C. Whitman. 26 June  
1968. v.p. charts, tables. CAM task MAT-  
03L-000/FOCS-98-01.

UNCLASSIFIED  
A class of transient random signals is modeled as the product of a deterministic envelope and a Gaussian random process. The linear filtering of such signals is studied, emphasizing the mean and variance of the total output energy. The "spectral covariance surface" of the ensemble plays an important role and this is derived and discussed for typical situations. We discuss the problem of ideal narrow band filtering, and draw implications for spectral analysis and monopulse signal processing.